UNIVERSITY OF LIVERPOOL

Papercrete Studies of the Mix Design and Sustainability for Construction Materials

Thesis submitted in accordance with the requirements of the University of Liverpool for the degree of Doctor in Philosophy

By
Xiang Wang

Monday, November 16, 2020

PGR Declaration of Academic Honesty

NAME (Print)	Xiang Wang
STUDENT NUMBER	1403820
SCHOOL/INSTITUTE	Department of Civil Engineering
TITLE OF WORK	Papercrete Studies of the Mix Design and Sustainability for Construction Materials

This form should be completed by the student and appended to any piece of work that is submitted for examination. Submission by the student of the form by electronic means constitutes their confirmation of the terms of the declaration.

Students should familiarise themselves with Appendix 4 of the PGR Code of Practice: PGR Policy on Plagiarism and Dishonest Use of Data, which provides the definitions of academic malpractice and the policies and procedures that apply to the investigation of alleged incidents.

Students found to have committed academic malpractice will receive penalties in accordance with the Policy, which in the most severe cases might include termination of studies.

STUDENT DECLARATION

I confirm that:

- I have read and understood the University's PGR Policy on Plagiarism and Dishonest Use of Data.
- I have acted honestly, ethically and professionally in conduct leading to assessment for the programme of study.
- I have not copied material from another source nor committed plagiarism nor fabricated, falsified or embellished data when completing the attached material.
- I have not copied material from another source, nor colluded with any other student in the preparation and production of this material.
- If an allegation of suspected academic malpractice is made, I give permission to the University to use source-matching software to ensure that the submitted material is all my own work.

SIGNATURE 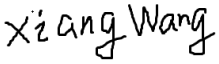

DATE Saturday, November 28, 2020

Abstract

Renewable or recycled materials have been widely used in construction materials to achieve a sustainable target, such as natural fibre or derivatives used in the construction industry. As a kind of short cellulose fibre, a massive amount of waste paper fibre was generated from industrial and constructional sections annually. However, the research on the waste paper fibre used in concrete or construction material to replace the traditional disposal of wasted paper is limited. This project aims to establish a systemic method to investigate the influence of waste fibre used in concrete blocks and find out the approximate mixed proportion.

Except for waste paper fibre, raw material used in this study for the concrete block include Portland cement, water, hydraulic lime (aims to improve interfacial properties of waste paper fibre), aggregates with an appropriate size, and additives. By using the response surface method, a set of mixed proportions was obtained (water-cement ratio, hydraulic lime to cement ratio, waste paper to cement, and aggregate ratio set to be the independent variables), to get a predictive function for each property. Further, the validation and optimization of the mixed proportion were conducted to meet the requirement of the ASTM standard. In the first stage, the influence of different mix ratios on the block's properties was explored based on the material performance test results, including density, water absorption, compression resistance, softening coefficient, heat transfer performance and microscopic structure. The experimental results show that waste paper fibre significantly reduces the strength of the block, water absorption and softening coefficient, but the thermal insulation performance is improved. In addition, hydraulic lime positively affects the

interface between cement and waste paper and improves the block's compressive strength. In the second stage, according to the experimental data obtained and the material specifications given in the ASTM standard, by establishing and verifying the second-order predictive function of the response surface, the design mixed proportion that meets the ASTM standard of non-load-bearing block can be found, and the volume replacement rate to cement can reach 11.7%. In the third phase, the paper block concrete's feasibility and sustainability as a building material were demonstrated based on a life cycle assessment (LCA) method through an in-depth analysis of its characteristics. The results show that waste paper fibre in concrete provides a potential treatment method for replacing waste paper in landfills or incineration, especially replacing cement.

Acknowledgment

During conducting my final year project, I gain immense support and help from my supervisors, classmates, friends, colleagues and my parents, to whom I am sincerely grateful.

First, I would like to express my heartfelt appreciation to my supervisor, Prof. Chee Seong Chin and Prof. Derrick Tate, for his guidance and support. His advice and assistance help me to work out difficulties and continue my work. I would like to thank Prof. Jun Xia for support and guidance during a laboratory experiment. I would like to thank Dr. Stephen Jones for their support and suggestions. Without their help, my dissertation cannot be accomplished.

I am sincerely grateful to the Department of Civil Engineering for the support of equipment and various apparatus to complete my graduate studies. I would like to express appreciation to my friends and colleagues for their support and advice in my work, especially Zuowei Liu and Xingyi Wang.

My sincere appreciation goes to all laboratory assistants who provide support to me in laboratory experiments. Finally, I sincerely thank my parents for their encouragement and support in my studies, they give me inspiration and love.

Tables of content

List of Figures

List of Tables

Chapter 1 Introduction

1.1 Background

Human activities that aim to improve living quality generally with energy and resources consumption impact the environment both directly and indirectly. Nevertheless, environmental carrying capacity is limited and environmental issues caused by inappropriate human activities conversely have a negative influence on human lives. Due to the dramatic increase in population and industry, environmental issues are becoming prominent and pressing. On a global scale, environmental issues involve global warming, resource depletion, ozone layer depletion and biodiversity degradation. The exceeding emissions and improper disposal would result in air pollution, acid rain, water pollution and other environmental issues[1].

To balance the conflict between development and the environment, the concept of sustainability is proposed and attracts wide attention. The UN World Commission firstly reports the relatively thorough concept of sustainable development on Environment and Development in 1987. The target of sustainability, which is still gradually improving, is required to comprehensively consider the coordination between social benefits, economic benefits and environmental benefits[1–3].

The sustainable concept is essential in the civil construction sector because it consumes a vast amount of energy and resources in fabrication, transportation and installation. The civil construction industry occupies 60%-70% of materials flow globally, particularly the building sector, which consumes approximately 24% of raw materials and 40% of energy worldwide, plays a vital role in human activities thus have a tremendous impact on the environment[4–8]. In addition, as a crucial source

of greenhouse gas (GHG), about 40%-50% of GHG is attributed to the civil construction sector in the worldwide scope [9,10]. For example, the USA's building sector is responsible for 40% of total CO_2 emission[11].

There are a lot of advantages of cement-based materials, such as easy assembly and shaping, relatively low cost, appropriate mechanical properties and durability[10]; thus concrete is the most widely used material in the civil construction field, globally the annual per capita production of the concrete is around 1 ton [12]. However, due to the high energy consumption and depletion of natural resources in production, transport and installation, based on the life cycle assessment (LCA) method, traditional concrete is not an eco-friendly product[13–15]. More than 5% of human-made carbon dioxide emissions are attributed to global concrete production [9]. Fig. 1 and Fig. 2[7] reported material manufacture process and transport are responsible for a majority of GHG emissions in the building sector, where the proportion of GHG emissions from concrete and steel is approximately 70%.

Cement as an essential component of concrete is specially produced and consumed in large quantities for civil construction. The cement production globally is increasing by 2.5% yearly and reaches up to 2.3 giga-tons (Gt) in 2005 and is estimated to 3.5Gt by 2020[16]. The cement production procedures and use are high energy and materials intensive industry, with discharging more than 5% of total human-made CO_2 and massive by-products, such as SO_2 and NO_x, to the environment[17–20]. The process of cement production generates around 0.9 tons of carbon dioxide per ton[21]. According to the case study based on LCA, production of 1 ton ordinary Portland cement consumes 1.5-1.6 tons of ingredients, over 3000 MJ of fossil fuel energy and more than 120 kWh of electricity[17,22]. Consequently, sustainable and

environmentally friendly strategies are gained more attention in the civil construction sector.

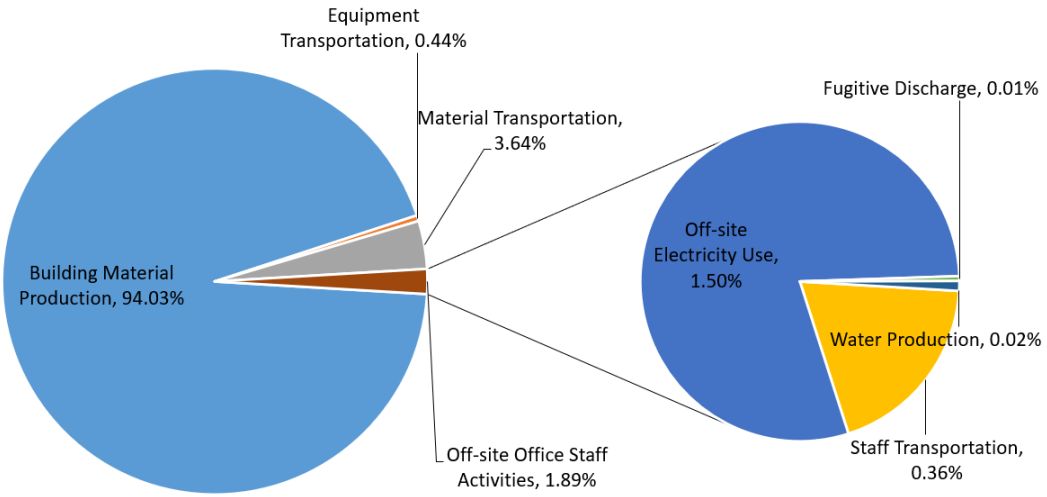

Fig. 1 The contribution of indirect GHG emissions [7].

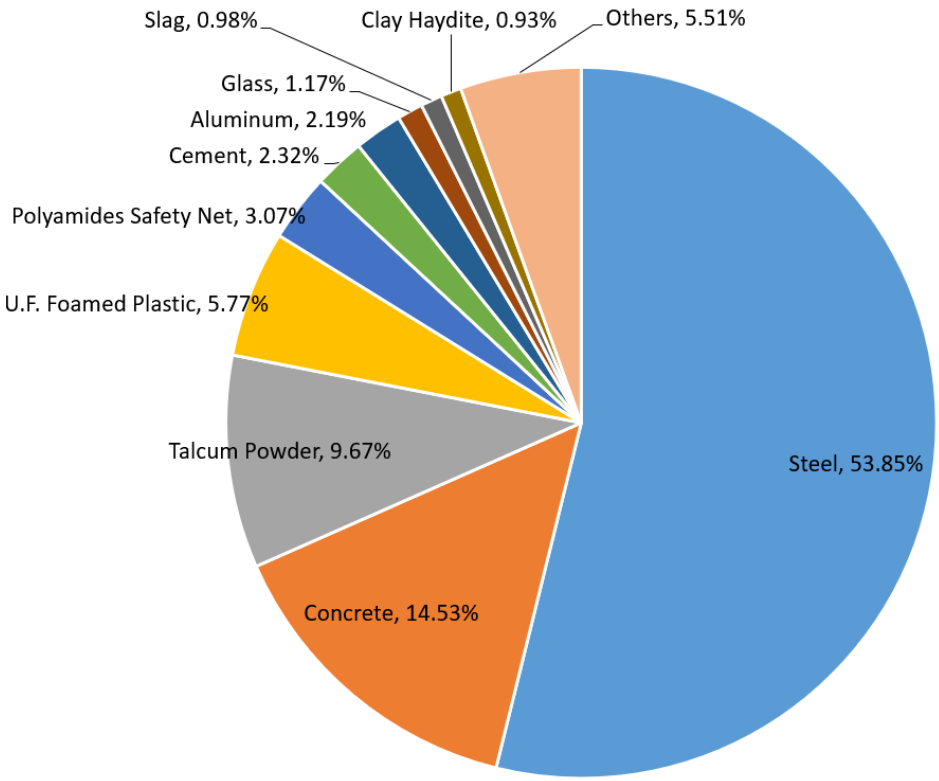

Fig. 2 The contribution of GHG emission generated by initial building materials [7].

Based on the target of sustainability in the civil construction sector, some criteria were established, including reducing the utilization of non-renewable resources, efficiently using resources, minimizing pollution, optimizing construction processes and a healthy environment[3,23]. As stated above, construction materials are

particularly important for the sustainability of the construction sector. Thereby, some alternative materials were selected and investigated to reduce the environmental footprint of traditional concrete. Alternative materials are mainly achieved from recycled construction materials and industrial waste, such as fly ash, Ground Granulated Blast Furnace Slag (GGBS), limestone, scrap tires, rice husk ash, wood ash and et. al.[24–26]. For instance, by using limestone to replace cement, the reduction of CO2 emission can reach up to 25%[27]. Both Flower et al.[28]and O'Brien et al.[29]reported that ordinary concrete mixing with fly ash and GGBS can reduce GHG emissions by around 15% and 22%, respectively. The alternatives to natural materials used in typical concrete can effectively reduce GHG emission further relieve the burden of the environment. The main reasons were summarized according to LCA in previous literature as following [29–33]: 1) The energy consumption in transport and installation was reduced due to the relatively low density of substitutes. 2) The disposal of industrial waste is avoided to some extent. The influence of landfill and incineration of waste is alleviated. 3) The depletion of natural resources is reduced. The dosage of cement and natural aggregates decreases because of adding the substitute.

The waste paper generated in quantity yearly is a potential construction resource. The concept of papercrete was proposed in 1928 initially and known as an environmental-friendly material due to the utilization of recycled components. Papercrete, which was one kind of sustainable construction material composed of recycled and re-pulped paper, gets wide attention from the engineering field [34,35]. On the one hand, papercrete provides a solution to waste paper disposal, comprising the most considerable fraction of municipal solid waste [36]. Additionally, the

material cost of papercrete ($21.53/m^2) was much lower than the cost of both the wood-frame structure ($64.58/m^2) and concrete construction ($96.88/m^2)[34]. Papercrete theoretically fulfils sustainability as a high-level requirement in the construction industry. The use of sustainable materials with lower energy consumption and fewer emissions than traditional construction materials could be crucial.

On the other hand, due to the increase in paper demand, the paper's production quantity is also increasing. Meanwhile, the paper recycling rate is increasing annually, and however, the rate is not enough for total production. For instance, with massive energy consumption, the production and depletion of pulp in China occupied 42.66% and 50.64% globally, respectively[37,38]. The recycling rate of waste paper remainsed steady in recent years (around 47.5%) in CEPT countries[39]. Therefore, waste paper recycling is an essential component of waste management.

Manufacture processes where the waste paper was re-pulped and re-produced to recycled paper had a great negative effect on the environment since the pulp and paper industry was an energy-intensive sector, thus waste paper recycling had no remarkable environmental benefits, even had higher indirect environmental impacts[40,41].

To sum up, waste paper with a relatively simple treatment can be used as an addition or substitute to make papercrete, which is a promising eco-friendly material with reasonable cost and favourable properties.

Some researchers investigate the manifold influence resulted from common lime and derivative product used in concrete. Ordinary cement with limestone, namely Portland limestone cement (PLC), is being used in several European countries.

Through the introduction of limestone, sulphate resistance and workability are improved, and bleeding of concrete is modified. In environmental impact, PCL with 20% of limestone can decrease up to 10% emissions and energy consumption compared with ordinary Portland cement (OPC)[42,43]. The early age compressive strength and sorptivity are improved by introducing silica fume and lime. Besides, compaction presented as permeability is enhanced because hydration of lime fills in a tiny void in concrete in Fig. 3[44].

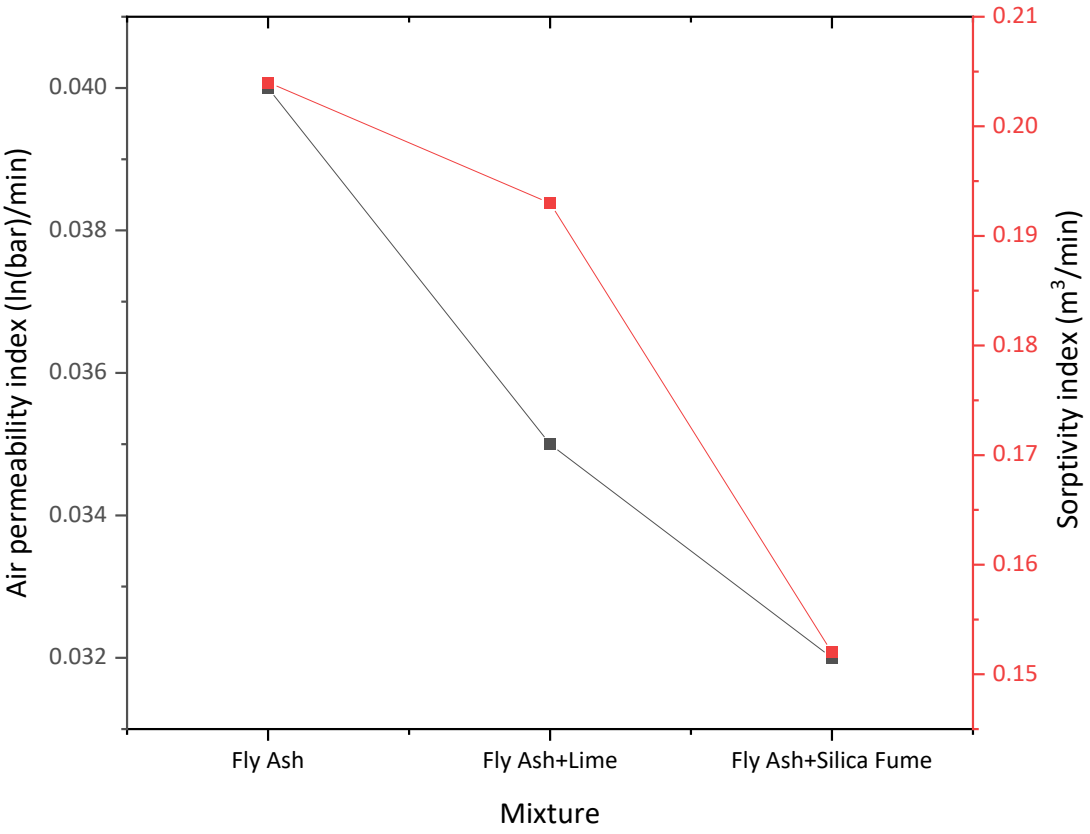

Fig. 3 The influence of lime used in concrete on air permeability and sorptivity[44].

According to relating chemical analysis (x-ray diffraction analysis), the major constitution of lime is calcium hydroxide ($Ca(OH)_2$). Therefore pozzolanic material can chemically combine with $Ca(OH)_2$, forming C-S-H gel. Previous research indicates the replacement ratio of lime in blended cement is from 5% to 10%, and optimized performance is achieved with 7% of lime replacement[44–46]. Additionally, the

inclusion of lime content can efficiently increase the thermal insulation of concrete. Especially, lime is a binder mix with hemp, which is a natural vegetal fibre to manufacture hemp-concrete[47,48].

The cement production process is a resource and energy-intensive industry, substitute of cement is usually used in practice. Lime is relatively cheap and abundant in nature. Due to easily extraction and utilization, lime is used all over the world almost throughout human history. Lime is a cement replacement material, generally used as a cementitious material. Even though the lime product's manufacturing processes have an impact on the environment as well because the required temperature during the calcining process is relatively low compared with cement production, lime consumes less energy and lower carbon emissions[48,49].

Paper pulp is sensitive to an alkaline environment, and especially both physical and chemical degradation occurs gradually. For instance, the alkaline hydrolysis of part of pulp fibre leads to the cellulose molecular chain's disruption. In addition, due to the concentration of pore water at the fibre's surface, where the hydration process occurs and hydration products fill up with the inner cores of pulp fibre, the mechanical performance of fibre is impaired[50]. The research indicates cementitious matrices with low alkalinity are beneficial to the conservation of mechanical performance of recycled fibre, especially the degradation of modulus of rupture and the reduction of specific energy [51].

1.2 Objectives

Fig. 4 shows the flow diagram of papercrete block (PB) design, and major aims of this research include: To achieve the expected performance of papercrete in the structural and non-structural applications, raw material selection and production

process of papercrete will be developed. To standardize the materials and testing relating to papercrete, Adapt American Society of Testing Materials (ASTM) material specifications will be used. Develop and characterize the model of micro-scale of different components in papercrete.

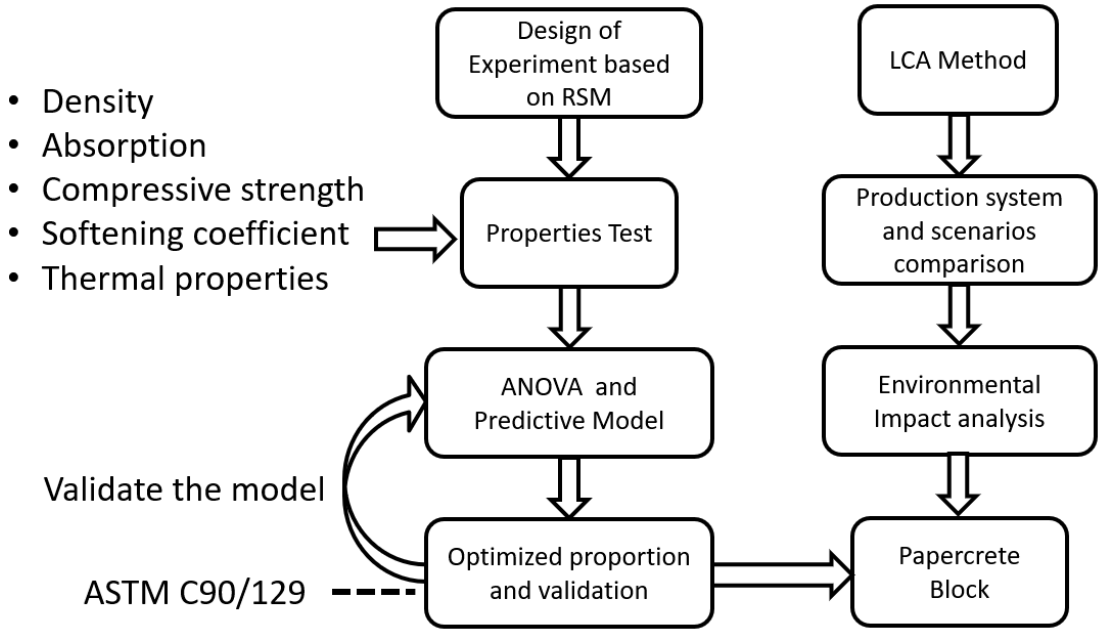

Fig. 4 The diagram of investigation on PB.

1.3 Layout of Thesis

This thesis introduces current research related to the papercrete. The experiment is designed based on the response surface method (RSM), and the results of various tests are presented and discussed. The optimized proportion design of PB is validated and explained. The life cycle assessment of PB is calculated and evaluated. This thesis includes six chapters and summarized as follows:

Chapter 1: Introduction of alternative materials used in concrete, sustainability for civil engineering, and the concept of papercrete. The main objectives of this research and the flowchart of research are presented. Additionally, the outline of this thesis is described.

Chapter 2: Literature reviews of previous relevant studies are presented. Not only waste paper fibre is introduced, but the materials relating to the waste paper fibre used in concrete are also presented, such as the natural cellulose fibre. The influence of such cellulose used in concrete is introduced, including general properties, mechanical properties, and environmental effects.

Chapter 3: Describe in detail the experiment procedures, including raw materials, design of experiment, mix design based on RSM, waste paper fibre properties and preparation of PB. The selection of standards is explained and comparisons with British standards and Chinese standards are conducted.

Chapter 4: Analysis of Variance (ANOVA) for results of an experiment based on RSM, the regression model is created, diagnose and explained. The optimized proportion of papercrete is tested and validated.

Chapter 5: Establish the development of the life cycle assessment model of PB production, make a comparison between papercrete production and conventional concrete blocks production combined with waste paper disposal.

Chapter 6: The conclusion of this research is described, and further investigations are proposed and discussed based on current results.

Chapter 2 Literature review: the studies on the concrete with waste paper

2.1 Introduction to papercrete

Papercrete, as a sustainable construction material composed of ***recycled or re-pulped waste paper*** mixing with bonded materials and aggregates, was achieved wide attention from the engineering field. The waste paper generated in quantity yearly is the potential construction resource, and disposal of waste paper is a noticeable issue with the increase of paper consumption. Therefore, the concept of papercrete was proposed to solve these problems by introducing waste paper fibre into concrete. Typically, the raw materials of papercrete mainly included cementitious materials, aggregates, and waste paper pulp.

There are no uniform and systematic methods for the mixed design of papercrete in existing studies, and most research involved two common methods to design the papercrete recipe. One method is a waste paper pulp is used as the substitute of cement; another method is a waste paper pulp is added as extra composition.

Studies of waste paper used as a substitute for cement are limited. Yun et al.[52]considered waste paper pulp had a good binding with cement paste, and cement at 5%, 10% and 15% by weight was replaced by waste paper pulp and other ingredients include sand and superplasticizer. Relatively low density (1.44g/cm^3) and an acceptable compressive strength (17.4MPa) were achieved with 3:17:17:10 of paper : water : cement : sand. The results demonstrated this method and mixed proportion was possibly feasible but preliminary.

More studies use the second method, adding extra waste paper pulp. Based on this method, the multifarious mix proportion is designed and tested. Fuller et al.[35]report a variety of mix proportions. Ingredients used in Fuller's experiment, except for cement and waste paper, contain fly ash, sandglass, clay, lime, Styrofoam with different recipes. As Fig. 5 shows, Sangrutsamee et al.[53]and Akinwumi et al.[54]mixed cement and sand with different types of waste paper to make papercrete. Aigbomian et al.[55] created a kind of papercrete which has good thermal insulation with sawdust and lime. In addition, Subramani et al.[56]tried to use recycled aggregates to replace coarse aggregates in papercrete.

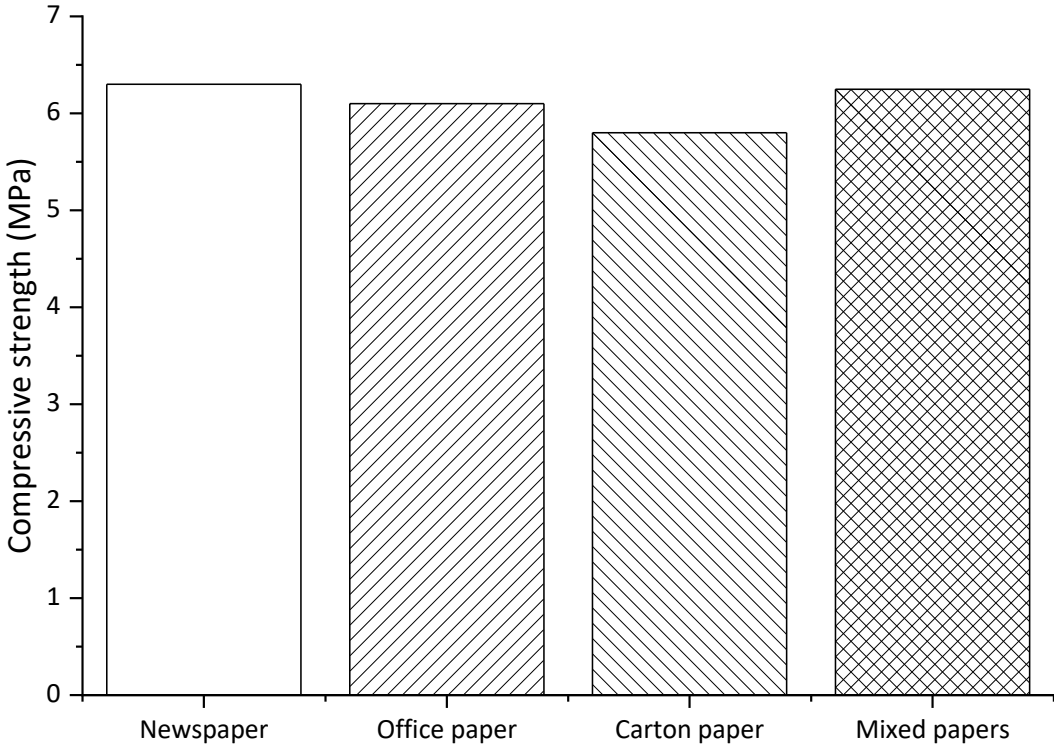

Fig. 5 Compressive Strength for Different Types of Recycled Waste Paper with 20% of pulp content[53].

Based on the research status, experiments should be designed to investigate the reasonability of these two mix schemes due to a lack of comparison between schemes.

There were several advantages to using natural cellulose fibre or waste paper fibre in concrete. The waste paper used as an alternative to the raw materials of the concrete was sustainable, renewable, and recyclable. Typically, incineration, landfill, and recycling are the most used technologies for the disposal of waste paper. Landfill and incineration indeed have a negative effect on the environment, even though waste paper recycling is a developed scheme, and the recycling rate is increasing continuously. Processes of paper recycling are regarded as potentially environmental harmfulness with using multiple chemicals and energy consumption[57]. The concept of the papercrete provides a new treatment, which avoids a set of pollution from waste paper disposal. On the other hand, due to the introduction of cellulose fibre, the density of the concrete decreases according to the amount of usage of waste paper. Furthermore, as a result of both low thermal conductivity of paper fibre and pores in papercrete, which was considered to have favourable thermal insulation.

However, the influence of cellulose fibre on the mechanical properties of the concrete was not explicit, and the research on papercrete only focus on the influence of a single factor. Moreover, Sangrutsamee et al.[53] have investigated the influence of waste paper types used in concrete on compressive strength. There are no significant differences in papercrete with various waste paper, and papercrete with office paper pulp have a relatively higher strength due to physical property difference. The search relating to flexural strength is limited. Selvaraj et al.[58] carried out the experiment to cast the papercrete with a designed proportion and waste paper pulp is added as the extra component by the mass fraction of cement. Experimental results indicate that the variation of flexural strength is not monotonous. The enhancement of flexural strength is likely to be attributed to paper fibre, which has similar principle

to fibre-reinforced concrete. There was no investigation on the multi-factor influences of the properties of papercrete, and the design of mix proportion of papercrete is not systematized.

Waste paper fibre or cellulose fibre was used to replace the cement or the aggregates in concrete. Most current literature concentrated on the replacement of cement in the low ratio [59,60]and there was limited literature using waste paper to replace aggregates[61]. Consequently, in this study, recycled waste paper fibre was used to mix with a concrete block with lime, which aims to decrease the use of cement and aggregates. Based on the experimental design of the response surface method (RSM), density, water absorption, and compressive strength were measured to investigate the interaction of various factors, and the predictive model for responses was established.

2.2 The influence of waste paper used in concrete

2.2.1 General properties

Waste paper pulp have relatively lower density compared with other composition, and by using waste paper pulp, the density of concrete obtains a distinct reduction. A lot of literature reports unit weight of papercrete decreases with increasing the amount of waste paper pulp[52,54,55,58,62–64]. Aigbomian et al.[55]propose a new building material called wood-Crete, consisting of sawdust, waste paper, and lime. The density of wood-Crete reduces by around 33% when the addition of waste paper increases from 10% to 75%.

2.2.2 Workability

Due to the properties of the paper pulp, such as high-water absorption and hydrophobicity of cellulose, workability of papercrete, such as shrinkage ratio, waster absorption of papercrete, slump value, have great differences with conventional

concrete. Fig. 6 illustrates the negative effect of pulp fibre on the workability of fresh concrete, results indicate there is a significant reduction of slump and slump flow with 0.28 and 0.5 water-cement ratio[65].

Due to the hygroscopicity of cellulose fibre, papercrete has higher water absorption, and the increase of paper content leads to the increase of water absorption[52,53,59]. Selvaraj et al.[58]report that water absorption reaches up to 50% when adding 35% waste paper in concrete. Anandaraju et al.[63]make water absorption of papercrete brick reduce through introducing GGBS.

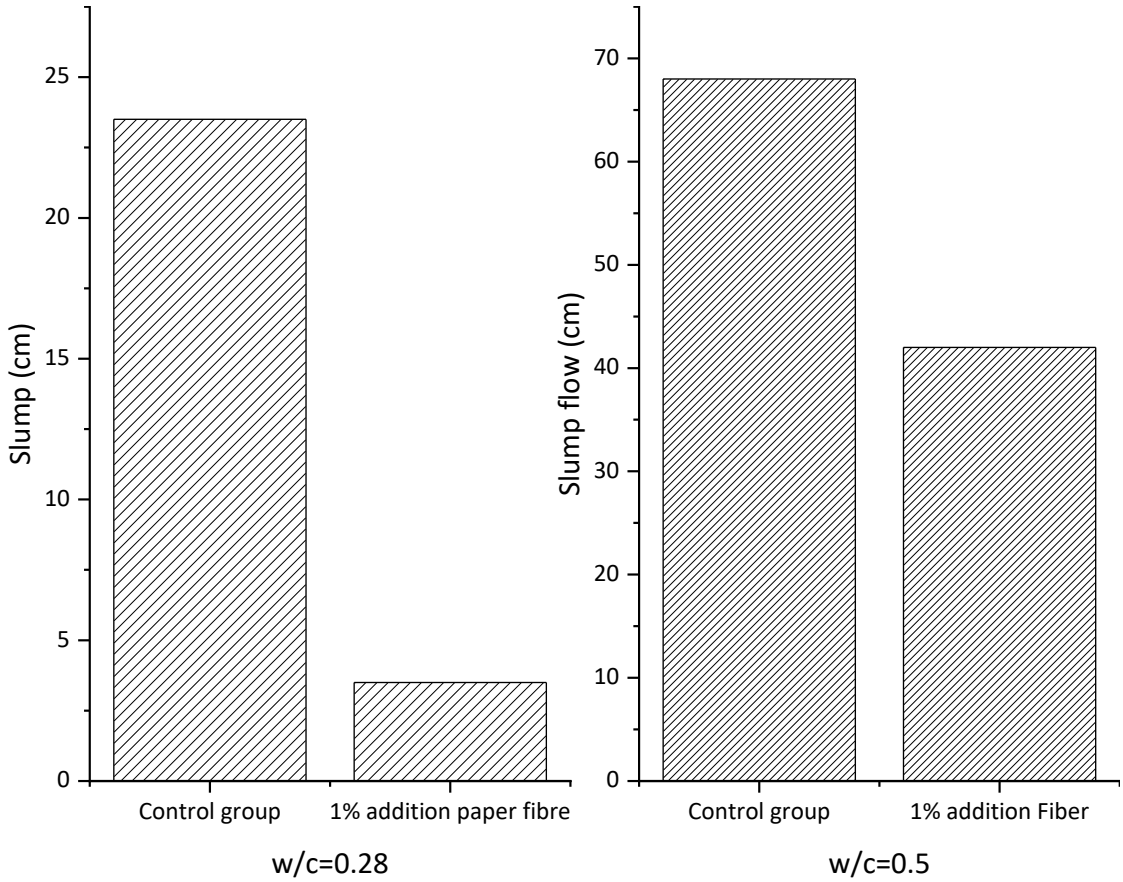

Fig. 6 Slump test on mortar (paper fibre was used as 1% addition) [65].

The drying shrinkage ratio has a slight increase when the proportion of waste paper content increases[52,59,62,66]. However, there is no more detailed analysis for shrinkage or swelling of papercrete. Nevertheless, the huge amount of water

retained in papercrete during a long period have a non-negligible influence on the drying behaviour of papercrete.

2.2.3 The mechanical properties influence

a) Modulus of elasticity

Elastic modulus, as a significant parameter, determines the deflection of materials with a load. All existing studies showed that the elastic modulus of papercrete had a remarkable reduction when waste paper content increases[62,67,68]. The main reason, which leads to the decrease of elastic modulus, was the relatively low elastic modulus of paper fibre. Generally, cellulose fibre, as a basic constituent of paper, was the elastic modulus fibre with 10GPa[69].

b) Compressive strength

Almost all studies demonstrate compressive strength had a remarkable reduction due to adding paper content, and compressive strength decreases continuously with the increase of paper content[52,54,55,58,62–64,70]. There were different results obtained by Kumar et al. [59]. In this experiment, the compressive strength increases monotonously until the cement/paper ratio is 3, and then the compressive strength curve drops down rapidly. Especially, the experimental results from Anandaraju et al. [63] show the influence of GGBS on papercrete brick when cement/paper/quarry dust ratio was 1:2:4 with increasing of GGBS content, the compressive strength of papercrete increases from 6.35Mpa to 9.2 MPa at 28 days.

Moreover, Sangrutsamee et al.[53]investigate the influence of waste paper types used in concrete on compressive strength. There are no significant differences in papercrete with various waste paper. Papercrete with office paper pulp have a relatively higher strength due to physical property difference.

c) Flexural strength

The search relating to flexural strength is limited. Selvaraj et al.[58] designed the papercrete with cement : sand : coarse aggregate ratio of 1:1.5:2 and waste paper pulp was added as the extra component by the mass fraction of cement. Experimental results indicate that the variation of flexural strength was not monotonous. Flexural strength decreased to 4.36MPa with 2.5% paper content and then increased up to 10.84MPa with 35% paper content, compared with 6.81MPa of concrete in the control group. The enhancement of flexural strength was likely to be attributed to paper fibre, which had a similar principle to fibre-reinforced concrete.

d) Splitting tensile strength

The experiment conducted by Yun et al.[52]used the waste paper pulp as a substitute for cement with a replacement ratio ranging from 5% to 15%, which indicated that the splitting strength decreased when the replacement ratio increased. However, a slightly different result was achieved in the experiment of Selvaraj et al. [58]. Compared with control group concrete with 2.89MPa at 28 days, the splitting tensile strength had a slight increase when addition paper mass was less than 2.5% and then continuously decreases to 0.79MPa with 35% addition paper. In Selvaraj's experiment, coarse aggregate, which had a positive influence on the strength of concrete, was used in papercrete. Moreover, the minimum addition mass of waste paper pulp for Yun's experiment, exceeded the range where splitting tensile strength increases in the experiment of Selvaraj. The paper content in the experiment of Yun was used as the replacement of cement, but for Selvaraj's mix design, the waste paper pulp was introduced as an addition. The difference of proportion is likely to lead to a result in the difference of concrete structure and affect the mechanical

property of concrete. Besides, further studies should be made to investigate potential and accurate reasons.

2.2.4 The durability

The introduction of waste paper pulp affects the durability of concrete, mainly due to the increase of the water absorption of waste paper. Fig. 7 shows the influence of waste Kraft pulp with different treatment on the water absorptions, reported by Booya et al[60].

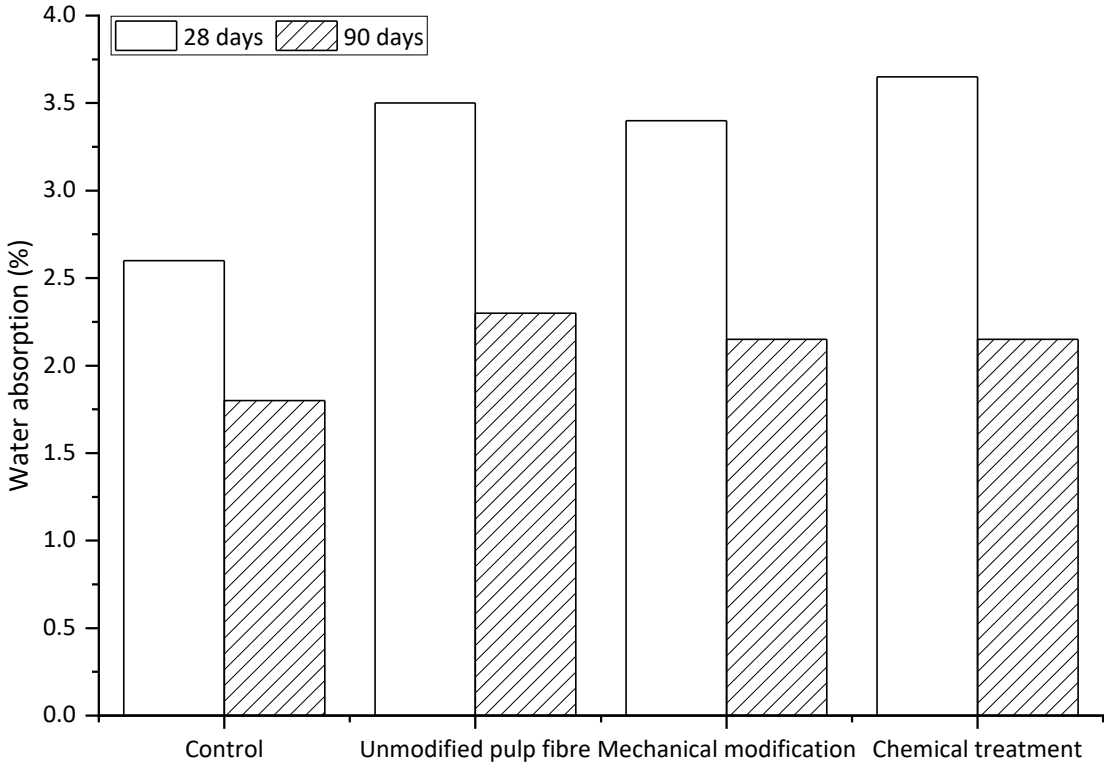

Fig. 7 Variation in water absorption[60].

Generally speaking, PB have favourable fire resistance as construction materials and cannot be ignited with open flame[63,64,67]. Generally, most research reports that R-value for papercrete brick is higher than traditional concrete but is affected by the amount of cement and sand used in papercrete[34,35,71]. The experimental results of Sangrutsamee et al.[53]indicate thermal conductivity of papercrete decreases significantly with the increase of waste paper content. Besides, the effect of waste paper type is investigated and papercrete mixing with carton paper can achieve lower

thermal conductivity compared with papercrete with newspaper or office paper. The wood-Crete was designed by Aigbomian et al.[55], which is made up of sawdust, waste paper, and lime, obtain a rather low thermal conductivity with a minimum of 0.046 W/m K. As a good performance insulation material with low cost and lightweight, papercrete has great potential value.

2.2.5 Other properties

The ultimate strain was achieved from the stress-stain curve in the experiment of Choi et al.[52,62]have a remarkable increase with increasing the replacement ratio of waste paper in papercrete. The cellulose fibre of waste paper is likely to enhance the ductility of papercrete through combination with the cement matrix.

In another experiment conducted by Santamaria and Fuller[35,67], according to the creep test, the deformation of papercrete increase nonlinearly and continuously until maximum value. The creep, which is rather small and has no significant effect on structures, increases when cement content increases. However, the pull-out test in this experiment does not clarify the influence of the waste paper on the pull-out capacity of a driven bar for papercrete.

The experiment performed by Selvaraj et al.[58]indicated that the impact resistance increases with the increase in waste paper content. The main reason was the cellulose fibre has a positive influence on impact force absorption. A similar result was obtained by Decard et al.[72], papercrete has higher damping and capacity of energy absorption basing on the low-velocity impact test.

Several articles report that acoustic property of papercrete, Fuller et al.[35,67] report papercrete has favourable sound absorption. In addition, the sound insulation of

hollow concrete blocks designed by Modry[73] meets the requirement of the partition wall, according to ISO 717-2[74] test.

2.3 Utilization of hydraulic lime in papercrete

Hydraulic lime (HL) and lime derivative as an ancient binder are widely used in various cementitious materials, such as plastering motor, grouts, restoration materials, or lime-based concrete. According to the research of Grist[75]and Pozo-Antonio[76], the improvement of mechanical strength caused by the hydraulic reactivity of natural hydraulic lime was achieved, and HL was demonstrated to improve the stability of the compound. Aerial lime was widely used and investigated in most studies where the effect of lime ratio on such as mechanical properties, durability has been completed, however further, there are limited investigations that the concrete including cement and HL.

The utilization of HL production was. The alite (Ca_3SiO_5), which is the essential component of CEM Ⅰ is formed at the temperature of above 1300°C in the kiln, while compared with CEM Ⅰ, the alite is only trace amount (＜0.7%), the major compound in HL is belie ($(CaO)_2 \cdot SiO_2$) which is generated at 900° C in the kiln, particularly as Table 1 shows the comparison between Natural Hydraulic lime (NHL5) in line with BS EN 459[77] and typical CEM Ⅰ as an example. It is clear that the energy consumption of CEM Ⅰ manufacture is higher than that of HL.

The aim of introducing lime into papercrete is to explore the effect of hydraulic HL or alkaline environment on waste paper fibre mixing with concrete. HL and lime dust are widely used in cementitious ingredients as an alternative of cement, such as plastering mortar [78,79], and lime-based concrete[80]. Especially, the mixture of

cellulose derivatives and HL has a mutual effect on the mortar. Water retention, mechanical strength growth and variation of compressive strength depend on the chemical properties of cellulose derivation. Introducing cellulose ether into lime mortar has a negative influence on compressive[81]. Whereas Hui Liu et al. [82] demonstrated that utilization of carboxymethyl cellulose (CMC) in lime motor significantly improve the compressive strength of the lime motor, according to experimental results introducing CMC into the lime motor can slow down the procedure of lime hydration and steadily produce the calcite of $CaCO_3$ crystals. In this study, HL is used as an alternative of cement, which is to investigate the interactions on the strength reduction caused by the effect of waste paper.

Table 1 The comparison of mineralogical constituent between NHL with CEM Ⅰ [77].

Compositions	Typical NHL5 (% / mass)	Typical CEMI% / mass)
Insoluble substance	4	Trace
Free lime, $Ca(OH)_2$	21	2
Unburnt calcium carbonate, $CaCO_3$	23	0
Alite, Ca_3SiO_5	Trace	58
Belite, $(CaO)_2 \cdot SiO_2$	45	13
Tricalcium aluminate, $3CaO \cdot Al_2O_3$	2	9
Gehlenite, $Ca_2Al(AlSiO_7)$	2	0
Calcium aluminoferrite, $Ca_2(Al \cdot Fe)_2O_5$	2	8
Gypsum, $CaSO_4$	Trace	5
Other	1	5

2.4 Application of papercrete

In the laboratory, some structural elements are designed and poured into testing for papercrete. Interlocking arch, seating, shed, compound walls with or without rebar, and infill constructed with other frameworks, are designed and tested to be feasible[66,67]. Furthermore, some structures with or without footings and slabs on the ground are designed and tried[67].

Papercrete has already been applied in practice. Papercrete is used to build vaults, domes, walls, and stucco[67,71]. Even a small house partly adopted papercrete was constructed in the rural area, as shown in Fig. 8[67].

Fig. 8 Building using papercrete[67].

2.5. Statement of problem and motivation of study

2.5.1 Advantages

As stated previously, the most significant advantage of papercrete compared with conventional concrete is lightweight due to the use of waste paper. Even though in a similar condition of compressive strength, the density of papercrete reduces by roughly 26% compared with typical clay brick[53]. The reduction of density can efficiently decrease energy consumption during fabrication and transportation. Meanwhile, waste paper content seems to improve flexural strength and splitting strength and make concrete more ductile.

Secondly, due to favourable thermal insulation and sound absorption, papercrete can be used as a thermal insulation material or infill material in the partition wall and convenient for installation and teardown.

Besides, the waste paper, which is generally disposed of through landfill or incineration, is re-pulped and reused to mix with the concrete. Therefore, papercrete can be regarded as an eco-friendly material. Even though the waste paper is reprocessed to be recycled paper, papercrete has a positive influence on the environment and sustainability. Furthermore, compared with conventional concrete, the cost of paper is relatively lower, and papercrete would be a sustainable construction material economically.

2.5.2 Disadvantages

Generally, although there have been some investigations on the properties of papercrete, the formal testing standards and specifications for papercrete are not established yet [83]. In addition, according to the study of Santamaria [67], the compressive strength of papercrete is around 140-160 psi, and the compressive strength of a part of the specimen even can be up to 260 psi or more. Elastic modulus is observed in the range from 220 psi to 3000 psi with more than 40 different mix designs.

Moreover, based on different applications, the investigation on other important properties such as tensile strength, heat and sound insulation, creep, fire resistance, and long-term durability is limited and not available for the public. In general, to some extent, waste paper content has a negative influence on most mechanical properties of concrete. However, the reduction seems to be acceptable and is affected by ingredients significantly. Some studies should be established to explore the potential use of papercrete as sustainable construction in Civil Engineering. In a word, although the concept of papercrete was proposed previously, the research on papercrete was still limited and incomplete. The main problems of the investigation on papercrete

concentrate on the lack of standards and have no systematic methodologies. Basing on existing research, the main issues which limit the application of papercrete involve three aspects:

1) Papercrete has a poor performance when it is soaked in the water.

2) The strength of papercrete is not as good enough as conventional concrete.

3) The application prospect is not clear because not all properties of papercrete are clarified and analysed. Papercrete is a promising lightweight concrete for a specific potential application.

2.6 Summary

Most research investigates the influence of natural fibre with concrete, the research of waste paper used in concrete is limited. Overall, there are different used schemes of waste paper (addition, replacement of raw materials). Studies involving waste paper fibre used in concrete have indicated several potential advantages by using waste paper fibre in concrete, such as density reduction, thermal properties, and resistance to freeze-thaw. Literature indicates there is no systematic mixing schemes for the proportion design of concrete with waste paper. Besides, for all most all studies, the mixing ratio is at a low level. Some literature presented the positive influence of lime used in concrete on the mechanical strength and durability of concrete. Additionally, there is no study investigating the environmental effect on the utilization of waste paper in concrete, the production and processing of waste paper should be defined and clarified to investigate the environmental credit of this recycled treatment.

Chapter 3 Experimental procedures

3.1 Introduction

In this chapter, firstly, the standards are determined based on the requirement of building blocks in ASTM (American Society for Testing Material) standards, the comparison of possibly applicable standards is made to clarify the rationality of standards selections. Accordingly, mixed proportions design and test standards relating to building blocks are adopted. The detailed experimental procedures aiming to investigate the properties of PB are designed based on the response surface method (RSM) in this study. The properties of PB include density, absorption, 7-day and 28-day compressive strength, softening coefficient, and thermal resistance. All experiment for all properties test mentioned above was conducted at the department of civil engineering of Xi'an Jiao-tong Liverpool University.

3.2 Standard selection

There are several standards involving building blocks so-called concrete masonry units (CMU) in ASTM standards, including ASTM C55[84], ASTM C90[85] and ASTM C129[86]. A brief comparison of involved standards is listed in Table 2. ASTM C55 only covers solid concrete building bricks with greater than 17.2 MPa of compressive strength. Considering the strength reduction of papercrete as the literature review described previously, it is difficult to satisfy this strength limitation. Similarly, even ASTM C90 covers the hollow masonry blocks, and the compressive strength should be greater than 13.8 MPa for an average of 3 blocks. ASTM C129 of non-loadbearing concrete masonry blocks was adopted to assign the requirement of PB. The standard specifics dimension requirement, the density classification, linear drying shrinkage

and strength requirement for both hollow and solid nonloadbearing concrete masonry blocks. The masonry blocks involve not only the conventional concrete mixture but also the concrete mixture with other alternative materials. Therefore, ASTM C129 was selected to access the properties of PB in this study. Requirements in ASTM C129 are listed in Table 3 to Table 5.

A set of tests were conducted to determine the properties of blocks. According to the requirement of CMU, the test project was determined and referring to the requirement of ASTM C140[87]. The oven-dry density, absorption, moisture, 7-day, and 28-day compressive strength were measured.

ASTM D7357[88] as a reference covers the minimum requirements for cellulose fibres used for fibre-reinforced concrete, and the limitations of using this standard are fibre categories only involve natural cellulose fibre. Although some properties are not included in the relevant ASTM standards, considering the high-water absorption of waste paper fibre, according to GB T 4111[89], the softening coefficient is taken into account.

Additionally, the thermal properties of PB, which is an advantage reported in the literature but without sufficient clarification, should be investigated. Thus the thermal transmission properties are measured by the heat flow meter apparatus according to ASTM C518[89] and ASTM C1058[90]. In fact, there are some optional standards in ASTM. ASTM C687[91], and ASTM C1363[92] and ASTMC 1045[93] are also used to measure the thermal properties of specific materials or structures. Due to the scope of application and the limitation of apparatus, ASTM C518 was adopted to measure the thermal transmission properties of PB. Additionally, the scope of ASTM C177 is to measure the steady-state heat flux through the flat, homogeneous

specimen(s) when their surfaces are in contact with solid, parallel boundaries held at constant temperatures using the guarded-hot-plate apparatus.

Table 2 The comparison of standards related to CMU available in ASTM.

Code of ASTM standard	Name of standards	Scope	
C55	Specification for concrete building brick	Solid, dry-cast, concrete building brick used for constructing structural masonry	Strength requirement is high
C90	Specification for loadbearing concrete masonry	Hollow and solid non-loadbearing concrete masonry units consisting of traditional raw materials.	Strength requirement is relatively low
C129	Specification for non-loadbearing concrete masonry		

Table 3 Requirements of Density classification

Density classification	The oven-dry density of concrete (average of three samples, lb/ft^3(kg/m^3))
Lightweight	Less than 105 (1680)
Medium Weight	105 to less than 125 (1680 to 2000)
Normal Weight	125 (2000) or more

Table 4 The compressive strength requirements for non-loadbearing concrete masonry units in ASTM.

Samples	Compressive strength (the mean value of net area) Min. psi (MPa)
Average of 3 units	600 (4.14)
Individual unit	500 (3.45)

According to the requirement of ASTM standards for generally no-load bearing concrete masonry, As the show in Table 3 to Table 5, all the requirement of non-load bearing masonry in ASTM.

Table 5 Requirements of dimensions with permissible variations.

	Limitation
Minimum face shell thickness	≥1/2 in (13 mm)
Differences for the overall dimension (width, height, and length)	±1/8 in (3.2 mm)

3.3 Materials

The desired PB in this study was designed by using the conventional concrete mixture design as a reference. There is a total of six ingredients used for PB manufacture. Part

physical properties of all these ingredients were measured according to the corresponding ISO and ASTM standards or achieved from local suppliers.

The ordinary Portland Cement was used in this study, namely CEM Ⅰ/42.5 cement in Fig. 13, complying with the requirement of Chinese standard, GB 8076[94]. The chemical analysis and physical properties were listed in Table 6, where the specific density was verified according to ASTM D1480[95], so that volume replacement in the proportion design. This type of cement is widely used for common purpose concrete and benefit for investigating the influence of additive on the concrete.

Table 6 Chemical constitutes and physical properties of cement.

Chemical analysis	%
SiO_2	22.89
Al_2O_3	4.54
FeO	3.47
CaO	61.98
MgO	2.06
SO_3	2.76
Na_2O	0.53
$Free\ CaO$	0.88
$Loss$	1.23
Cl^{-1}	0.022
Physical properties	
Density (kg/m^3)	3.14
Fineness ($0.08/\%$)	0.9
28-day compressive strength (MPa)	48.6

Table 7 The physical properties of aggregates used in the study.

Materials	Properties	Value
Coarse aggregate (crushed gravel)	Specific gravity (OD)	2.68
	Absorption (%)	0.70
	Dry bulk density (kg/m^3)	1512.30
Fine aggregate (river sand)	Specific gravity (OD)	2.64
	Fineness modulus	2.72
	Absorption (%)	0.50

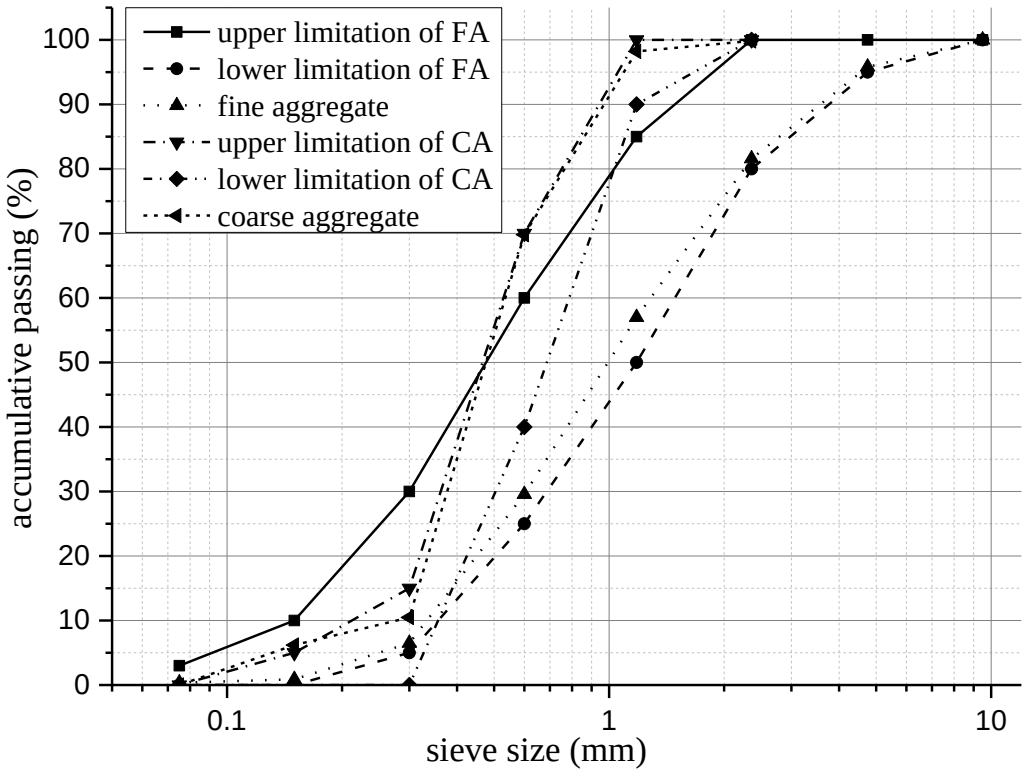

Fig. 9 The results of the sieve test with the limitation for fine and coarse aggregates.

Fig. 10 Gravel and sand used in the sieve test for building blocks.

Fine and coarse aggregates, including river sand and crushed gravel, was purchased from the local market in China. The properties of this sand and gravel are listed in Table 7, and especially the bulk density of crushed gravel measured was used to calculate quantities for the papercrete design. The sieve test was conducted according to ASTM C136-14[96] and the results, as Fig. 9 and Fig. 10 shown, complying with the grading requirement in ASTM C33[97]. The main physic properties were tested according to ASTM C127[98] and ASTM C128[99]. The specific gravity, water absorption and bulk density of this crushed gravel were 2.68, 0.7, and

1512.3 kg/m^3. The specific gravity, fineness modulus and water absorption of this river sand were 2.64, 2.72, and 0.5%, respectively.

Waste paper fibre (WPF) used in this study was commercially available, which was purchased from a millwork plant of the mineral products in China in Fig. 11. WPF adopted is made from a mixed source mainly consisting of newspaper, roll paper, book paper, etc. All fibres were bleached and cut into a short scale with an average length of 1.34 mm. The basic properties, including specific gravity, average dimensions, coarseness, and water retention value, were measured according to the corresponding standards as following content described. The average length and coarseness were tested according to the standards of the Technical Association of the Pulp and Paper Industry (TAPPI), namely T232[100], T233[101] and T234[102]. Additionally, there is no specific standard for testing the density or related properties of WPF and similar materials. Thus, the gravimetric pycnometer method, which is the same standard to fine and coarse aggregate, was used to measure the specific gravity according to ASTM C128. Properties of WPF are presented in Table 8. Considering the water absorption of WPF, water retaining value (WRV) was determined by using centrifugal method with and TAPPI Useful Method (UM) 256[103].

$$WRV = \frac{m_1 - m_2}{m_2} \times 100\% \quad (3\text{-}1)$$

where, m_1 is the total weight of centrifuged WPF, and m_2 is the weight of dried WPF.

Table 8 Physical properties of WPF.

Material	Properties	Values
Waste paper fibre (WPF)	Average length (μm)	1344
	Average width (μm)	24.4
	Coarseness (mg/m)	0.3269
	Water retention (g)	1.25
	Specific gravity	0.58

Fig. 11 Flocculent WPF used in the PB.

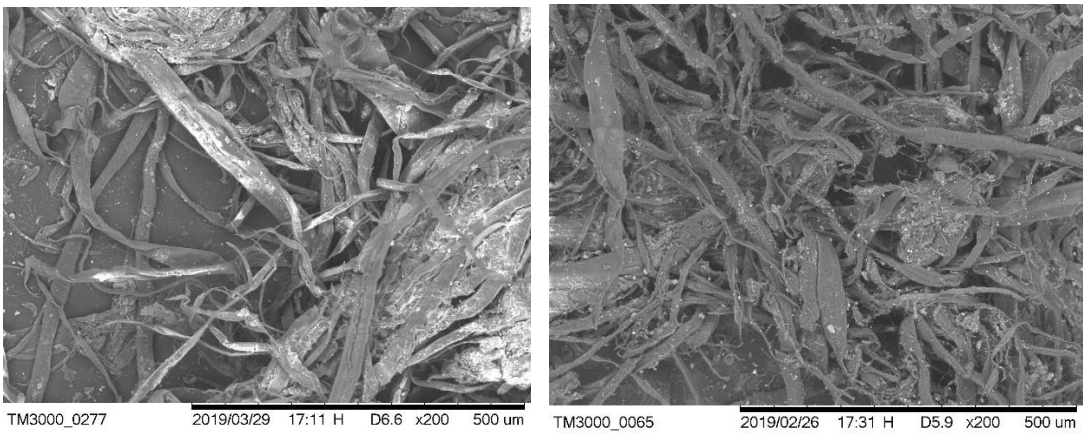

(a) Untreated WPF (b) WPF with treatment of Ca(OH)2

Fig. 12 SEM images of WPF with and without treatment at 500 of magnification.

Hydraulic lime adopted in this study was Natural Hydraulic Lime (NHL) purchased from Hessler Kalk Company in Fig. 13. There are two major reasons for the introduction of NHL into the papercrete. On the one hand, to adjust the alkaline environment of concrete for WPF and achieve the aim of treating the surface of WPF[82,104,105]. On the other hand, the environmental benefit is achieved due the simplified production process compared with cement[106]. The content of CaO is greater than 58% and bulk density is 0.78 kg/m^3, and this information is sourced from the supplier.

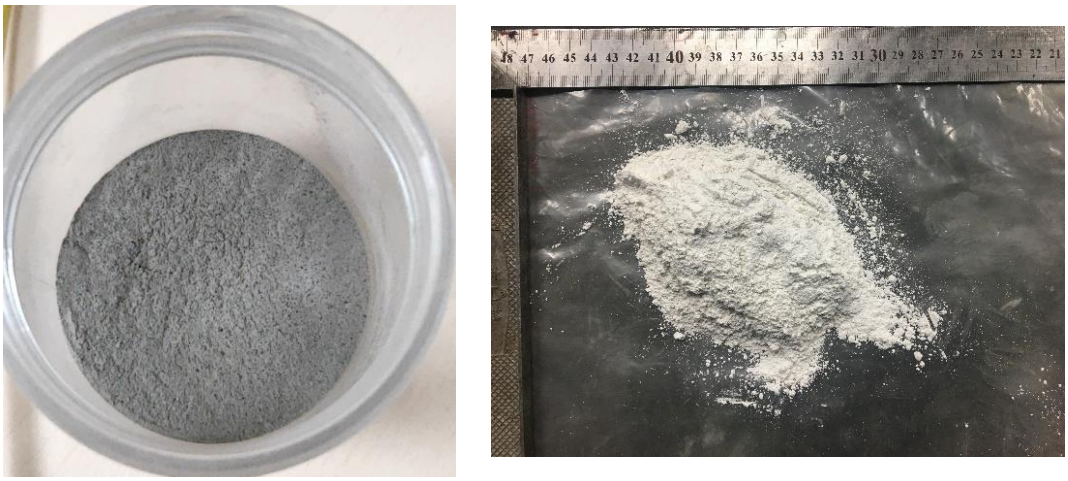

Fig. 13 Cement (left) and hydraulic lime (right) used in PB.

Superplasticizer was used to adjust water dosage and flowability (such as slump) of fresh concrete, and a polycarboxylate-based high-range water-reducer (HRWR) was adopted in the investigation as recommended in ACI 211[107] to achieve favourable workability.

3.4 Experimental design

3.4.1 Design of experiment

According to the requirement of concrete blocks with almost zero even less than zero slumps, the initial mix proportions of PB are determined according to ACI-211.3R (standards for the design of mix proportions of no-slump concrete)[108]. These standard addresses procedures of selecting mix proportions of expected concrete with the slump in the range of 0-25mm, especially including the guild of concrete masonry units. Considering the raw materials used and introduced previously, the center point of the experiment was determined in Table 9.

The influence and optimization of mix proportions for PB is required in this study, Response Surface Method (RSM) was adopted for Design of Experiment (DOE), which is a combination of the statistical and numerical method based on the least square method with the minimum error of meta-model, especially this method is typically

used to investigate the influence of multiple factors on interested responses, further, create and analyse the regression model[109]. RSM is also used for multi-objective optimization by specifying the limitations of independent variables or responses[110,111]. RSM is widely applied in a different field for reliability analysis or optimum design, such as agriculture, biology, food, chemistry, manufacturing, civil engineering and etc.[112–115].

RSM aims to establish the relationship between input variables and responses as Equation (3-2) shows, particularly if the independent variables are the linear function of response, and the approximate first-order model is presented in Equation (3-3)[116]:

$$y = f(x_1, x_2, \dots, x_k) + \in \tag{3-2}$$

$$y = \beta_0 + \sum_{i=1}^{k} \beta_i x_i + \in \tag{3-3}$$

where β_0 and β_i are the regression coefficients with $i = 1, 2, \dots, k$, x_i are the i'th independent variables and $\in$ is the error of the approximation model.

Moreover, in most cases, a higher-order model is more applicable, and the polynomial with a higher degree should be used if the approximate system is non-linear, or in other words the curvature occurring in the system, typically the form of quadratic polynomial models as a most common second-order model is presented:

$$y = \beta_0 + \sum_{i=1}^{k} \beta_i x_i + \sum_{i=1}^{k} \beta_{ii} x_i^2 + \sum_i \sum_j \beta_{ij} x_i x_j + \in \tag{3-4}$$

where especially $i < j$, x_i and x_j are the independent variables, β_i, β_{ii} and β_{ij} are the regression coefficients of the first degree, second degree, and cross degree, k is the number of effect factors. $\in$ is the model error, including both of measuring error and regress error.

Central Composite Design (CCD) was adopted in this study to ensure the uniformity of design. Central Composite Circumscribed (CCC) Design was used to achieve the rotatability of design. For general DoE procedures, the selection of the design points for the generation of the response surface is important. CCC design with two factors and three factors is illustrated in Fig. 14, which is more appropriate compared with Center Composite Face-centered design (CCF) design and Center Composite Inscribed (CCI) design. There are three types of design points, including cubic points, center points and axial points (start points). Particularly, the selection of star points is important to ensuring the orthogonality and rotatability make the predicted variance of all the star points is constant [109,117].

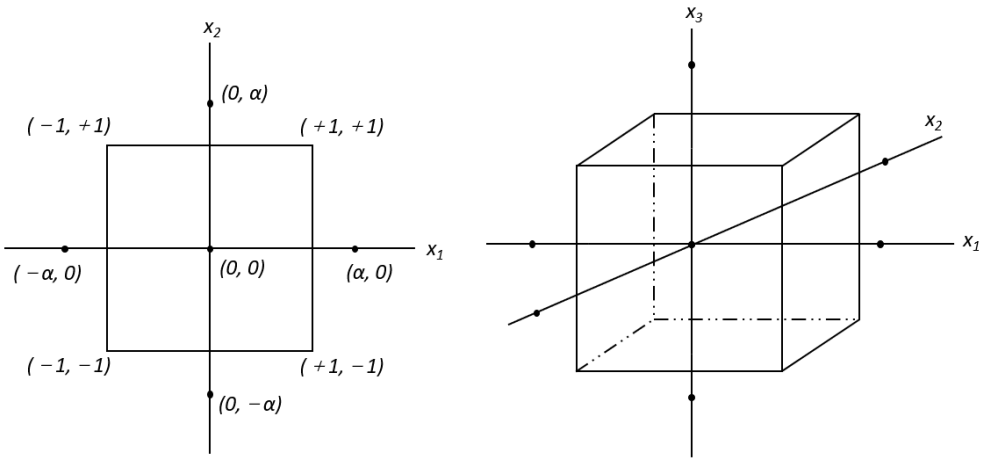

a) CCC design with k=2 b) CCC design with k=3

Fig. 14 The schematic diagram of CCC design.

In order to satisfy the rotatability for design, the level of star points is determined:

$$\alpha = {n_f}^{1/4} \tag{3-5}$$

$$n_f = 2^k \tag{3-6}$$

where, the α is distance to the center point, so-called star design point, n_f is the number of factorial points, k is the factor numbers.

Particularly, it is impossible to complete all the casting in one experiment since the amount of concrete block is a large quantity, the casting and test should be completed several times, blocking of experiment design are used to eliminate the error caused by potential factors, such as a difference of mixing condition on different dates. According to the requirement of blocking (approximately orthogonal between blocks), in this study, the experiment blocks was set to be 3 to reduce variation in regression coefficients.

Additionally, the data analysis for RSM should be conducted and discussed in the next section. Especial, Analysis of Variance (ANOVA) is conducted to evaluate the significance of each independent variable based on a P-value of 0.5%. The P-value of the major and the interaction terms, which are significant for the response, are less than 0.5%. Oppositely the terms with a p-value＞5% are insignificant for the statistic. Generally, only significant terms should be considered when establishing the predictive models. Finally, multiple objectives optimized design should be obtained and verified according to the developed models.

In this study, the proportion of the concrete mix is shown in Table 9. The independent variables of the designed proportion include w/c ratio, HL ratio, WPF-C and WPF-A. Particularly, HL is the cement replacement ratio by weight and is in the range from 0-10%. According to the relative research[55,56], WPF was not only used as an alternative material, also as aggregates introduced into concrete, thus two mixing schemes were adopted in this study. WPF WPF-C is the cement replacement ratio by weight using papercrete fibres and is ranging from 0-15% and WPF-A is the aggregates replacement ratio by volume in the range of 0-7%. Additionally, water reducing agent is used to adjust the workability of PB due to high water absorption

of WPF. Thus, the number of non-center points and center points is 24 and 3, respectively. RSM was adopted to investigate the influence of various mixing ratios of WPF and NHL on the PB.

An appropriate mix proportion based on zero slump concrete design is adopted as the lowest limitation of mix proportion. By using (central composites design) CCD, factors of mixing design with three levels were obtained as

Table 10 shows, where the code presents the standardized level of each factor and α is the axial point in the design of the experiment.

Table 9 The mix design of the concrete blocks as control group.

Raw materials	Cement	Gravel (coarse aggregate)	Sand (fine aggregate)	Water	Water reducing agent
Dosage (kg/m^3)	354.17	1238.57	626.77	170	5%

Table 10 Design of RSM factors.

Factors	Code	Levels of code				
		-α	-1.00	0	1.00	α
w/c ratio	X_1	0.38	0.43	0.48	0.53	0.58
HL ratio (%)	X_2	0	2.5	5	7.5	10
WPF-C ratio (%)	X_3	0	3.75	7.5	11.25	15
WPF-A ratio (%)	X_4	0	1.75	3.5	5.25	7

3.4.2 Mix design

The building blocks, namely CMU in ASTM, are the designed target; therefore, the prospective slump of fresh concrete should be as small as possible. The initial concrete mixing scheme was designed in accordance with ACI 211[107] as a control group. With the high replacement ratio, there are two schemes of replacement adopted in this study. WPF was not only used to replace the content of cement, also to substitute the aggregates in concrete. There is some literature exhibiting different mixing strategies as an alternative to cement or aggregate. The detailed mix design

was listed in Table 11. Especially some identifiable influence can result in variation of experimental results, such as the change of experimental data, or the change of the experimental environment, particularly the block is irrelevant with independent variables considered in the experiment. To remove this variation in mathematics, CCD is conducted in blocks design in Table 11.

Table 11 Actual design point and blocks for RSM design.

Block	Run of Experiment	Factor-1	Factor-2	Factor-3	Factor-4
		X_1: w/c	X_2: HL, (%)	X_3: WPF-C, (%)	X_4: WPF-A, (%)
Block-1	1	0.43	2.5	3.75	5.25
	2	0.53	7.5	3.75	5.25
	3	0.43	2.5	11.25	1.75
	4	0.53	2.5	3.75	1.75
	5	0.48	5	7.5	3.5
	6	0.53	7.5	11.25	1.75
	7	0.53	2.5	11.25	5.25
	8	0.43	7.5	3.75	1.75
	9	0.43	7.5	11.25	5.25
Block-2	10	0.43	2.5	3.75	1.75
	11	0.43	2.5	11.25	5.25
	12	0.48	5	7.5	3.5
	13	0.53	7.5	11.25	5.25
	14	0.53	2.5	3.75	5.25
	15	0.43	7.5	11.25	1.75
	16	0.53	2.5	11.25	1.75
	17	0.43	7.5	3.75	5.25
	18	0.53	7.5	3.75	1.75
Block-3	19	0.48	5	7.5	7
	20	0.48	5	15	3.5
	21	0.48	5	7.5	3.5
	22	0.58	5	7.5	3.5
	23	0.48	10	7.5	3.5
	24	0.48	5	7.5	0
	25	0.38	5	7.5	3.5
	26	0.48	0	7.5	3.5
	27	0.48	5	0	3.5

3.5 Preparation of specimens

3.5.1 Casing and mix procedures

During the procedures of mixing, to avoid non-uniform distribution of WPF in fresh concrete (considering the viscosity of fresh concrete and the density of WPF,

sedimentation and motion of WPF in concrete was perceived to be negligible), all dry ingredients were completely mixed in a mixer of 500kg capability for around 5 minutes in a mixer before adding water. Then tap water and superplasticizer were introduced and mixed with dry ingredients for around 5 minutes to achieve an acceptable condition. The temperature measured during the mixing process is less than 38° C.

In this study, PB were manufactured in steel moulds with 4000kN of forming pressure for the 30s by using brick making machine as Fig. 15 b) illustrated. Based on the requirement of ACI 211 and expected dimensions of PB were designed to be 200 mm ×200 mm×400 mm (widely used dimensions) with a hollow percentage of 33.28%, detailed configurations are listed in Table 12. Additionally, to satisfy the subsequent test requirement, including the oven-dry density, absorption, moisture and compressive strength test in ASTM C140, entire PB were adopted as prepared specimens for tests (The half of concrete blocks or blocks cut with a regular shape are acceptable in standards if considering the size of apparatus).

Table 12 Designed dimension of PB.

Length (mm)	Width (mm)	Height (mm)	Expected Net area (mm^2)	Hollow Percentage
400	200	200	47232	33.28%

Fig. 16 shows the process of fresh concrete mixing and manufactured blocks. After casting and forming, the fabricated PB were cured in the air at room temperature of 20±5° C and relative humidity of 40±5% until the day of the test.

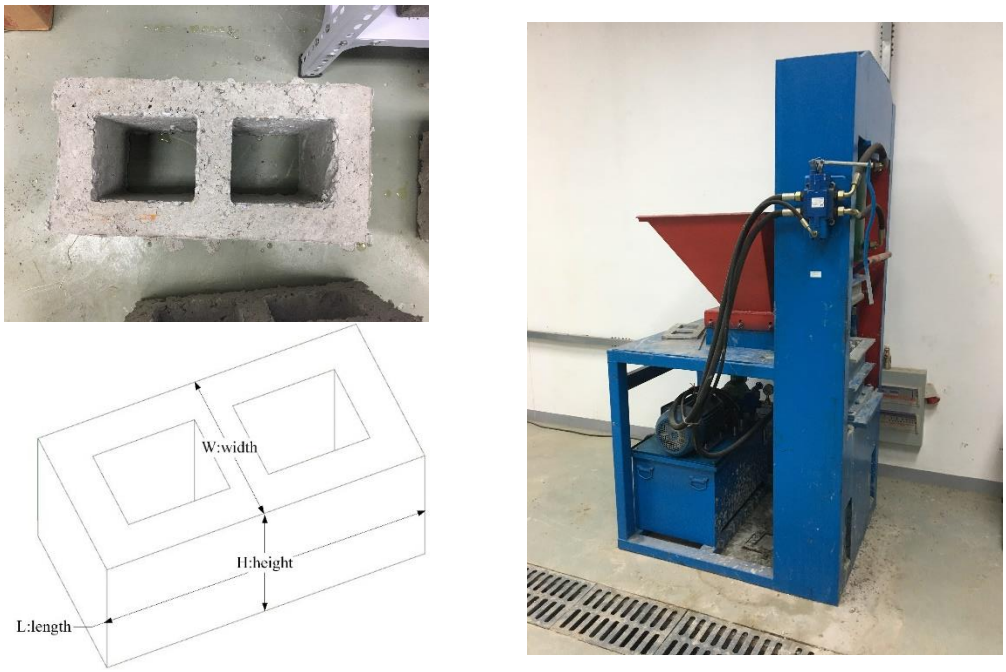

(a) profiles of PB (b) block making machine

Fig. 15 Dimensions of PB and block making machine for moulding.

Fig. 16 The concrete mixing and prepared blocks curing in room temperature.

3.5.2 General properties test

The oven-dry density, absorption and moisture were measured according to the requirement of ASTM C140[87]. Three samples of PB were prepared for these general properties test. After curing at 28 days with 20° C, specimens were completely immersed in water at a temperature of 15 to 27° C for 24 to 28 hours, then w_i of specimens immersed in water were weighed. w_s was measured after specimens were removed from the water, dried for 60±5s to remove the surface water. Subsequently, specimens were aeration-dried in an oven at 110±5° C for ≥24 hours,

w_d was recorded after completely dried. The calculation of indexes is presented in Equation (3-7) to (3-11)

$$Absorption, \% = 100 \times [(w_s - w_d)/w_d] \quad (3\text{-}7)$$

$$Moisture, \% = 100 \times [(w_r - w_d)/(w_s - w_d)] \quad (3\text{-}8)$$

$$Density, kg/m^3 = 1000 \times [w_d/(w_s - w_i)] \quad (3\text{-}9)$$

$$Net\ Volume\ (V_n), cm^3 = (w_s - w_i) \times 10^3 \quad (3\text{-}10)$$

$$Net\ Area\ (A_n), mm^2 = (V_n \times 10^3)/H \quad (3\text{-}11)$$

where: w_s is the saturated weight of PB, kg, w_d is the oven-dry weight of PB, kg, w_r is the received weight of PB, kg, w_i is the immersed weight of PB, kg, V_n is the net volume of PB, cm^3, A_n is the net area of PB, mm^2, H is the height of PB, mm.

3.5.3 Compressive strength test

According to ASTM C1552[118], high strength gypsum recommended (Compressive strength at 2 hours≥24.1 MPa) was used as a capping material that was required to ensure the surface applied the loaded flat during the strength test, the thickness of the gypsum cap is required to be less than 2 mm.

Fig. 17 shows the gypsum capping schematic and actual capping processes. The compressive strength tests were carried out following ASTM C140[87]. The hollow blocks with their hollow cores in a vertical direction were set up in a universal testing machine. Three samples of PB prepared were tested for each group at 28 days. The uniform rate of 2mm/min was applied on the top surface of blocks to meet the requirement of the test standard that ensures test duration in the range of 1 to 2 mins.

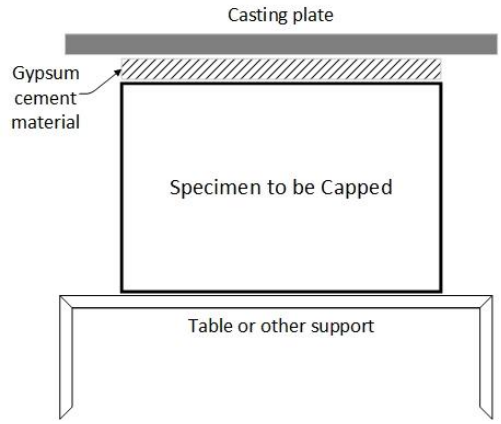

a) The schematic diagram of capping

b) Capping for PB in the lab.

c) The set-up of the compressive strength test for PB.

Fig. 17 Capping on the surface of PB and set-up of compressive strength test.

3.5.3 Softening coefficient

The experiment was conducted as GB T4111[89] required. A total of six specimens of PB are selected. Three specimens of PB were immersed in the water at 15-25° C for four days after curing, and the distance of specimens to the water should be greater than 20 mm. Then specimens were put on the shelf to drain water and wipe the surface of specimens to achieve the condition of saturated surface dry.

$$K_1 = \frac{f_1}{f} \tag{3-12}$$

where K_1 is softening coefficient, f_1 is the average compressive strength of 5 specimens with saturated surface dry, f is the average compressive strength of 5 specimens with air-seasoning.

3.5.4 Thermal properties test

The experiment of thermal properties was conducted according to ASTM C518. The configuration of the experimental set-up is illustrated in Fig. 18. The specimens were set between two plates, where one side and on the other side. The heat flow meter, as Fig. 19, was used to measure the heat flow through the PB, the thermal insulation materials used to avoid the dispassion of heat. As equation (3-13) and (3-14) shows, thermal conductivity and thermal resistance are typically used to evaluate the heat transfer performance to materials, and in some extent, these two parameters describe the equivalent performance-based different aspect[119], especially the thermal conductivity was adopted in this study.

$$\lambda_T = S \cdot E(\frac{L}{\Delta T}) \tag{3-13}$$

$$R_t = \frac{\Delta T}{S*A} \tag{3-14}$$

where, λ_T is the thermal conductivity of materials ($W/(m \cdot K)$), S is the calibration factor of the heat flux transducer ($W/(m^2V)$, E is heat flux transducer output (V), particularly, $S \cdot E$ is presented as heat flux in heat flow meter here, L is the distance between the two plate (m), ΔT is the temperature difference of two plate (K) and A is the area of heat source.

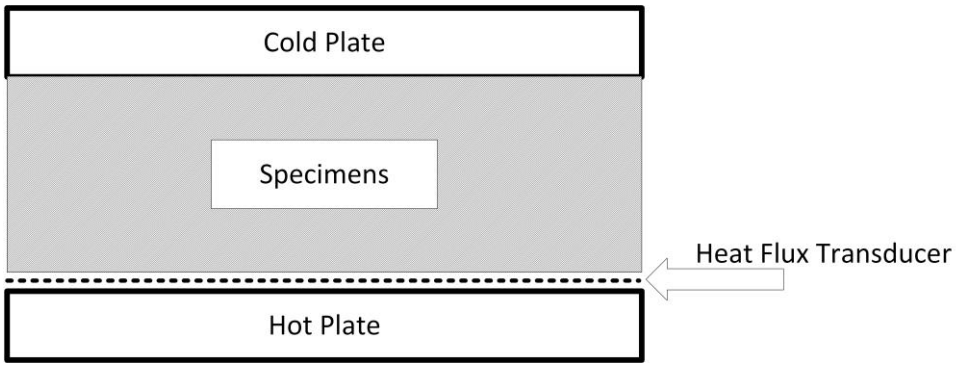

Fig. 18 Heat flow meter with one transducer and one specimen.

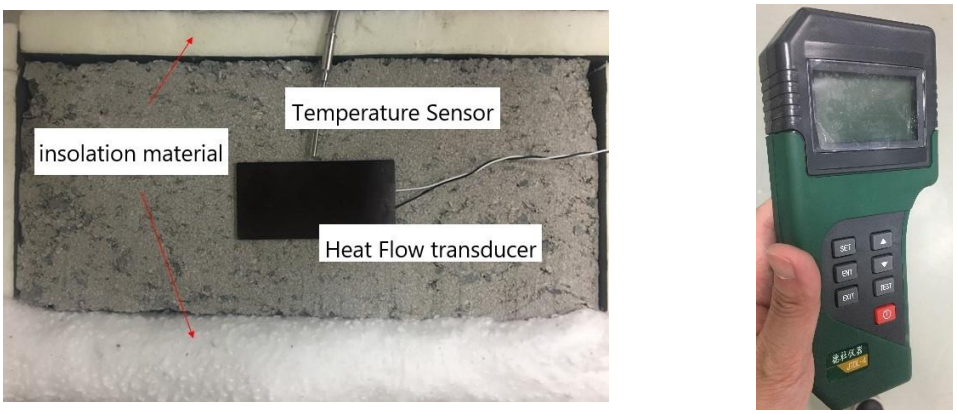

a) Set-up of a thermal transmission experiment b) Heat flow meter

Fig. 19 Thermal transmission experiment and apparatus.

3.5.5 Microstructure test

The SEM study was conducted to explore the interface change of WPF and PB with and without chemical treatment at the age of 28 days (air curing at room temperature). Fig. 20 illustrate that samples are cleaned and attached to the support, then placed in the SEM machine. The air in SEM machine is eliminated to be vacuum. Samples are scanned at various image magnification ranging from 50X to 4000X in order to achieve an appropriate image where the cement and WPF can be identified clearly.

In order to investigate the microstructure of PB, an analysis of a scanning electron microscope (SEM) images was conducted to explore the interface between the cement matrix and paper fibre. Small samples from four mixed design (experimental serial number 20, 21,23,26 and 27, as shown in Table 11) were prepared for SEM

scanning. Samples with and without surface coating were measured at various image magnification.

Fig. 20 Samples placed on the support and SEM used.

3.6 Summary

In this section, the relevant standards in ASTM for PB are considered and compared to select appropriate assessment standards and test standards. The density, water absorption, compressive strength and thermal transfer test in ASTM are determined to prepared, which are significant for the utilization of building concrete blocks. Additionally, considering the introduction of WPF, the moisture effect on the concrete blocks during the use stage are significant and there is no related standard in ASTM, thus the softening coefficient test in Chinese standard is used for test. Micro structure is selected to investigate the influence of WPF and NHL used in concrete block, where the mixing proportion with NHL and without NHL is prepared for this comparison. All the experimental processes, calculation and specimens preparation are described. Furthermore, RSM is not only used to investigate the influence of mixed proportion on the physical properties of PB, but also to achieve an optimized proportion.

Chapter 4 Experimental Results and Discussion

4.1 Response and analysis

In this chapter, all results of the experiment, including density, absorption, 7-day and 28-day compressive strength, softening coefficient and thermal conductivity of all blocks, are shown according to the corresponding test and results of tests are analysed based on ANOVA of RSM.

4.1.1 Response surface results of density

The unit's weight of PB is significant for concrete blocks, which effects the installation and transportation. The energy consumption can be saved by the reduction of the density of PB. Additionally, density is also relating to mechanical strength to some extent.

The reduction of the density is mainly caused by the addition of WPF. The experiments listed in Table 13 were conducted to indicate the influence of WPF fraction and HL fraction on the density of papercrete. The highest and lowest density of PB was measured to be 2204.85kg/m^3 and 1758.45kg/m^3, respectively. The maximum density of PB is greater than 2000 kg /m^3, which is a normal weight CMU. The minimum density is in the range of medium weight (1680 kg/m^3＜CMU＜2000 kg/m^3).

Table 13 Results of density in the experimental design matrix.

	Run of Experiment	X_1: w/c	X_2: HL, %	X_3: WPF-C, %	X_4: WPF-A, %	Density (kg/m^3)
Block-1	1	0.43	2.5	3.75	5.25	2065.33
	2	0.53	7.5	3.75	5.25	1968.90
	3	0.43	2.5	11.25	1.75	1941.30
	4	0.53	2.5	3.75	1.75	2029.13
	5	0.48	5.0	7.50	3.50	1930.55
	6	0.53	7.5	11.25	1.75	1834.62
	7	0.53	2.5	11.25	5.25	1763.71
	8	0.43	7.5	3.75	1.75	2183.02

	9	0.43	7.5	11.25	5.25	1857.33
Blcok-2	10	0.43	2.5	3.75	1.75	2189.78
	11	0.43	2.5	11.25	5.25	1878.92
	12	0.48	5.0	7.50	3.50	1933.39
	13	0.53	7.5	11.25	5.25	1774.87
	14	0.53	2.5	3.75	5.25	1940.79
	15	0.43	7.5	11.25	1.75	1945.30
	16	0.53	2.5	11.25	1.75	1838.79
	17	0.43	7.5	3.75	5.25	2069.91
	18	0.53	7.5	3.75	1.75	2049.42
Blcok-3	19	0.48	5.0	7.50	7.00	1833.34
	20	0.48	5.0	15.0	3.50	1758.45
	21	0.48	5.0	7.50	3.50	1940.55
	22	0.58	5.0	7.50	3.50	1856.64
	23	0.48	10	7.50	3.50	1948.23
	24	0.48	5.0	7.50	0.00	2010.08
	25	0.38	5.0	7.50	3.50	2013.09
	26	0.48	0.0	7.50	3.50	1897.00
	27	0.48	5.0	0.00	3.50	2204.85

The P-value and F-value are derived from ANOVA, which is used to clarify the level of significance of both major factors and interactive terms. Specifically, F-value based on the Fisher test is used to compare the data's mean square to the residual mean square, and P-value (Prob＞F) is the probability of model hypothesis failure. A high-value of P-value indicates the invalidation of the hypothesis. Terms with P-values ≤0.05 are considered to have a great influence on the responses. However, terms with P-value＞0.05 are supposed to be statistically insignificant. Residual indicating lack of fit means the amount the predictive models miss the observation, which is the difference between the actual and predicted value for all designed points[120,121]. Table 14 shows the average values of tree samples of PB based on the density test results. The F-value for this initial quadratic model is 76.67, indicating the significance of this model, and there is only a 0.01% chance that the F-value this large could occur due to noise.

The 95% confidence interval (CI) is used to determine the significance of terms, and as a previous discussion, the model terms with P＜0.05 are significant. In this case of the density, the significance of these quadratic model terms can be ascertained, specifically X_1, X_2, X_3, X_4 and X_3^2 are significant, indicating the model and these terms have a vital influence on the density of PB, while insignificant terms (including X_1X_2, X_1X_3, X_1X_4, X_2X_3, X_3X_4, X_1^2, X_2^2 and X_4^2) indicate that the influence of these terms and interactions is not remarkable or even negligible.

To achieve the predicted function, the insignificant terms are removed from the initial model and the criterion of simplification is set to be Adj.R2 of model⩾0.85. The reduced quadratic model with an F-value of 193.46 and P-value＜0.0001, implying the significance of this modified model. Accordingly, R^2 (0.9876), $Adj.R^2$(0.9825), $Pre.R^2$(0.9673) and $Adeq.precision$(42.249) from the ANOVA table is listed in

Table 15, which is greater than 0.85, namely reliable. $Adj.R^2$ is A measure of the amount of variation around the mean explained by the model, adjusted for the number of terms in the model. The $Adj.R^2$ decreases as the number of terms in the model increase if those additional terms don't add value to the model. $Pre.R^2$ is A measure of the amount of variation in new data explained by the model. $Adeq.precision$ measures the signal to noise ratio, when the ratio greater than 4 is desirable. Consequently, this model can be used to guide the design space.

The prediction modified equation in terms of actual factors is obtained at the end of the analysis, as Equation (4-1) presented:

$$Density = 2941.273 - 1308.693X_1 + 2.301X_2 - 64.969X_3 - 33.543X_4 + 36.318X_1X_3 + 1.155X_3X_4 + 1.001X_3^2 \quad (4\text{-}1)$$

Table 14 ANOVA for response surface of density based on the quadratic model.

Source	Sum of Squares	Degree of Freedom (Df)	Mean Square	F-Value	P-value
Block	1480.14	2	740.07		
Model	3.908E+005	14	27917.57	76.67	< 0.0001
X_1: w/c	64436.23	1	64436.23	176.96	< 0.0001
X_2: HL (%)	794.49	1	794.49	2.18	0.1704
X_3: WPF-C (%)	2.718E+005	1	2.72+005	746.54	< 0.0001
X_4: WPF-A (%)	45508.91	1	45508.91	124.98	< 0.0001
X_1X_2	352.95	1	352.95	0.97	0.3481
X_1X_3	741.93	1	741.93	2.04	0.1839
X_1X_4	443.43	1	443.43	1.22	0.2956
X_2X_3	201.75	1	201.75	0.55	0.4738
X_2X_4	4.95	1	4.95	0.014	0.9095
X_3 X_4	918.63	1	918.63	2.52	0.1433
X_1^2	192.74	1	192.74	0.53	0.4836
X_2^2	0.067	1	0.067	1.85E-004	0.9894
X_3^2	4611.87	1	4611.87	12.67	0.0052
X_4^2	1.71	1	1.71	4.69-003	0.9468
Residual	3641.35	10	364.13		
Cor Total	3.960E+005	26			

Table 15 Reduced Quadratic Model fitting results for the RSM analysis of density.

Response	R^2	$Adj.R^2$	$Pred.R^2$	$Adeq.Precision$	SD	Mean
Density (kg/m^3)	0.9876	0.9825	0.9673	42.249	16.96	1950.27

Fig. 21 indicates interactions between significant variables on the destiny of PB, and only the significant interactive terms are illustrated. Within the defined range, it is clear that the increase of w/c and the amount of WPF decrease the density of PB, except for the HL ratio. According to the results from Khedari et al.[122] , the density of concrete by introducing flexible fibre (such as cellulose fibre or natural fibre) achieved a slight reduction due to the generation of more void in concrete. A similar tendency is achieved in this study, and the density of concrete by introducing cellulose fibre decreases as Fig. 22 (3-dimensional response surface plot of density with corresponding variables) shows. Fig. 22 illustrates the relationship between the response (density of PB) and independent variables. On the one hand, Fig. 22 (a)

indicates the influence of HL on density is more significant with a low w/c ratio than that of HL on density with a high w/c ratio. Furthermore, the influence of HL on density is negligible when the w/c ratio is low. The interactions between HL and WPF is limited, which probably indicates the improvement of the interface between WPF and aggregates in the concrete is limited and there are no remarkable interactions between HL and WPF.

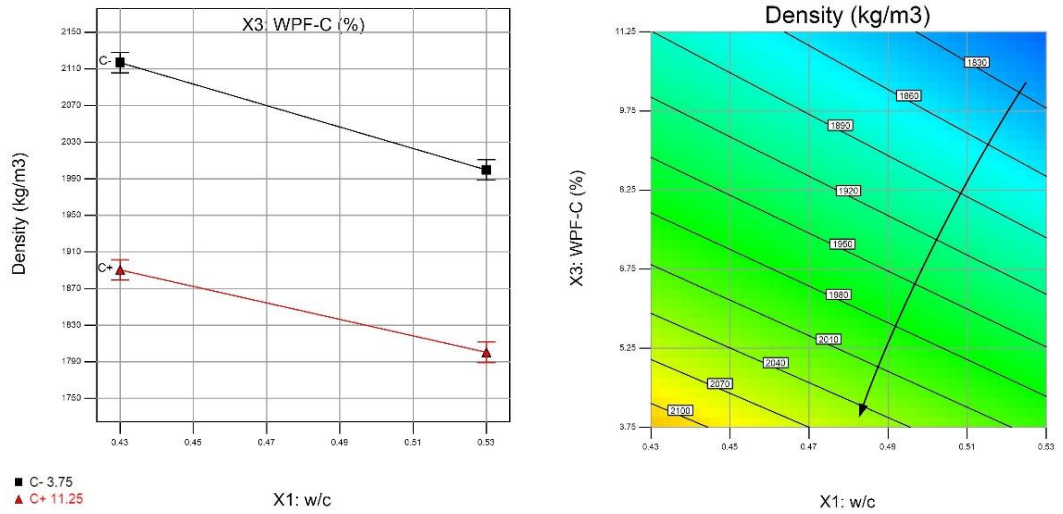

a) Interactive effects of w/c and WPF-C on softening coefficient (HL is 5% and WPF-A is 3.5%)

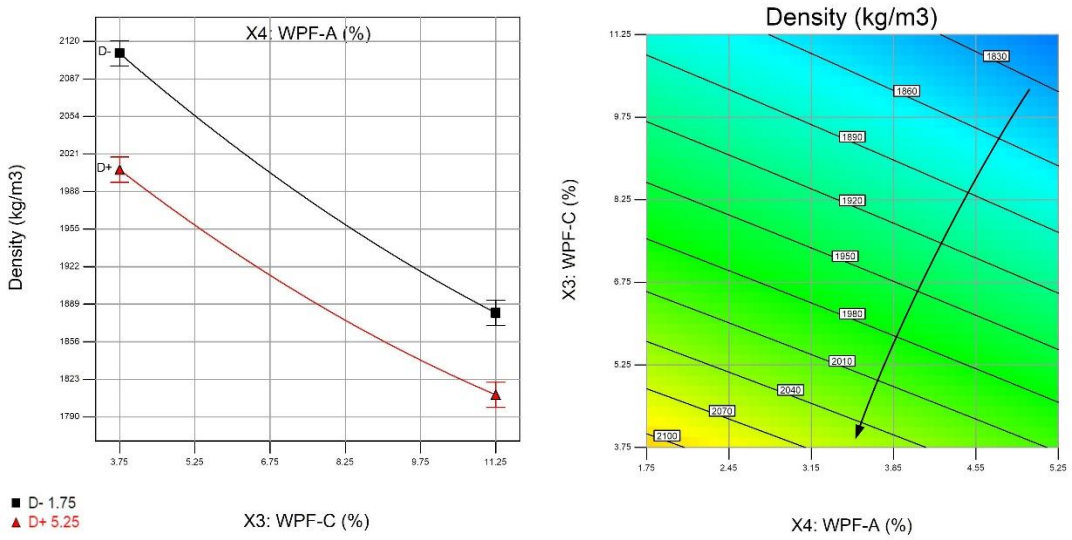

b) Interactive effects of WPF-A and WPF-C on softening coefficient (w/c is 0.48 and HL is 5%)

Fig. 21 Interaction effects of significant variables on the density of PB.

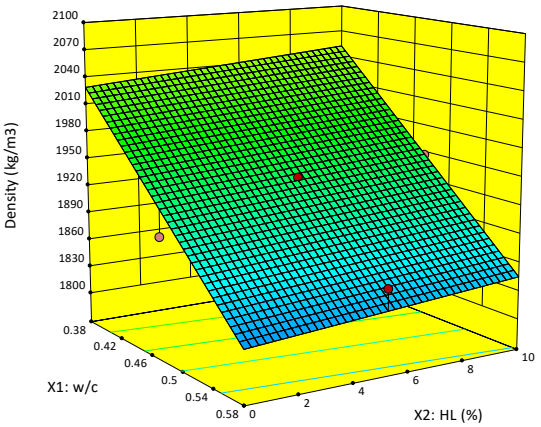

(a) Relationship between w/c, HL (%), and density (WPF-C=7.5% and WPF-A=3.5%)

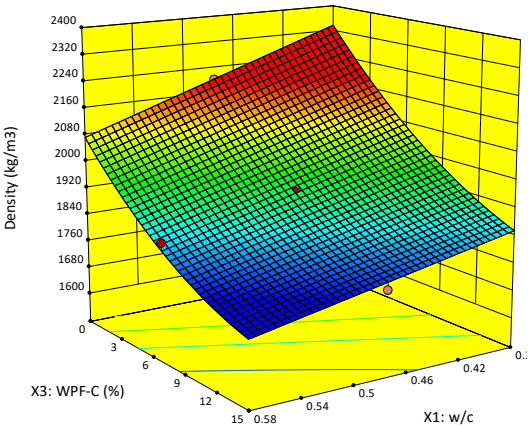

(b) Relationship between w/c, WPF-C (%), and density (WPF-A=3.5% and HL=5%)

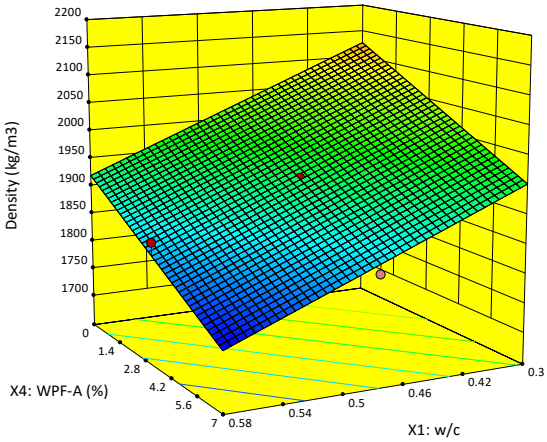

(c) Relationship between w/c, WPF-A (%), and density (WPF-C=7.5% and HL=5%)

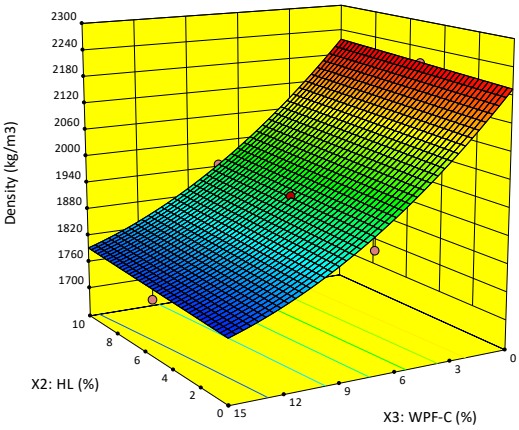

(d) Relationship between HL (%), WPF-C (%), and density (w/c=0.48 and WPF-A=3.5%)

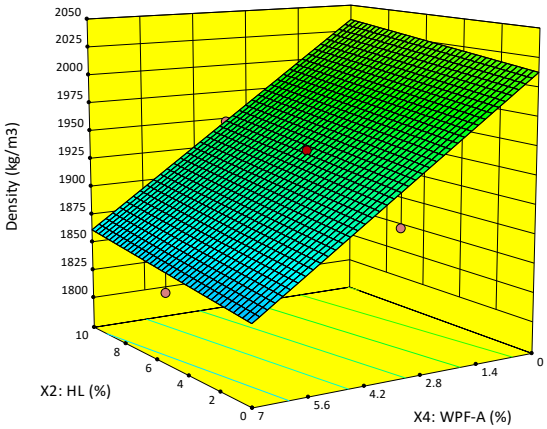

(e) Relationship between HL, WPF-A (%), and density (w/c=0.48 and WPF-C=7.5%)

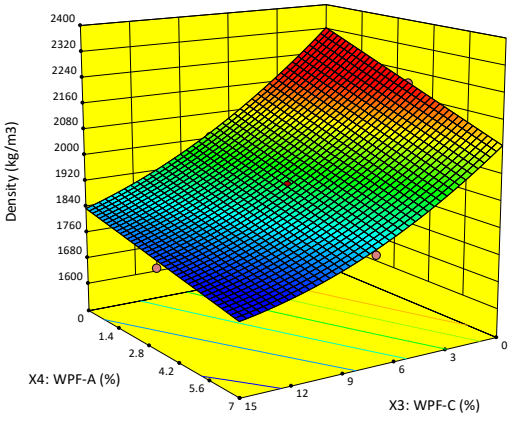

(f) Relationship between WPF-C (%), WPF-A (%) and density (w/c=0.48 and HL=5%)

Fig. 22 The interaction of each independent variable for density.

4.1.2 Response surface results of water absorption

According to the water absorption tests conducted previously, water absorption values of PB are listed in Table 16 in the form of RSM design. The maximum of water

absorption is 20.16%, with 0.48 of w/c, 5% of HL, 15% of WPF-C and 3.5% of WPF-A. The minimum of water absorption is 5.17%, when the factors (w/c, HL, WPF-C and WPF-A) is 0.48, 5%, 0% and 3.5%, respectively.

Table 16 Results of water absorption in the experimental design matrix.

	Run of Experiment	X_1: w/c	X_2 HL, %	X_3: WPF-C, %	X_4: WPF-A, %	Water Absorption, %
Block-1	1	0.43	2.5	3.75	5.25	11.31
	2	0.53	7.5	3.75	5.25	12.00
	3	0.43	2.5	11.25	1.75	13.62
	4	0.53	2.5	3.75	1.75	9.39
	5	0.48	5	7.5	3.5	14.26
	6	0.53	7.5	11.25	1.75	16.83
	7	0.53	2.5	11.25	5.25	18.67
	8	0.43	7.5	3.75	1.75	6.18
	9	0.43	7.5	11.25	5.25	15.74
Blcok-2	10	0.43	2.5	3.75	1.75	6.68
	11	0.43	2.5	11.25	5.25	15.95
	12	0.48	5	7.5	3.5	13.93
	13	0.53	7.5	11.25	5.25	17.82
	14	0.53	2.5	3.75	5.25	13.47
	15	0.43	7.5	11.25	1.75	12.37
	16	0.53	2.5	11.25	1.75	17.07
	17	0.43	7.5	3.75	5.25	7.35
	18	0.53	7.5	3.75	1.75	8.73
Blcok-3	19	0.48	5	7.5	7	15.95
	20	0.48	5	15	3.5	20.16
	21	0.48	5	7.5	3.5	14.60
	22	0.58	5	7.5	3.5	16.16
	23	0.48	10	7.5	3.5	13.32
	24	0.48	5	7.5	0	10.58
	25	0.38	5	7.5	3.5	9.75
	26	0.48	0	7.5	3.5	15.15
	27	0.48	5	0	3.5	5.17

Similarly, to access the effect of each independent variable and interactive terms on water absorption based on P-value, the significant terms of water absorption are determined as Table 17 shows. Table 17 indicates the significant terms include the model function, X_1, X_2, X_3, X_4, X_1^2, X_3^2 and X_4^2, while based on the same consideration, $\mathrm{X_1X_2}$, $\mathrm{X_1X_3}$, $\mathrm{X_1X_4}$ and $\mathrm{X_2^2}$ are insignificant, thus to ensure

$Adj.R^2$ of each term⩾0.85, the reduced quadratic model is obtained as Equation (4-2) :

$$\text{Water Absorption} = -49.611 + 180.776X_1 - 0.223X_2 + 1.441X_3 + 2.099X_4 + 0.027X_2X_3 - 0.055X_2X_4 - 0.046X_3X_4 - 155.663X_1^2 - 0.0328X_3^2 - 0.102X_4^2 \quad (4\text{-}2)$$

Table 17 ANOVA for response surface of water absorption based on the quadratic model.

Source	Sum of Squares	Df	Mean Square	F-Value	P-value
Block	3.16	2	1.58		
Model	407.32	14	29.09	69.92	< 0.0001
X_1: w/c	58.93	1	58.93	141.63	< 0.0001
X_2: HL (%)	6.82	1	6.82	16.39	0.0023
X_3: WPF-C (%)	286.60	1	286.60	688.80	< 0.0001
X_4: WPF-A (%)	43.12	1	43.12	103.64	< 0.0001
X_1X_2	0.46	1	0.46	1.10	0.3195
X_1X_3	0.028	1	0.028	0.066	0.8021
X_1X_4	0.15	1	0.15	0.37	0.5580
X_2X_3	1.02	1	1.02	2.45	0.1484
X_2X_4	0.92	1	0.92	2.21	0.1678
X_3 X_4	1.47	1	1.47	3.53	0.0897
X_1^2	3.83	1	3.83	9.21	0.0126
X_2^2	0.23	1	0.23	0.56	0.4726
X_3^2	5.25	1	5.25	12.62	0.0052
X_4^2	2.56	1	2.56	6.16	0.0324
Residual	4.16	10	0.42		
Cor Total	414.65	26			

Table 18 shows the fitting indexes, and the Pred.R^2 of 0.9497 is in reasonable agreement with the Adj.R^2 of 0.979, where the difference is less than 0.2. These indexes indicate the reduced quadratic model is reliable. Additionally, $Adeq.Precision$ of 33.325 indicates an adequate signal, within the range of satisfaction.

Table 18 Model fitting results for the RSM analysis of water absorption.

Response	R^2	$Adj.R^2$	$Pred.R^2$	$Adeq.Precision$	SD	Mean
Density	0.9878	0.979	0.9497	33.325	0.6	13.04

Fig. 23 shows the interactions of significant terms on the water absorption of PB. In Fig. 23 a) water absorption decreases gradually at 0.48 of w/c and 3.5% of WPF-A when WPF-C is in the high level of replacement ratio, while water absorption decreases remarkably with low replacement ratio level of WPF-C. Diagram b) in Fig. 23 shows there is the positive effect of decreasing WPF-A on water absorption when WPF-A decreases from 5.25% to 1.75% at 0.48 of w/c and 7.5% of WPF-C. Diagram c) in Fig. 23 indicates the synergistic effect of WPF-A and WPF-C on water absorption of PB, and the 2-dimensional contour in Diagram c) demonstrates the change of the gradient of water absorption is inapparent.

As Fig. 24 shown, the 3-D response surface plots illustrate the relationship between each variable, including w/c, HL (%), WPF-A (%), WPF-C (%) and water absorption. Fig. 24 (a)-(f) shows the change of response (water absorption) is influenced by the relationship of each factor, the range of factors is w/c (0.38-0.58), HL ratio (0-10%), WPF-C ratio (0-15%) and WPF-A ratio (0-7%), respectively, with other parameters at a central point for each correlation group (particularly HL ratio of 3.5% for each group). Furthermore, as a comparison of Fig. 29 (a)-(f), the increase of WPF-C, WPF-A and w/c increase the water absorption capability of PB. Compared to WPF-A and w/c, WPF-C makes a more significant contribution to water absorption. Specifically, the increase of water absorption caused by w/c is due to the void content expansion generated in concrete, while the increase of water absorption caused by WPF-C and WPF-A is owing to the high water absorption capability of WPF. In addition, the positive effect of HL on water absorption is remarkable when w/c is high. It is possible to due to the improvement of interface with other materials and decrease the voids in concrete. Moreover, the effect of WPF-C is most significant.

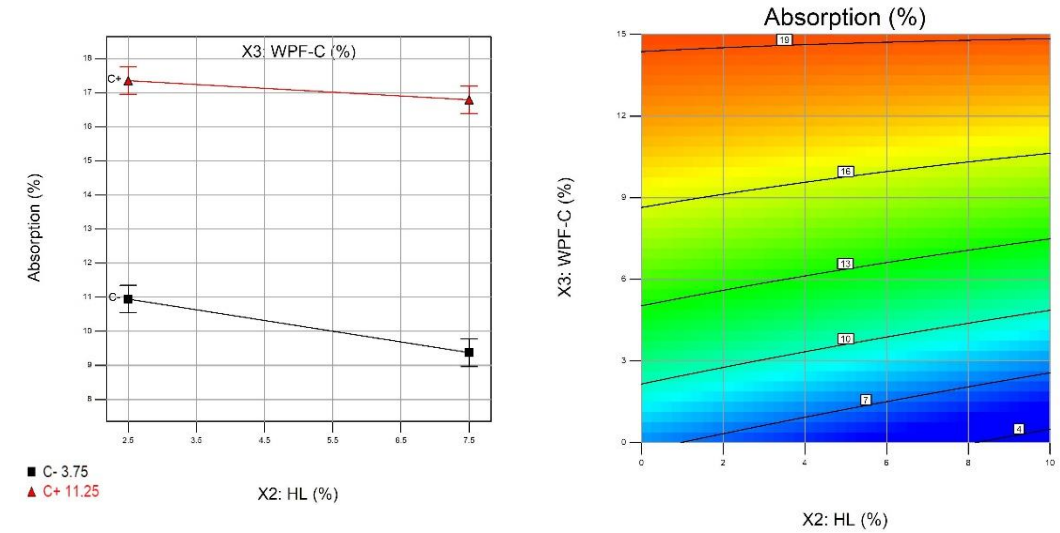

a) Interactive effects of HL and WPF-C on water absorption (w/c is 0.48 and WPF-A is 3.5%)

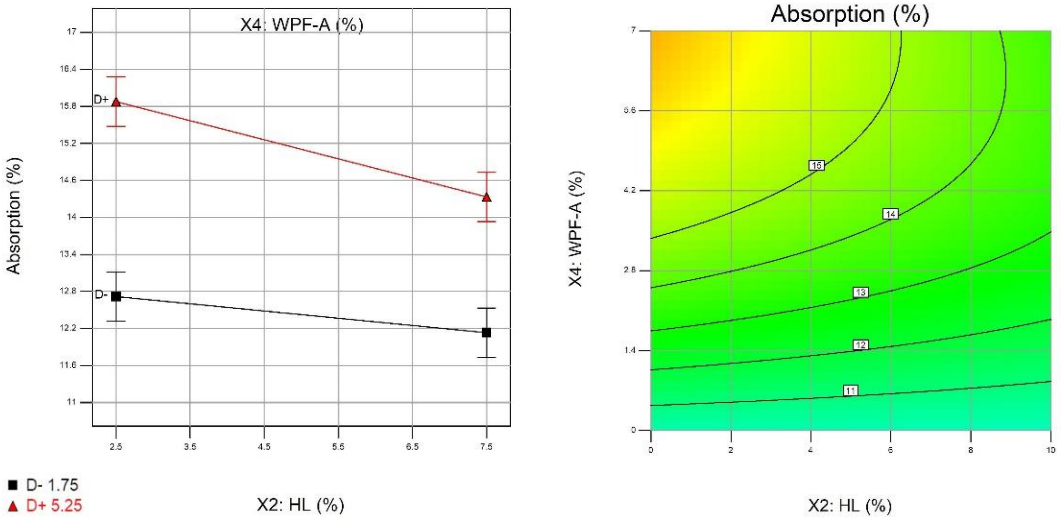

b) Interactive effects of HL and WPF-A on water absorption (w/c is 0.48 and WPF-C is 7.5%)

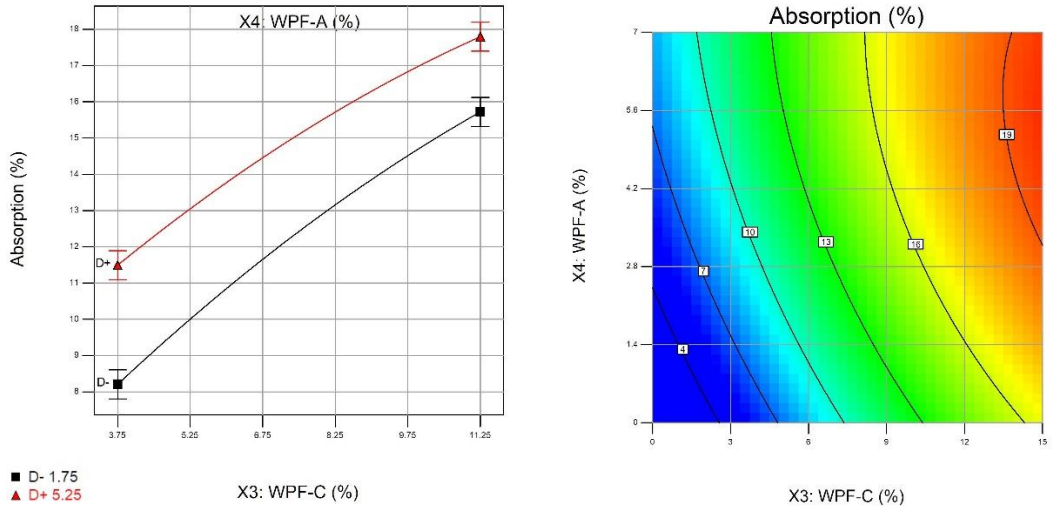

c) Interactive effects of WPF-C and WPF-A on water absorption (w/c is 0.48 and HL is 5%)

Fig. 23 Interaction effects of significant variables on water absorption.

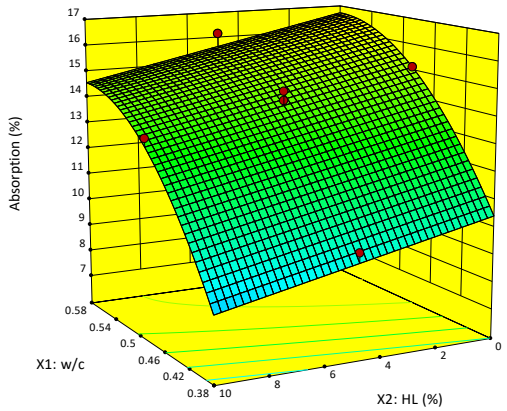

a) Relationship between w/c, HL (%), and water absorption (WPF-C=7.5% and WPF-A=3.5%)

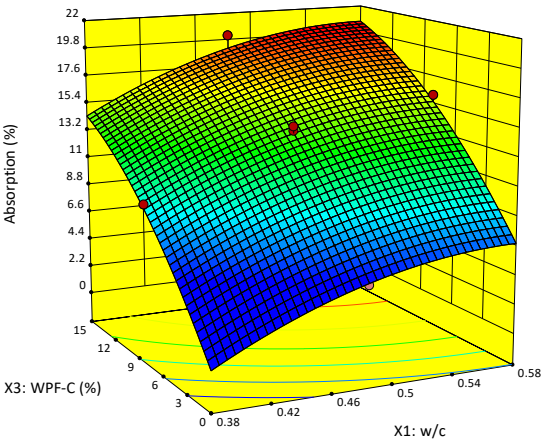

b) Relationship between w/c, WPF-C (%), and water absorption (WPF-A=3.5% and HL=5%)

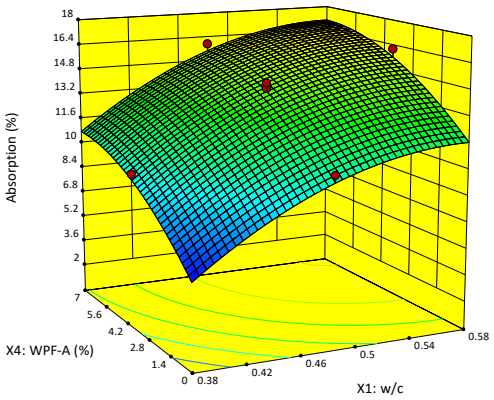

b) Relationship between w/c, WPF-A (%), and water absorption (WPF-C=7.5% and HL=5%)

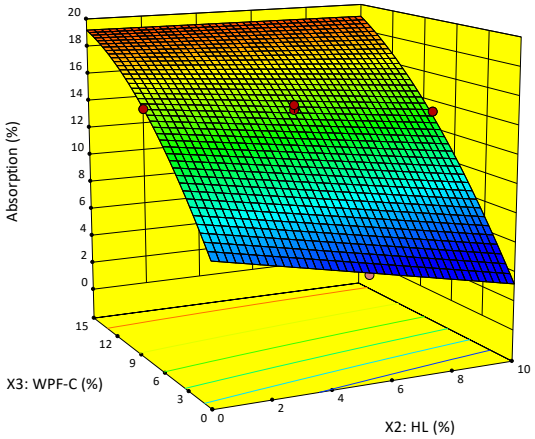

b) Relationship between w/c, WPF-C (%), and water absorption (WPF-A=3.5% and HL=5%)

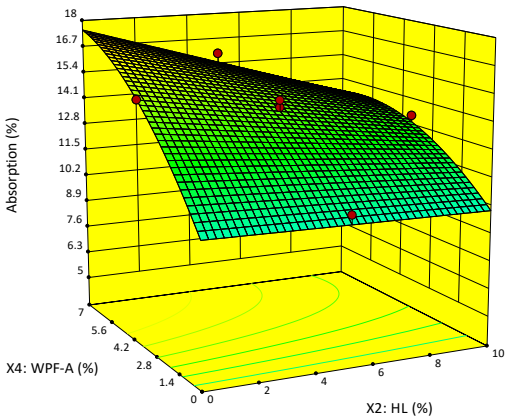

b) Relationship between w/c, WPF-C (%), and water absorption (WPF-A=3.5% and HL=5%)

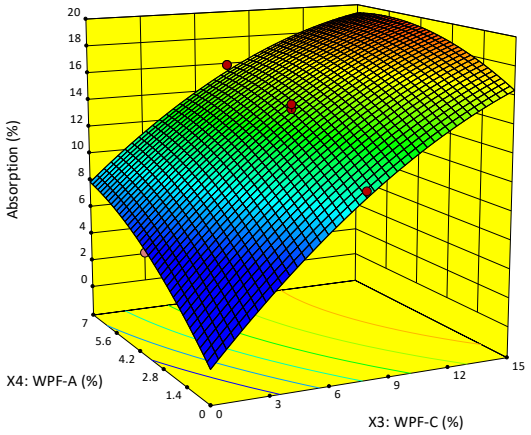

b) Relationship between w/c, WPF-C (%), and water absorption (WPF-A=3.5% and HL=5%)

Fig. 24 The interaction of each independent variable for absorption.

4.1.3 Response surface results of 7-day and 28-day compressive strength

Fig. 25 shows the failure specimens after the compressive strength test. The main crack occurs near the middle web of PB, which means the fracture first appears in the middle and then affect the surrounding area where several minor cracks observed at other positions.

Fig. 25 Typically tested papercrete sample under compression.

Table 19 shows the results of the 7-day and 28-day compressive strength of PB with corresponding proportion factors and levels. In the range of design space, the maximum of 7-day compressive strength is 6.46 MPa when w/c, HL (%), WPF-C (%) and WPF-A is 0.48, 5%, 0% and 3.5%, respectively. The minimum compressive strength at 28 days is 2.01 MPa with 0.48 of w/c, 5% of HL (%), 15% of WPF-C (%) and 3.5% of WPF-A (%). The maximum compressive strength at 28 days is 8.07 MPa with 0.48 of w/c, 5% of HL, 0% of WPF-C and 3.5% of WPF-A. The minimum compressive strength at 28 days is 2.95 MPa with 0.48 of w/c, 5% of HL, 15% of WPF-C and 3.5% of WPF-A.

Table 19 Results of compressive strength in the experimental design matrix.

	Run of Experiment	X_1: w/c	X_2 HL, %	X_3: WPF-C, %	X_4: WPF-A, %	7-day compressive strength, MPa	28-day compressive strength, MPa
	1	0.43	2.5	3.75	5.25	4.92	6.21
	2	0.53	7.5	3.75	5.25	4.66	5.92
	3	0.43	2.5	11.25	1.75	3.86	5.51
	4	0.53	2.5	3.75	1.75	4.92	6.35
Block-1	5	0.48	5	7.5	3.5	4.11	5.5
	6	0.53	7.5	11.25	1.75	2.95	4.07
	7	0.53	2.5	11.25	5.25	2.11	3.05
	8	0.43	7.5	3.75	1.75	5.92	7.71
	9	0.43	7.5	11.25	5.25	3.32	4.83
	10	0.43	2.5	3.75	1.75	5.37	7.05
	11	0.43	2.5	11.25	5.25	3.15	4.51
	12	0.48	5	7.5	3.5	4.00	5.38
	13	0.53	7.5	11.25	5.25	2.32	3.31
Blcok-2	14	0.53	2.5	3.75	5.25	4.19	5.53
	15	0.43	7.5	11.25	1.75	4.08	5.81
	16	0.53	2.5	11.25	1.75	2.65	3.81
	17	0.43	7.5	3.75	5.25	5.14	6.84
	18	0.53	7.5	3.75	1.75	5.00	6.67
	19	0.48	5	7.5	7	2.97	4.01
	20	0.48	5	15	3.5	2.01	2.95
	21	0.48	5	7.5	3.5	3.90	5.3
	22	0.58	5	7.5	3.5	3.08	4.22
Blcok-3	23	0.48	10	7.5	3.5	4.05	5.56
	24	0.48	5	7.5	0	4.51	6.25
	25	0.38	5	7.5	3.5	4.52	6.28
	26	0.48	0	7.5	3.5	3.56	5.01
	27	0.48	5	0	3.5	6.46	8.07

Table 20 and Table 21 show the summarized results of ANOVA for the responses of 7-day and 28-day compressive strength. The F-value of the 7-day and 28-day compressive model is 117.59 and 85.07, respectively. According to similar reasons as mentioned before, for both 7-day and 28-day compressive strength, the insignificant terms include X_1X_2, X_1X_4, X_2X_3, X_2X_4, X_3X_4, X_1^2, X_2^2 and X_4^2 which can be removed, while the significant terms are X_1, X_2, X_3, X_4, X_1X_3 and X_3^2.

Based on the settings of $Adj.R^2 > 0.15$, in consequence, the reduced quadratic model is obtained as Equation (4-3) and (4-4), the F-value of the modified models of

7-day and 28-day compressive strength is 354.36 and 263.24, respectively. These two reduced quadratic models are significant.

Table 22 and Table 23 show the rationality of the obtained models. For 7-day compressive strength, the $Adj.R^2$ of 0.9712 is in reasonable agreement with the $Pred.R^2$ of 0.9888, since the difference between these two indexes is less than 0.2. Moreover, a desirable value of $Adeq.Precision$ (58.228) indicates an adequate signal, which means the model is predictable for the design space. For 28-day compressive strength, the $Adj.R^2$ of 0.9595 is in reasonable agreement with the $Pred.R^2$ of 0.9850. $Adeq.Precision$ achieves a desirable value, 49.418＞4.

$$P_7(7\_day\ compressive\ strength) = 8.523 - 3.69X_1 + 0.054X_2 - 0.093X_3 - 0.191X_4 - 0.6X_1X_3 + 0.007X_3^2 \quad (4\text{-}3)$$

$$P_{28}(28\_day\ compressive\ strength) = 10.342 - 3.867X_1 + 0.071X_2 + 0.116X_3 - 0.268X_4 - 1.027X_1X_3 + 0.005X_3^2 \quad (4\text{-}4)$$

Table 20 ANOVA for response surface of 7-day compressive strength based on the quadratic model.

Source	Sum of square	Df	Mean Square	F-value	P-value
Block	0.165	2	0.082		
Model	32.860	14	2.347	117.59	＜0.0001
X_1: w/c	4.025	1	4.025	201.65	＜0.0001
X_2: HL (%)	0.432	1	0.432	21.63	0.000907
X_3: WPF-C (%)	25.179	1	25.179	1261.44	＜0.0001
X_4: WPF-A (%)	2.672	1	2.672	133.85	＜0.0001
X_1X_2	0.001	1	0.001	0.05	0.835381
X_1X_3	0.203	1	0.203	10.15	0.009721
X_1X_4	0.013	1	0.013	0.64	0.44289
X_2X_3	0.011	1	0.011	0.56	0.47066
X_2X_4	0.000	1	0.000	0.02	0.879626
X_3X_4	0.007	1	0.007	0.35	0.569543
X_1^2	0.017	1	0.017	0.84	0.380104
X_2^2	0.015	1	0.015	0.74	0.40911
X_3^2	0.142	1	0.142	7.11	0.023653
X_4^2	0.039	1	0.039	1.96	0.191324
Residual	0.200	10	0.020		

Cor Total	33.224	26

Table 21 ANOVA for response surface of 28-day compressive strength based on the quadratic model.

Source	Sum of Squares	Df	Mean Square	F Value	P-value
Block	0.14	2	0.07		
Model	46.69	14	3.34	85.07	＜0.0001
X_1: w/c	8.03	1	8.03	204.77	＜0.0001
X_2: HL (%)	0.75	1	0.75	19.11	0.0014
X_3: WPF-C (%)	31.79	1	31.79	810.83	＜0.0001
X_4: WPF-A (%)	5.28	1	5.28	134.76	＜0.0001
X_1X_2	0.03	1	0.03	0.74	0.4107
X_1X_3	0.59	1	0.59	15.12	0.0030
X_1X_4	0.02	1	0.02	0.57	0.4662
X_2X_3	0.05	1	0.05	1.18	0.3030
X_2X_4	0.00	1	0.00	0.01	0.9411
X_3X_4	0.00	1	0.00	0.08	0.7868
X_1^2	0.00	1	0.00	0.05	0.8202
X_2^2	0.00	1	0.00	0.00	0.9773
X_3^2	0.06	1	0.06	1.65	0.2284
X_4^2	0.03	1	0.03	0.87	0.3727
Residual	0.39	10	0.04		
Cor Total	47.23	26			

Table 22 Reduced Quadratic Model fitting results for the RSM analysis of 7-day compressive strength.

Response	R^2	$Adj.R^2$	$Pred.R^2$	$Adeq.Precision$	SD	Mean
Density	0.9916	0.9888	0.9712	58.228	0.12	3.99

Table 23 Reduced Quadratic Model fitting results for the RSM analysis of 28-day compressive strength.

Response	R^2	$Adj.R^2$	$Pred.R^2$	$Adeq.Precision$	SD	Mean
Density	0.9887	0.9850	0.9595	49.418	0.17	5.4

Fig. 26 and Fig. 27 indicates the interactions between significant variables on the 7-day and 28-day compressive strength of PB, and only the most significant interactive terms are illustrated. Within the defined range, it is clear that the increase of w/c and the amount of WPF decrease the strength of PB. Fig. 28 and Fig. 29 shows the 3-D response surface plots of 7-day and 28-day compressive strength, the tendency of plot at 7 days and 28 day is consistent, thus the 28-day compressive strength is analysed.

As Fig. 29 shows, the 3-D response surface plots illustrate the interaction between each variable (w/c, HL WPF-A and WPF-C ratio) on 28-day compressive strength.

Fig. 29 (a)-(c) shows the interaction of w/c (0.38-0.58) and HL ratio (0-10%), the interaction of w/c (0.38-0.58) and WPF-C ratio (0-15%) and the interaction of w/c(0.38-0.58) and WPF-A ratio (0-7%), respectively, with other parameters at central point for each correlation group (particularly HL ratio of 3.5% for each group). The reduction of compressive strength increases while increasing WPF-A and w/c. Especially, the decreasing tendency of compressive strength slows down with a decrease of WPF-C. The influence of WPF-C on compressive strength is significant, with a high w/c ratio. The reduction of w/c ratio results in the reduction of cement content and the increase of cavity in concrete. Therefore, the w/c ratio has a significant influence on compressive strength, as observed from the figure. Furthermore, as a comparison of Fig. 29 (a)-(c), the effect of HL is inconspicuous, it is possible due to the improvement of interface with other materials. Moreover, the effect of WPF-C is most remarkable, and cohesion of WPF is limited compared with conventional cementitious material is a major reason for the decrease of compressive strength. Fig. 29 (d)-(e) shows the interaction of HL ratio (0-10%) and WPF-C (0-15%), and the interaction of HL ratio (0-10%) and WPF-A (0-7%), respectively. It is explained the alkaline environment generated by HL can relieve the degradation of compressive strength caused by adding WPF due to the improvement of surface properties of WPF, which is like the alkaline treatment on fibre. Booya et al.[60] achieve the reduction of 28.9% by using Kraft pulp fibres to replace 2% weight of cement, and indicates compressive strength adding the Kraft pulp fibres with chemical treatment can be improved due to generation of fibrils.

Fig. 29 (f) shows the interaction of w/c (0.38-0.58) and WPF-A ratio (0-10%) with other parameters at central point (WPF-C ratio of 7.5% and WPF-A of 3.5%). The cement and aggregates are replaced by WPF can lead to the rapid decrease of the compressive strength. The effect of WPF-A and WPF-C ratio on compressive strength is equally significant.

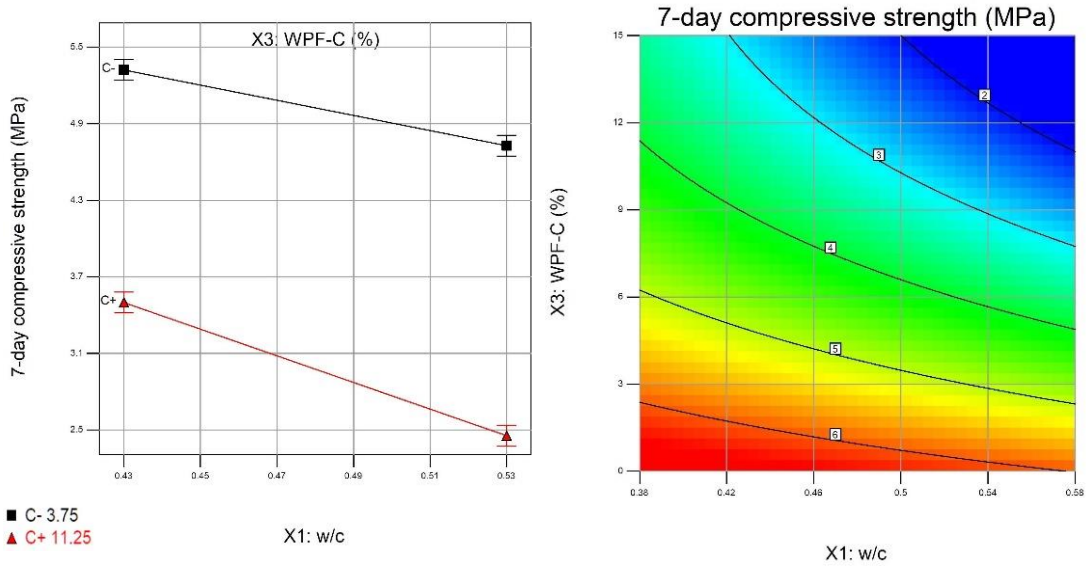

a) Interactive effects of w/c and WPF-C on water absorption (HL is 5 and WPF-A is 3.5%)

b) Contour of the relationship between w/c, WPF-C and 7-day compressive strength

Fig. 26 Interaction effects of change of independent variables on 7-day compressive strength.

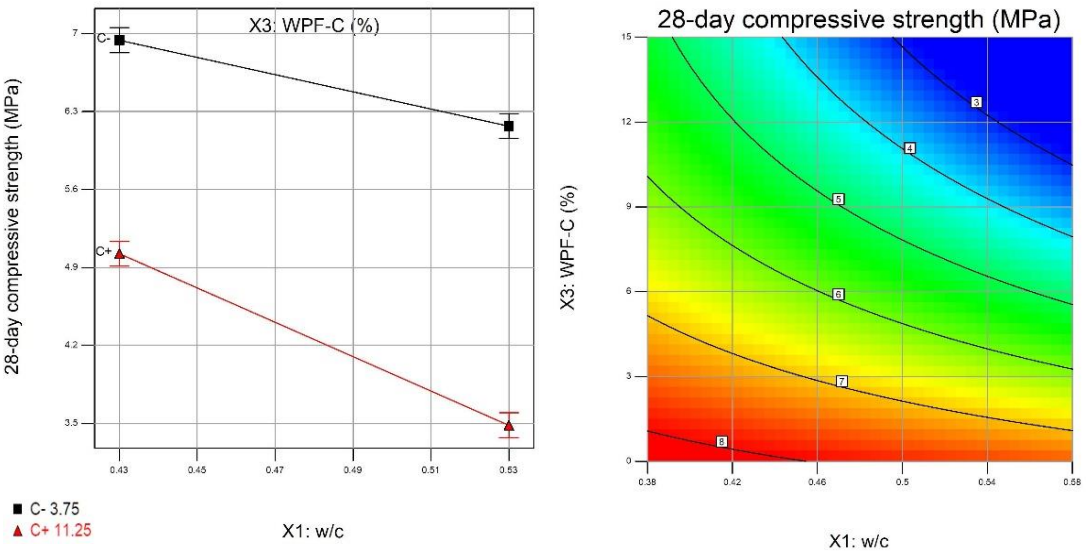

a) Interactive effects of w/c and WPF-C on water absorption (HL is 5 and WPF-A is 3.5%)

b) Contour of the relationship between w/c, WPF-C and 28-day compressive strength

Fig. 27 The tendency of 28-day compressive strength with the change of independent variables.

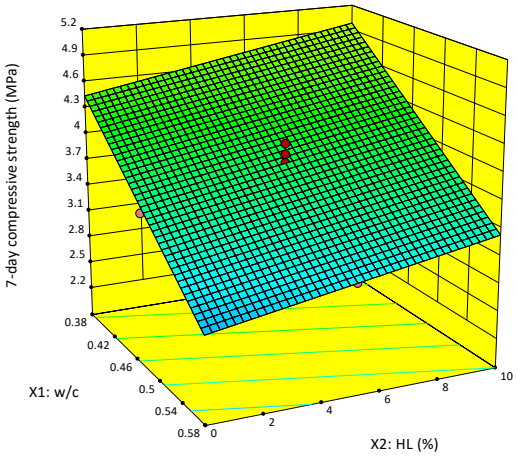

a) Relationship between w/c, HL (%), and 7-day compressive strength (WPF-C=7.5% and WPF-A=3.5%)

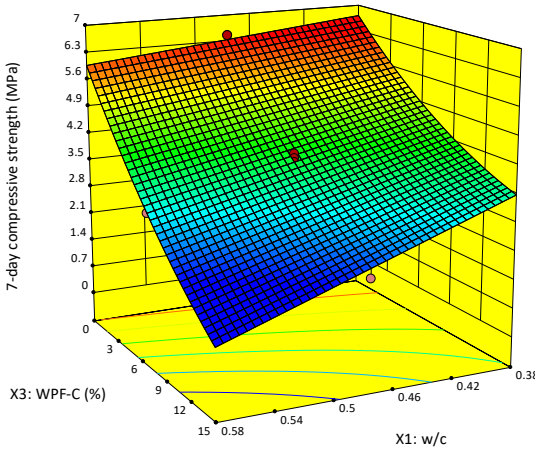

b) Relationship between w/c, WPF-C (%), and 7-day compressive strength (WPF-A=3.5% and HL=5%)

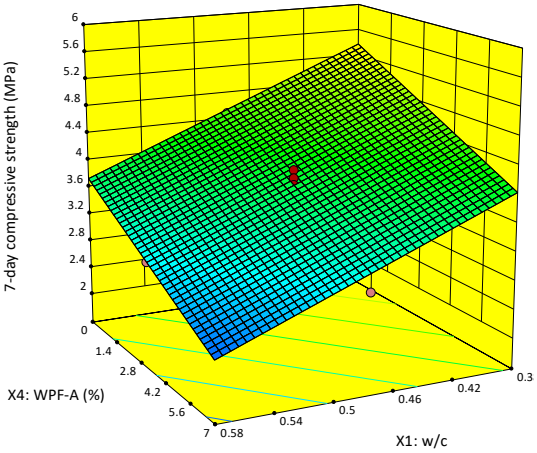

(c) Relationship between w/c, WPF-A (%), and 7-day compressive strength (WPF-C=7.5% and HL=5%)

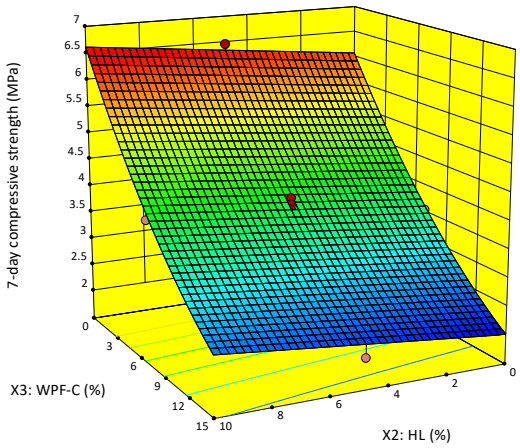

(d) Relationship between HL (%), WPF-C (%), and 7-day compressive strength (w/c=0.48 and WPF-A=3.5%)

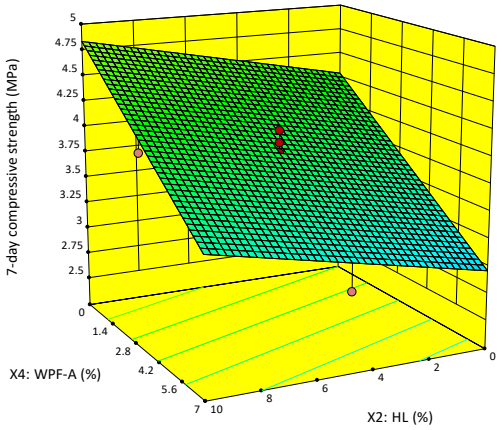

(e) Relationship between HL, WPF-A (%), and 7-day compressive strength (w/c=0.48 and WPF-C=7.5%)

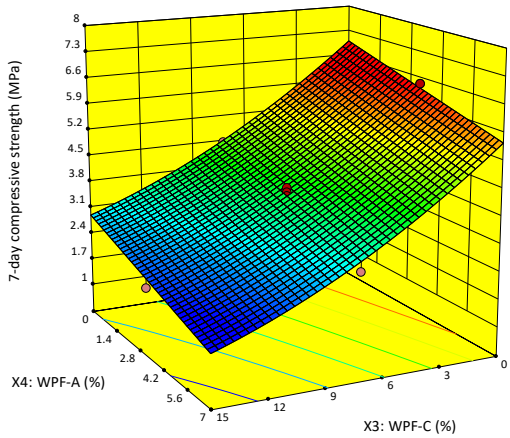

(f) Relationship between WPF-C (%), WPF-A (%) and 7-day compressive strength (w/c=0.48 and HL=5%)

Fig. 28 The interaction of each independent variable for 7-day compressive strength.

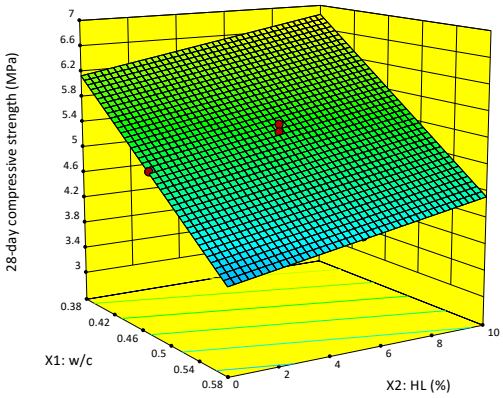

a) Relationship between w/c, HL (%), and 28-day compressive strength (WPF-C=7.5% and WPF-A=3.5%)

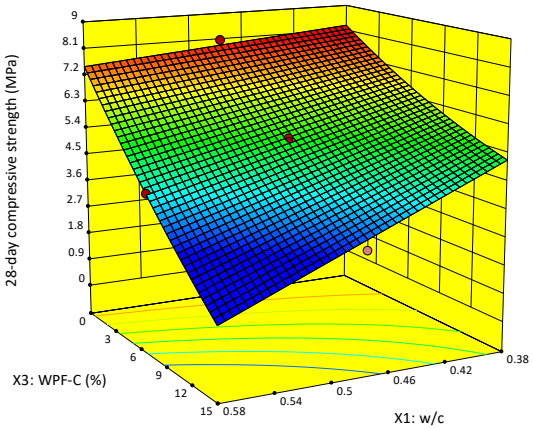

b) Relationship between w/c, WPF-C (%), and 28-day compressive strength (WPF-A=3.5% and HL=5%)

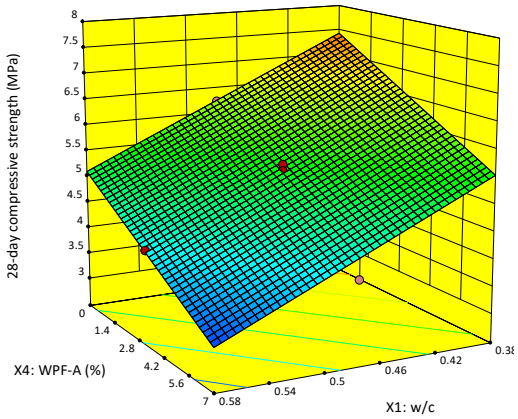

(c) Relationship between w/c, WPF-A (%), and 7-day compressive strength (WPF-C=7.5% and HL=5%)

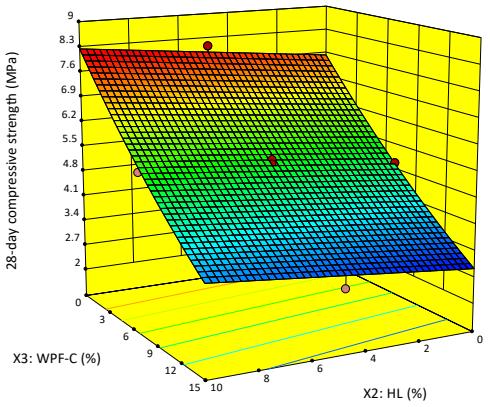

(d) Relationship between HL (%), WPF-C (%), and 7-day compressive strength (w/c=0.48 and WPF-A=3.5%)

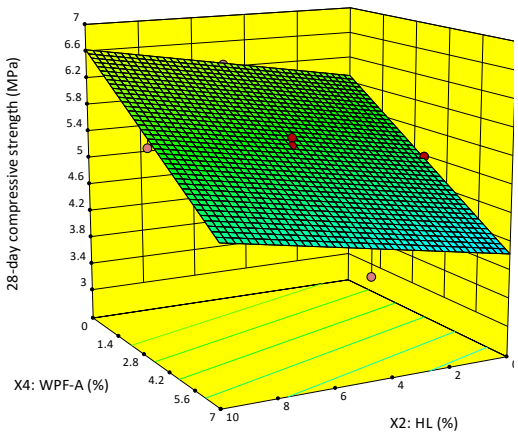

(e) Relationship between HL, WPF-A (%), and 28-day compressive strength (w/c=0.48 and WPF-C=7.5%)

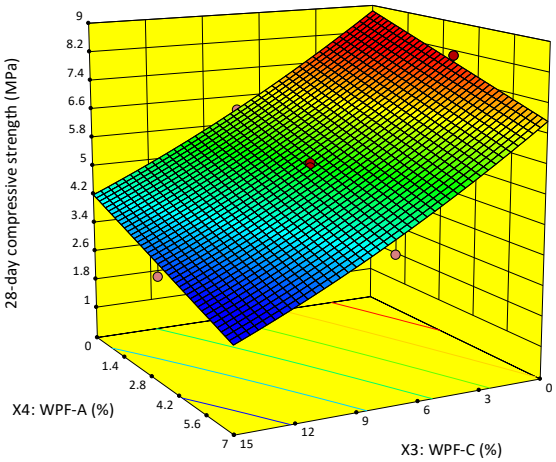

(f) Relationship between WPF-C (%), WPF-A (%) and 28-day compressive strength (w/c=0.48 and HL=5%)

Fig. 29 The interaction of each independent variable for 28-day compressive strength.

4.1.4 Response surface results of Compressive Softening Coefficient

All results of the softening coefficient of PB based on GB T4111 test are listed in Table 24. 0.687 of the softening coefficient is achieved at 0.48 of w/c, 5% of HL, 15% of WPF-C and 3.5% of WPF-A, indicating the maximum reduction of compressive strength, while 0.902 of the softening coefficient is presented at 0.48 of w/c, 5% of HL 0% of WPF-C and 3.5% of WPF-A, indicating the minimum reduction of compressive strength.

The softening coefficient of compressive strength is a parameter to access the performance of concrete blocks treated by water immersion, which is not included in ASTM standards for CMU, but high-water absorption of WPF influences the properties of concrete blocks possibly. The compressive softening coefficient indicates water-resistance of the materials in the case of the water change in intensity.

Table 25 shows the summaries of the ANOVA for the response of the water-resistance properties of PB. The significance of each term is shown based on F-value similarly, thus the terms of X_1X_2, X_1X_4, X_2X_3 and X_2^2 are not significant, and the Reduced Quadratic model is achieved in Equation (4-5).

Table 24 Results of the softening coefficient in the experimental design matrix.

	Run of Experiment	X1: w/c	X2: HL, %	X3: WPF-C, %	X4: WPF-A, %	Softening coefficient
Block-1	1	0.43	2.5	3.75	5.25	0.83
	2	0.53	7.5	3.75	5.25	0.81
	3	0.43	2.5	11.25	1.75	0.78
	4	0.53	2.5	3.75	1.75	0.87
	5	0.48	5	7.5	3.5	0.77
	6	0.53	7.5	11.25	1.75	0.74
	7	0.53	2.5	11.25	5.25	0.70
	8	0.43	7.5	3.75	1.75	0.88
	9	0.43	7.5	11.25	5.25	0.74
Blcok-2	10	0.43	2.5	3.75	1.75	0.87
	11	0.43	2.5	11.25	5.25	0.74
	12	0.48	5	7.5	3.5	0.78

	13	0.53	7.5	11.25	5.25	0.72
	14	0.53	2.5	3.75	5.25	0.80
	15	0.43	7.5	11.25	1.75	0.78
	16	0.53	2.5	11.25	1.75	0.74
	17	0.43	7.5	3.75	5.25	0.85
	18	0.53	7.5	3.75	1.75	0.86
Blcok-3	19	0.48	5	7.5	7	0.76
	20	0.48	5	15	3.5	0.69
	21	0.48	5	7.5	3.5	0.78
	22	0.58	5	7.5	3.5	0.75
	23	0.48	10	7.5	3.5	0.79
	24	0.48	5	7.5	0	0.84
	25	0.38	5	7.5	3.5	0.83
	26	0.48	0	7.5	3.5	0.76
	27	0.48	5	0	3.5	0.90

Table 25 ANOVA for response surface quadratic model of the compressive softening coefficient.

Source	Sum of square	Df	Mean square	F value	p-value
Block	0.000	2	0.000		
Model	0.085	14	0.006	71.77	＜0.0001
X_1: w/c	0.006	1	0.006	75.59	＜0.0001
X_2: HL (%)	0.000	1	0.000	4.65	0.056408
X_3: WPF-C (%)	0.065	1	0.065	776.25	＜0.0001
X_4: WPF-A (%)	0.011	1	0.011	125.09	＜0.0001
X_1X_2	0.000	1	0.000	0.13	0.730668
X_1X_3	0.000	1	0.000	2.58	0.13919
X_1X_4	0.000	1	0.000	0.62	0.447991
X_2X_3	0.000	1	0.000	0.21	0.653303
X_2X_4	0.000	1	0.000	2.08	0.179508
X_3X_4	0.000	1	0.000	1.93	0.195021
X_1^2	0.000	1	0.000	4.29	0.065263
X_2^2	0.000	1	0.000	0.00	0.995921
X_3^2	0.001	1	0.001	6.95	0.024895
X_4^2	0.001	1	0.001	9.08	0.013038
Residual	0.001	10	0.000		
Cor Total	0.086	26			

According to the results of the ANOVA of the modified model listed in Table 26, the F-value of the Reduced Quadratic model is 128.18, R^2, $Adj.R^2$ and $Pre.R^2$ are 0.989, 0.982 and 0.95, respectively, which indicates the model is reliable.

$$\text{Softening Coefficient} = 1.451 - 1.7597X_1 - 0.001X_2 - 0.0118X_3 - 0.0331X_4 - 0.0197X_1X_3 + 0.0008X_2X_4 + 0.0005X_3X_4 + 1.6472X_1^2 + 0.0004X_3^2 + 0.002X_4^2 \quad (4\text{-}5)$$

Table 26 Reduced Quadratic Model fitting results for the RSM analysis of softening coefficient.

Response	R^2	Adj.R^2	Pred.R^2	SD	Mean
Density	0.9892	0.9815	0.95	0.081	0.79

Fig. 30 shows the interactive effects of variables on changes in softening coefficient values, indicating to be either collaborative effects or antagonistic effects. In Fig. 30,plot b) illustrates the interactions between HL and WPF-A at 0.48 of w/c and 7.5% of WPF-C, which demonstrates at the low level of replacement ratio of WPF-A (1.75%) softening coefficient is almost constant and increases slightly with the increase of HL replacement ratio, while at the relatively high level of replacement ratio of WPF-A (5.25%), softening coefficient increases with the increase of HL replacement ratio. Furthermore, diagram a) and c) illustrate the interactive effects of w/c and WPF-C, and the interactive effects of WPF-A and WPF-C. There is no remarkable changes of interactions.

Fig. 31 a) illustrates the relationship between w/c, WPF-C, and softening coefficient values. This plot shows the maximum value of the softening coefficient is 0.902 when w/c is 0.48 and WPF-C is 0%. It is clear that both the increase of WPF-C and w/c has negative effects on the softening coefficient. Additionally, the simultaneous effects of w/c and WPF-C are not remarkable. WPF-C is a dominant factor in weakening the water-resistance of PB compared to the effect of w/c.

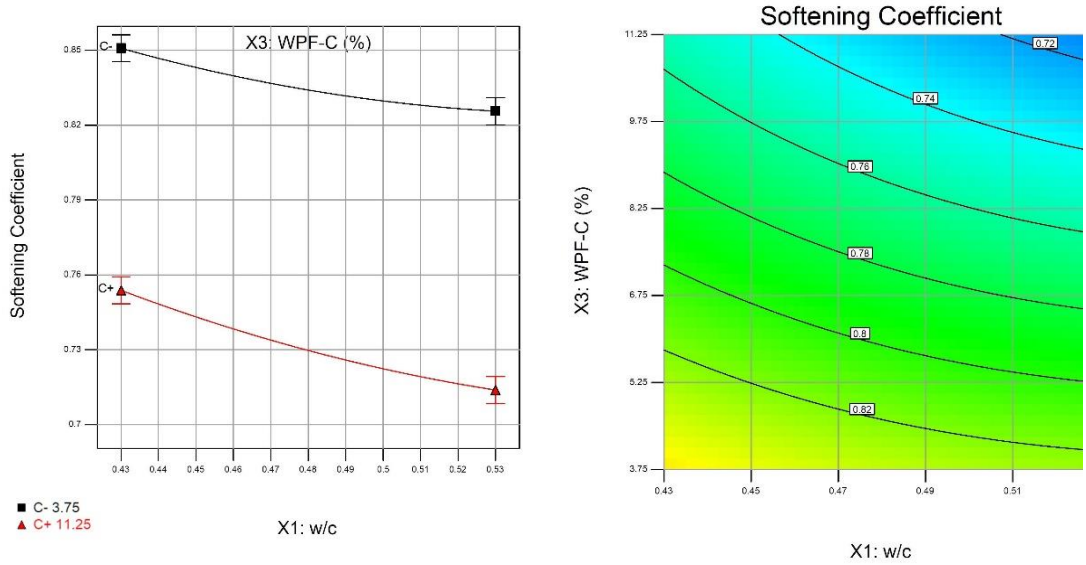

a) interactive effects of w/c and WPF-C on softening coefficient (HL is 5% and WPF-A is 3.5%)

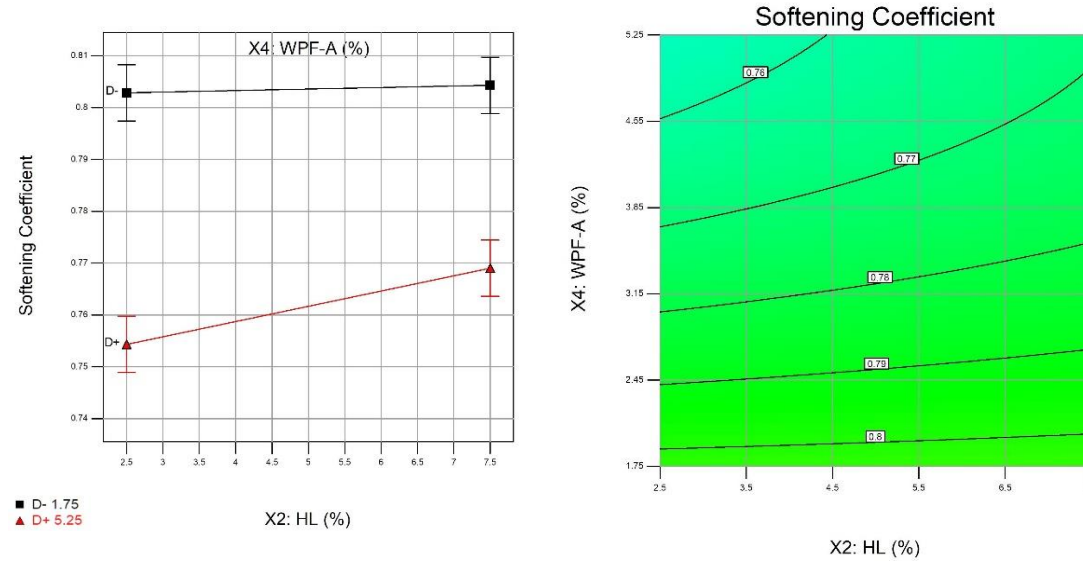

b) interactive effects of HL and WPF-A on softening coefficient (w/c is 0.48 and WPF-C is 7.5%)

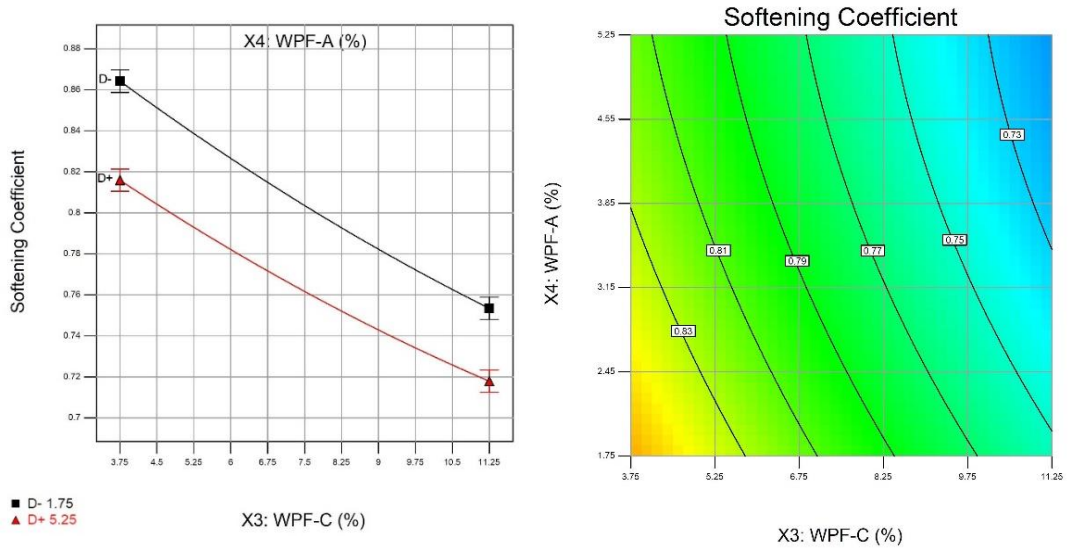

c) interactive effects of WPF-A and WPF-C on softening coefficient (w/c is 0.48 and HL is 5%)

Fig. 30 Interaction effects of variables on compressive softening coefficient.

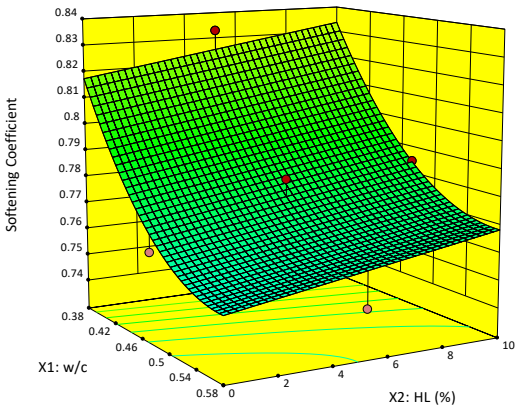

(a) Relationship between w/c, HL, and softening coefficient values (WPF-A=3.5% and WPF-C=7.5%)

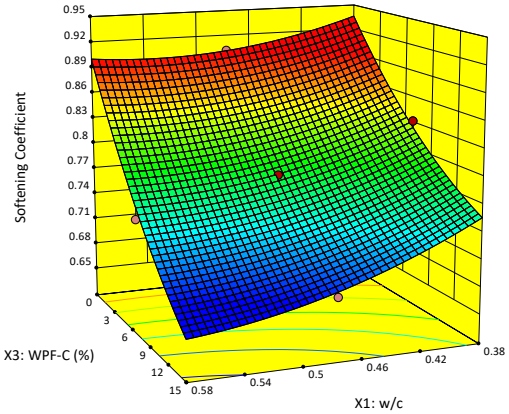

(b) Relationship between w/c, WPF-C, and softening coefficient values (WPF-A=3.5% and HL=5%)

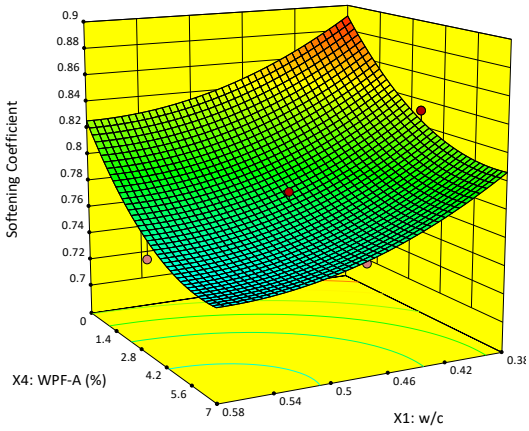

(c) Relationship between w/c, WPF-A, and softening coefficient values (HL=5% and WPF-C=7.5%)

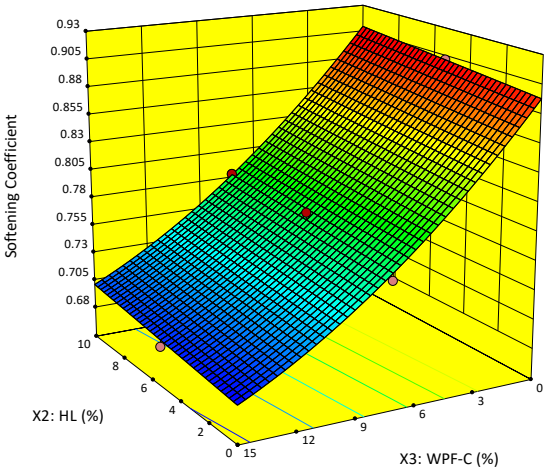

(d) Relationship between w/c, WPF-C, and softening coefficient values (WPF-A=3.5% and HL=5%)

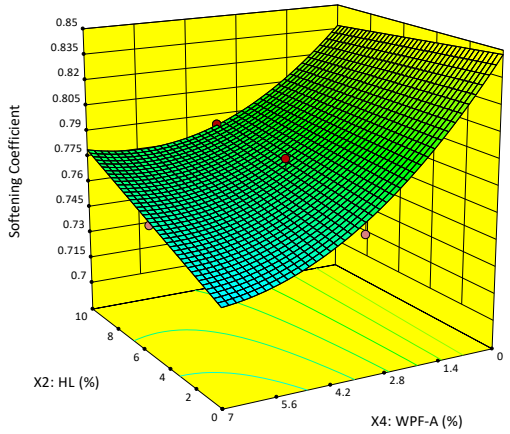

(e) Relationship between WPF-A, HL, and softening coefficient values (WPF-C=7.5% and w/c=0.48)

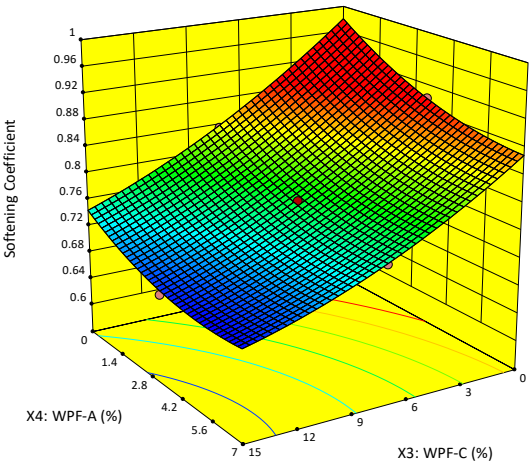

(f) Relationship between HL, WPF-A, and softening coefficient values (w/c=0.48 and WPF-C=7.5%)

Fig. 31 The interaction of each independent variables for softening coefficient.

4.1.5 Response surface results of Thermal performance

The thermal conductivity values of each PB in the design space are listed in Table 27. The maximum thermal conductivity is 1.33 W/m·K at 0.48 of w/c, 5% of HL, 0% of WPF-C and 3.5% of WPF-A, while the minimum thermal conductivity is 0.59 W/m·K at 0.48 of w/c, 5% of HL, 15% of WPF-C and 3.5% of WPF-A.

Table 28 shows the ANOVA results of thermal conductivities, the significance of major factors and interactive terms are determined and presented as F-value and P-value shows. Identical with the previous method, terms with P-value＜0.05 are considered to be non-negligible. Thereby, the reduced quadratic model is re-calculated with $Adj.R^2 > 0.15$, therefore, terms which make a great influence on the thermal conductivities include X_1, X_2, X_3, X_4, X_2X_3, X_2X_4, X_3X_4, X_1^2, X_3^2 and X_4^2 while other terms are removed from the predictive model. The new predictive model is presented in Equation (4-6).

$$\text{Thermal Conductivity} = 4.626 - 11.023X_1 + 0.01X_2 - 0.078X_3 - 0.126X_4 - 0.002X_2X_3 + 0.003X_2X_4 + 0.003X_3X_4 + 9.833X_1^2 + 0.002X_3^2 + 0.006X_4^2 \quad (4\text{-}6)$$

Table 27 Results of thermal conductivity of PB in the design space of RSM.

	Run of Experiment	X_1: w/c	X_2: HL, %	X_3: WPF-C, %	X_4: WPF-A, %	Thermal conductivity (W/m·K)
Block -1	1	0.43	2.5	3.75	5.25	1.09
	2	0.53	7.5	3.75	5.25	1.01
	3	0.43	2.5	11.25	1.75	0.89
	4	0.53	2.5	3.75	1.75	1.16
	5	0.48	5	7.5	3.5	0.85
	6	0.53	7.5	11.25	1.75	0.75
	7	0.53	2.5	11.25	5.25	0.62
	8	0.43	7.5	3.75	1.75	1.3
	9	0.43	7.5	11.25	5.25	0.77
Blcok -2	10	0.43	2.5	3.75	1.75	1.28
	11	0.43	2.5	11.25	5.25	0.79
	12	0.48	5	7.5	3.5	0.87
	13	0.53	7.5	11.25	5.25	0.68
	14	0.53	2.5	3.75	5.25	0.89

	15	0.43	7.5	11.25	1.75	0.9
	16	0.53	2.5	11.25	1.75	0.75
	17	0.43	7.5	3.75	5.25	1.22
	18	0.53	7.5	3.75	1.75	1.18
Blcok -3	19	0.48	5	7.5	7	0.76
	20	0.48	5	15	3.5	0.59
	21	0.48	5	7.5	3.5	0.88
	22	0.58	5	7.5	3.5	0.78
	23	0.48	10	7.5	3.5	0.94
	24	0.48	5	7.5	0	1.11
	25	0.38	5	7.5	3.5	1.13
	26	0.48	0	7.5	3.5	0.8
	27	0.48	5	0	3.5	1.33

Table 28 ANOVA for response surface quadratic model of thermal conductivity.

Source	Sum of Squares	DF	Mean Square	F-Value	P-value
Block	3.200E-003	2	1.600E-003		
Model	1.18	14	0.084	85.78	< 0.0001
X_1: w/c	0.15	1	0.15	153.36	< 0.0001
X_2: HL (%)	0.016	1	0.016	16.33	0.0024
X_3: WPF-C (%)	0.83	1	0.83	845.01	< 0.0001
X_4: WPF-A (%)	0.14	1	0.14	143.82	< 0.0001
X_1X_2	2.250E-004	1	2.250E-004	0.23	0.6423
X_1X_3	6.250E-004	1	6.250E-004	0.64	0.4433
X_1X_4	1.225E-003	1	1.225E-003	1.25	0.2899
X_2X_3	3.600E-003	1	3.600E-003	3.67	0.0844
X_2X_4	3.600E-003	1	3.600E-003	3.67	0.0844
X_3 X_4	4.900E-003	1	4.900E-003	5.00	0.0494
X_1^2	0.015	1	0.015	14.99	0.0031
X_2^2	5.333E-004	1	5.333E-004	0.54	0.4778
X_3^2	0.016	1	0.016	16.45	0.0023
X_4^2	9.633E-003	1	9.633E-003	9.82	0.0106
Residual	9.808E-003	10	9.808E-004		
Cor Total	1.19	26			

According to the results of the ANOVA of the modified model listed in Table 29, the F-value of the Reduced Quadratic model is 85.78, R^2, $Adj.R^2$ and $Pre.R^2$ are 0.9895, 0.9821 and 0.9585, respectively, which indicates the model is reliable.

Table 29 Reduced Quadratic Model fitting results for the RSM analysis of thermal conductivity.

Response	R^2	$Adj.R^2$	$Pred.R^2$	$Adeq.Precision$	SD	Mean
Density	0.9895	0.9821	0.9585	35.971	0.03	0.94

Fig. 32 illustrates the interactive relationship of major factors, only involving significant terms based on ANOVA on the thermal conductivities of PB. Fig. 32 a) indicates the growth rate of thermal conductivity to HL (%) increases when the WPF-C decreases from 11.25% to 3.75% at 0.48 of w/c and 3.5% of WPF-A. The quantities of WPF-C have a negative influence on the thermal conductivity when the HL ratio increases at 0.48 of w/c and 3.5% of WPF-A. Diagram b) illustrates the increased rate of thermal conductivity decreases when WPF-A decreases, which demonstrates WPF-A is a dominant effect on the thermal conductivity compared to HL (%). Diagram c) shows there is a slight change in the decrease rate of thermal conductivity with a decrease of WPF-C. The influence of WPF-A and WPF-C is both considerable.

Fig. 33 shows the 3-D diagrams of the relationship between 4 factors and the response (thermal conductivity). Overall the thermal conductivity reduces from 1.33 to 0.59 W/m • K, which indicates the performance of thermal insulation increases. It is clear that WPF-A and WPF-C enhance the performance of thermal insulation. This is an attribute to the positive effect of WPF with low thermal conductivity. Additionally, the thermal conductivity decreases with the increase of w/c. It is possible more void generated by the increase of w/c in concrete results in the decrease of thermal conductivity. Similar results were achieved in the study of Kim. et al. [123]. However, HL presents a slightly negative influence on the performance of thermal insulation. The thermal conductivity increases with increasing HL, and the interface around WPF is improved, which the void reduces in the concrete, resulting in an increase of thermal conductivity.

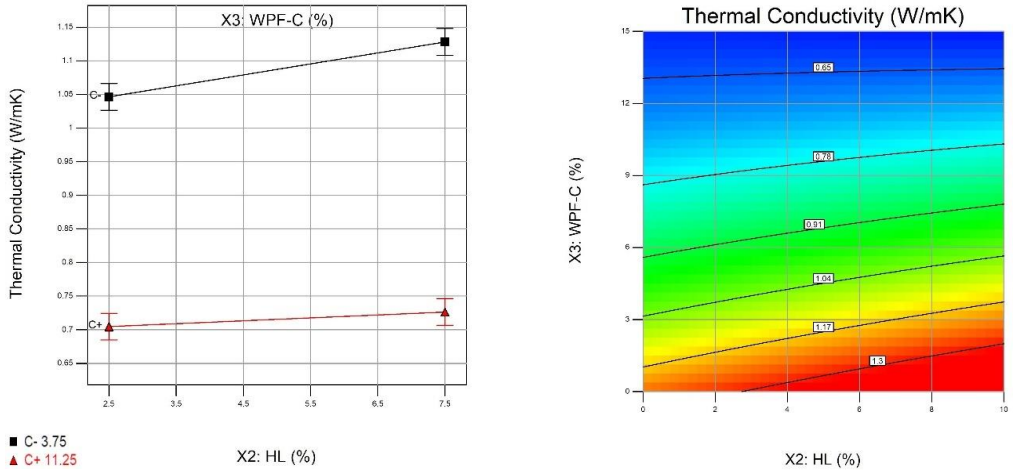

a) Interactive effects of HL (%) and WPF-C (%) on thermal conductivity (w/c is 0.48 and WPF-A is 3.5%)

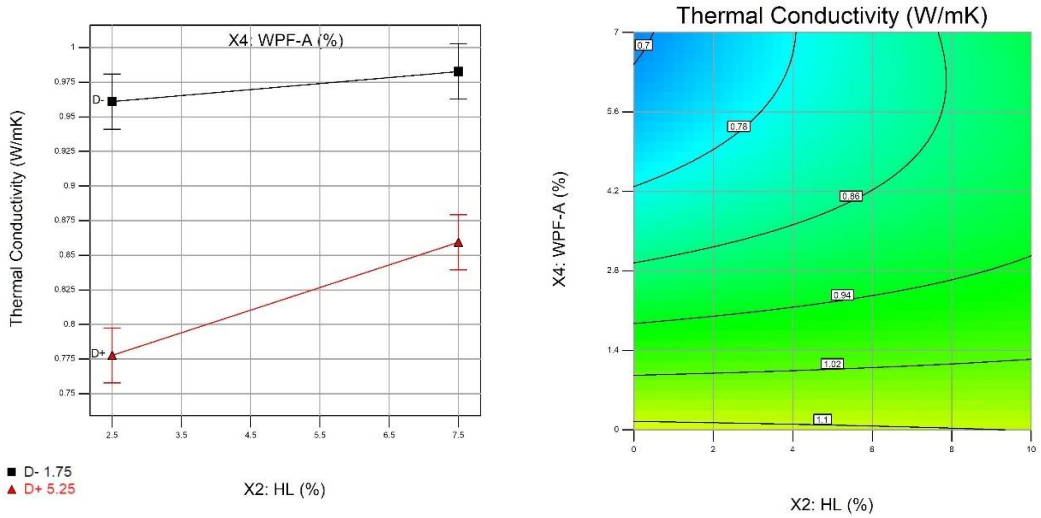

b) Interactive effects of HL (%) and WPF-A (%) on thermal conductivity (w/c is 0.48 and WPF-C is 7.5%)

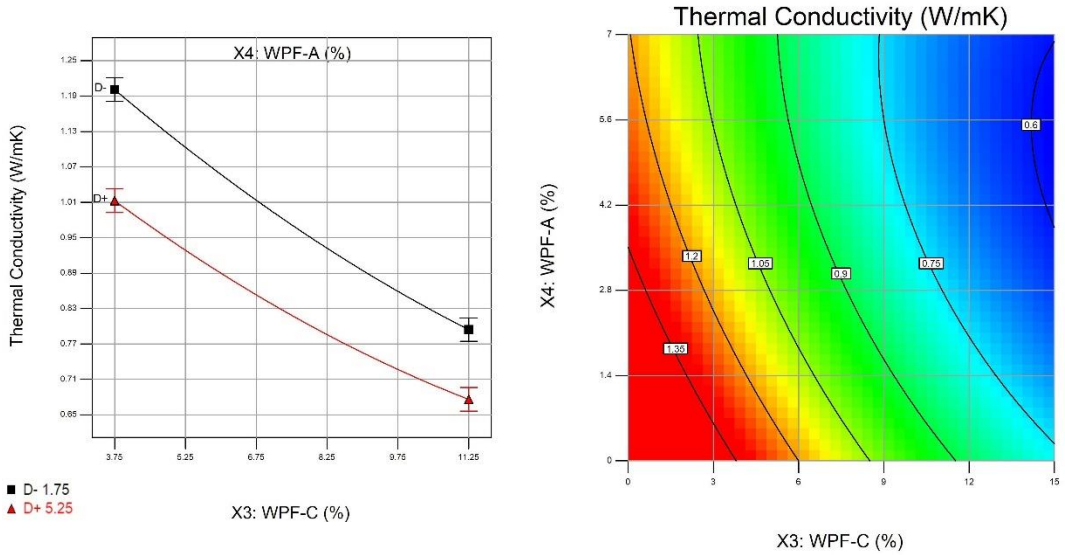

c) Interactive effects of WPF-A (%) and WPF-C (%) on thermal conductivity (w/c is 0.48 and HL is 5%)

Fig. 32 Interaction effects of variables on thermal conductivity (symbol of C in the plots represents WPF-C, symbol of D represents WPF-A).

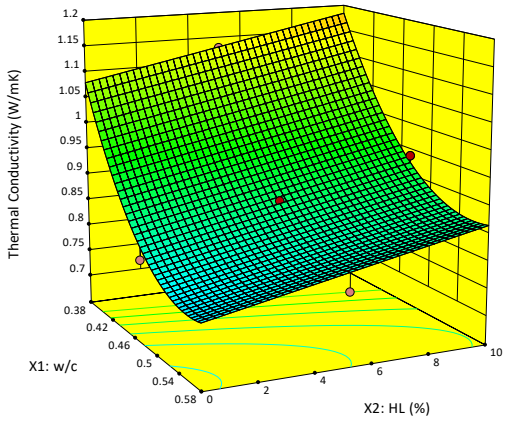

(a) Relationship between w/c, HL, and softening coefficient values (WPF-A=3.5% and WPF-C=7.5%)

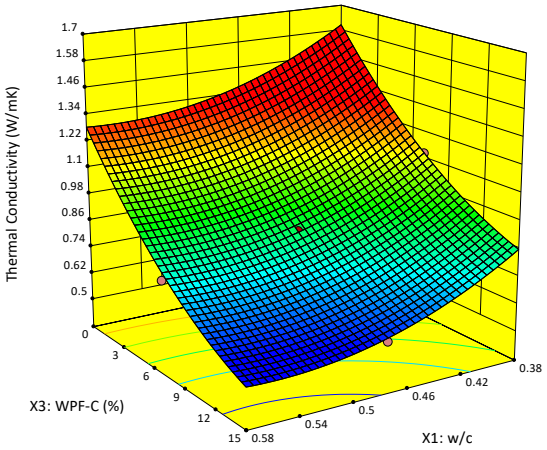

(b) Relationship between w/c, WPF-C, and softening coefficient values (WPF-A=3.5% and HL=5%)

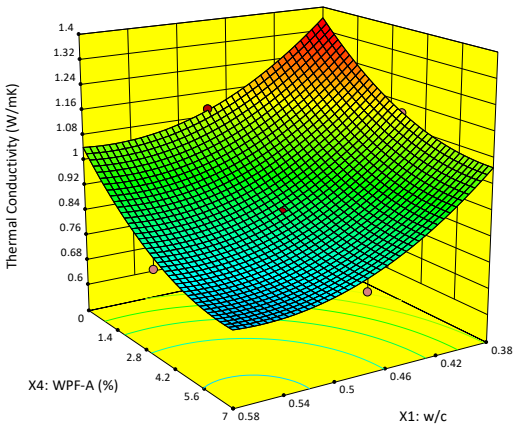

(c) Relationship between w/c, WPF-A, and softening coefficient values (HL=5% and WPF-C=7.5%)

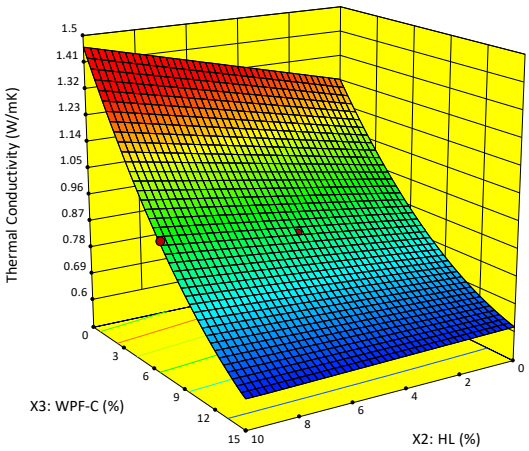

(d) Relationship between w/c, WPF-C, and softening coefficient values (WPF-A=3.5% and HL=5%)

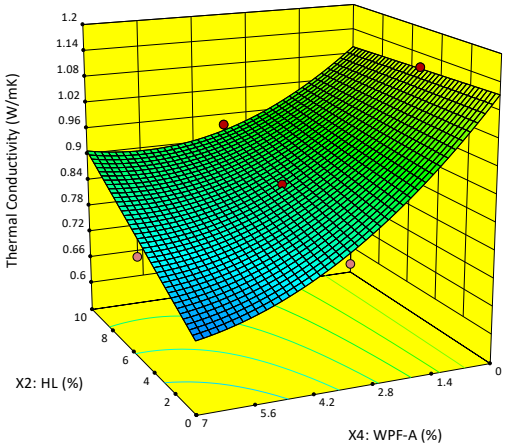

(e) Relationship between WPF-A, HL, and softening coefficient values (WPF-C=7.5% and w/c=0.48)

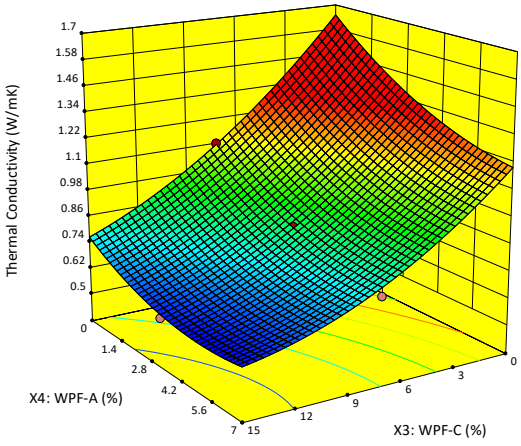

(f) Relationship between HL, WPF-A, and softening coefficient values (w/c=0.48 and WPF-C=7.5%)

Fig. 33 3-D response surface of relationship between each independent variable for thermal conductivity.

4.1.5 Correlation discussion

The ultrasonic pulse velocity (UPV) of the PB in full dried condition was tested at 28 days. The frequency was set to be 54 kHz and 100 Hz, according to ASTM C597-16[124]. Typically, compressive strength has a positive correlation with ultrasonic velocity, and UPV value is an indicator of the compactness for the concrete, which is affected by mesostructure or microstructure, such as crack or void. According to the results of the strength and ultrasonic test, Fig. 34 shows the relationship between compressive strength and velocity. There is a positive linear relationship achieved with R^2=0.97. Additionally, it is observed that the PB shows a comparatively low UPV value when the content of WPF is high, which demonstrates the results of the water absorption test.

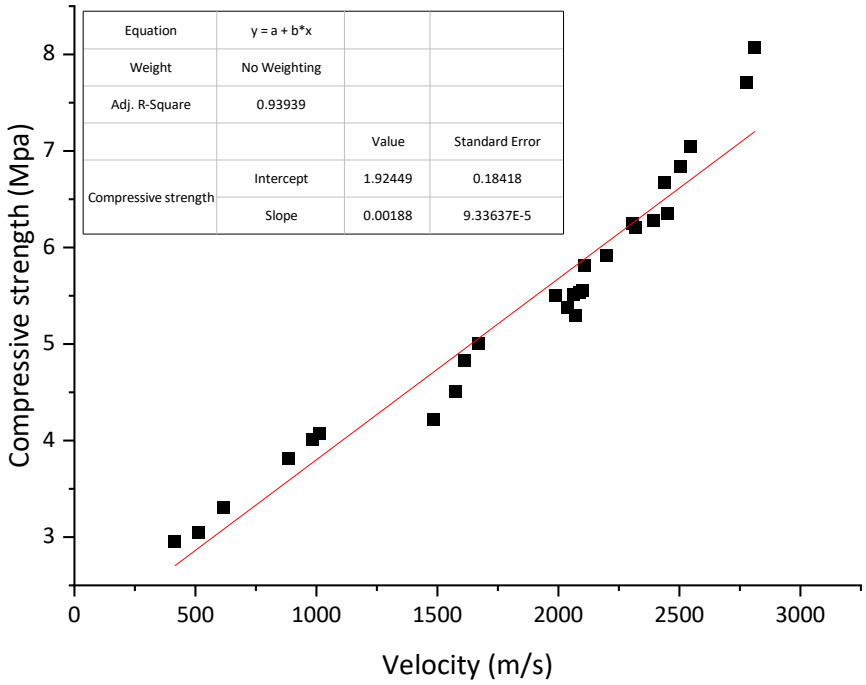

Fig. 34 The relationship between compressive strength and ultrasonic velocity of PB.

4.2 Validation and multi-objective optimization

A multiple optimized mix design was achieve considering density, water absorption and compressive strength. The experiment of predictive optimization was conducted

to validate the accuracy of the models. Table 30 shows the criteria of the variables with an upper and lower limit and the range considers the ASTM C129[86] to satisfy the strength requirement of non-loadbearing concrete, 4.14 MPa at least. The optimized proportion was performed by using Design Expert Software 10, and the results were given in Table 31.

A new mixture proportion of the PB was prepared to validate the optimized results from model prediction. The same experiment containing three samples was conducted. The results were listed in Table 31 and compared with the predictive results of models. The error calculated by absolute derivation was given, which acceptable indicating accordance, for compressive strength errors is larger than 5% slightly.

Table 32 shows the results of ANOVA for each parameter. The R^2 of the prediction model is 0.9141, considered in reasonable agreement with the Adj R^2, where is $Adeq.Precision$ is a signal-to-noise ratio, implying the model discrimination based on the ratio of predicted values range at design points and the average error (the model is adequate when the ratio is greater than 4).

Table 30 Criteria settings for multi-objective optimization.

Variables and responses	Target	Lower limit	Upper limit
w/c ratio	in range	0.38	0.58
HL ratio (%)	in range	0	10
WPF-C ratio (%)	in range	0	15
WPF-A ratio (%)	in range	0	7
Density (kg/m^3)	minimum	1758.45	2204.85
Absorption (%)	minimum	5.17	20.54
28-day compressive strength (MPa)	maximum	4.5	9

Table 31 Optimized proportion and response validation with prediction models of PB.

w/c	HL	WPF-C	WPF-A	Parameters	Experimental results	Predicated value	Error (%)
0.38	10	11.77	/	ρ	1967.18	2006.4	2
				Absorption	8.43	8.03	2.7
				P_{28}	6.26	7.14	14.1

Table 32 ANOVA validation for comparison of initial models and modified models.

Response	Models	R^2	Adj.R^2	Pre.R^2	SD	Adeq.Prec.	Mean
Density	Quadrautic	0.9908	0.9778	0.9267	28.5	28.5	1950.2
	Modified model	0.9908	0.9815	0.9376	17.4	33.21	1950.2
Absorption	Quadrautic	0.9899	0.9757	0.9141	0.65	27.45	13.04
P_{28}	Quadrautic	0.9917	0.9800	0.9296	0.2	30.57	5.4
	Modified model	0.9916	0.9833	0.9387	0.18	35.51	5.4

4.3 Scanning electron microscope (SEM)

Fig. 35 shows the scan images of papercrete samples with and without HL at 28 days. It was clear that hydraulic products were formed surrounding the WPF for both experimental serials. From Fig. 35 a), there was an indication of separation between the WPF and the cement matrix observed. The distribution of hydraulic products was nonuniform. Nevertheless, for the samples with a high ratio of lime, as Fig. 35 a) illustrated, the gaps between the cement matrix and WPF became narrow, which indicates the bound between the cement matrix and WPF is improved slightly compared with the PB without HL. The hydraulic products were distributed uniformly on the surface of WPF. The improved bonding condition between cement and WPF results in the improvement of the strength of PB. Further, Fig. 36 shows that hydration products disperse uniformly on the surface of WPF for papercrete with HL. There was no ettringite observed between the cement matrix and WPF. These results can be explained by Mohr et al.[105], ettringite was formed around kraft pulp fibre only after two wet/dry cycles.

Fig. 37 shows the scanned image of papercrete samples with an increment of the WPF ratio. It can be observed that there are remarkable voids in the PB with a high WPF ratio at 28 days. High water absorption of WPF results in voids and crack formed

around the interface zone with water loss. Moreover, in the case of a high ratio of WPF replacement, the gap between WPF and cement reduces by introducing HL, which demonstrates the effect of HL on the improvement of the interface is limited as a comparison between Fig. 37 a) and b).

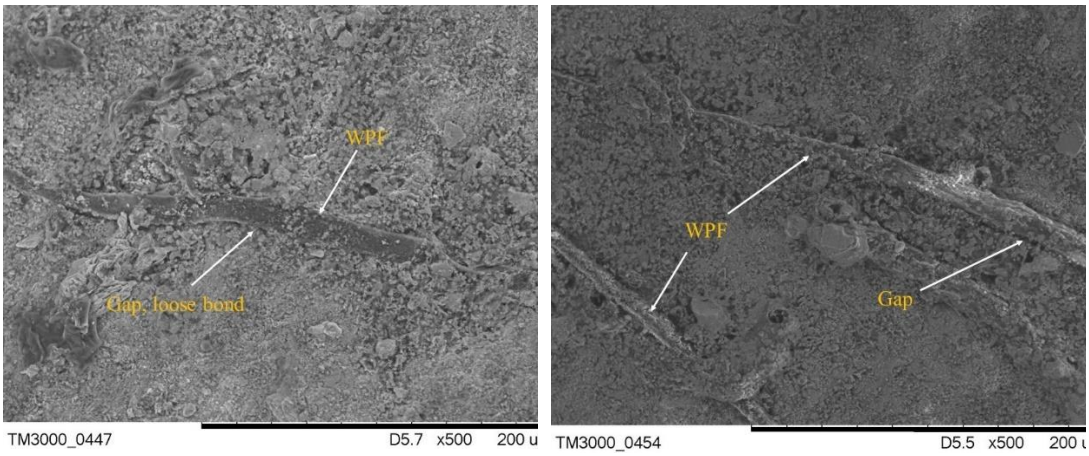

a) PB samples without HL, serial 26 b) PB samples with 10% HL, serial 23

Fig. 35 SEM images of PB with 7.5% of WPF-C and 3.5% of WPF-A (experiment serial 26 and 23) at×500.

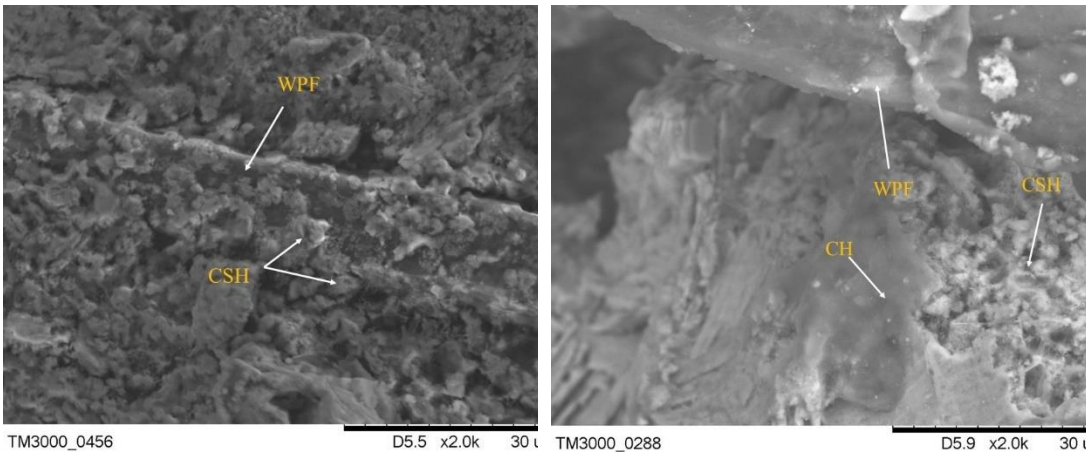

a) Interface in PB with 10% HL, serial 23 b) Voids and cracks in PB, serial 23

Fig. 36 The interface zone between WPF and cement matrix of PB sample at×2000.

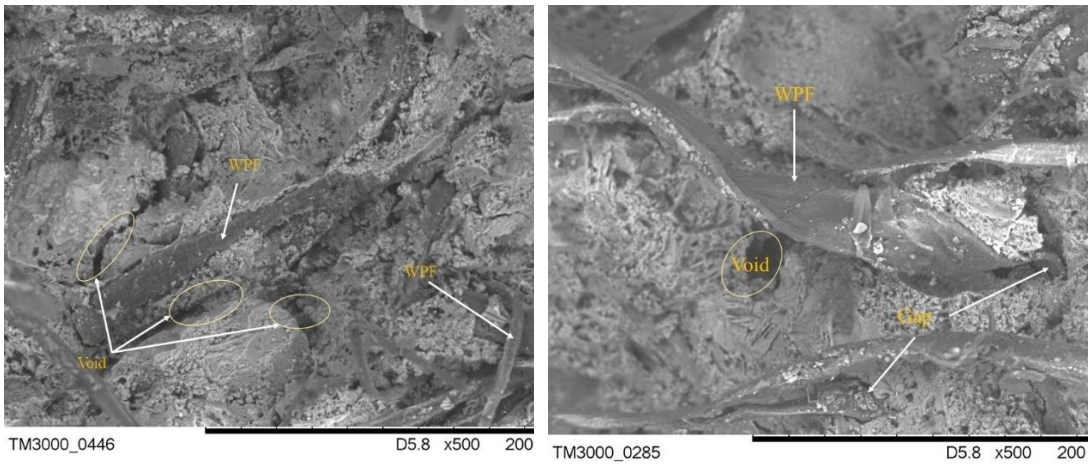

a) Papercrete with 7.5 % of WPF-C, serial 20 b) Papercrete with 15% of WPF-C, serial 21

Fig. 37 SEM images of PB without 5% of HL (mixture with 7.5% of WPF-C and 15% of WPF-C, respectively, namely experiment serial 20 and 21) at×500.

4.4 Summary

In this section, the results of the experiment were analysed based ANOVA, the influence of proportion variables on density, water absorption, compressive strength at 7 and 28 days, softening coefficient of compressive strength and thermal performance was investigated, the significance of major factors and interactive terms were clarified as well, accordingly, the predictive models of were established and validated based on the multi-objective optimized proportion of ingredients, an appropriate mixing proportion was achieved according to the requirement of ASTM. Additionally, SEM was used to investigate the mesostructure of papercrete with the change of proportion of ingredient. The influence of HL on the cohesion between WPF and cement was observed. Overall, the experimental results demonstrated that the introduction of WPF in the concrete decrease the strength significantly for cement and aggregates replacement schemes. The 3-D plots indicated that there was a slightly positive influence of HL on the strength and durability of PB.

Chapter 5 Life cycle assessment of papercrete

5.1 Introduction

Although the utilization of WPF in constructional materials is considered to be an environmentally friendly treatment due to the recovery of the resources in most pertinent literature[55,125,126], there is no quantification or specific analysis on the possible environmental benefits for WPF utilization in civil engineering materials. To assess the feasibility of WPF utilization in terms of environmental impact, an expanded production system was established in this section to analyses the overall environmental impact of PB production as well as WPF disposal by means of the life cycle assessment (LCA) method. Four scenarios of concrete block production systems with different WPF disposal (incineration, landfill, and recycling) were performed to investigate whether the use of WPF in concrete achieved a higher environmental credit than conventional production and treatment. Moreover, the sensitivity analysis was performed to study the effect of part input flow, the influence of mixing proportion change on the environmental impact was investigated by the comparison of three mixing proportion schemes, as well as transportation distance considered.

5.2 Methodology

LCA used in this study is a method to evaluates, by calculating the inputs and outputs, the potential environmental impact of certain processes or products in terms of specific lifecycles, qualitatively and quantitatively. Typically, a completed LCA method for a given product involves various processes in the production system, i.e., from raw material extraction to usage on site, either to final disposal or recycling (the definition system of LCA is summarized as from ‘cradle to grave’, ‘cradle to use’ or ‘cradle to cradle’). All environmental impacts are related to material, energy flows

and pollutant emissions to air and water. The LCA method is used effectively to compare different production plans. According to ISO 14040[127], ISO 14044[128] and ILCD handbook guidelines[129], LCA flowchart as shown in Fig. 38, the procedures of LCA are summarized to be four stages: 1) definition of the scope and objectives; 2) life cycle inventory (LCI) analysis; 3) life cycle impact assessment (LCIA) and 4) interpretation of results. In this section, the same steps were compiled to expound on the production of a PB.

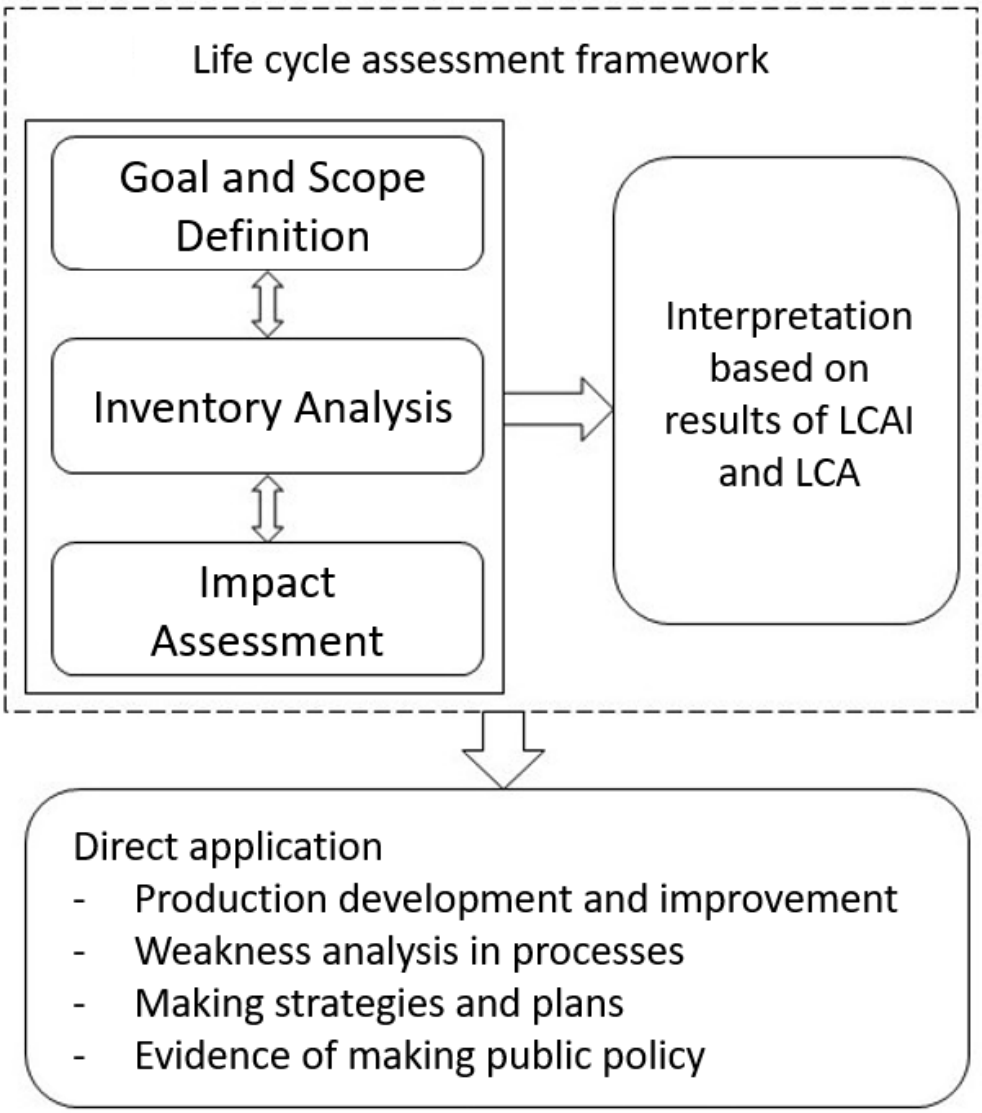

Fig. 38 Schematic diagram and objectives of the LCA method.

5.2.1 The goal and scope definition

Goal: The main objective of this LCA study was to investigate the environmental benefit of PB production compared to conventional concrete, demonstrate the reasonability of WPF used in concrete for environmental concerns, as well as identify the environmental impact contributions of each step in the production chain. Based on the LCA results, the possible suggestions for the technological process can be elucidated to improve the environmental performance of concrete block production combining with WPF disposal. Additionally, the LCA study aiming to obtain a cleaner manufacturing project was expected to provide supportive information for developers or policymakers to make an appropriate decision in terms of concrete production and waste paper management.

Scope definition: Two main parts of the scope definition of LCA should be clarified, the functional unit of production and system boundary.

Functional Unit (FU): It is important to select an appropriate functional unit for assessing the production system and comparing different production schemes. A volume or weight-based functional unit was adopted in earlier research relating to LCA of construction materials[130–132]. Damineli et al.[133] point out the inaccuracy of volume or weight-based functional unit since in most application cases the major function of concrete is physical or mechanical properties. Therefore, not only considering a constant volume or weight for the functional unit, the performance-based functional unit was proposed, a unit of functional performance including strength or durability such as compressive strength is widely considered to be appropriate and adopted in many articles[134–137]. The functional unit adopted in this study was 1 m^3 of concrete block for simplified calculation, which is comparable

to select one hollow CMU with the same dimension as a functional unit[138], since a CMU unit with the same configuration has the same apparent volume. Additionally, CUM is typically used for a non-loadbearing wall or partition wall with a specific cubage in practice, owing to the decreased density of PB caused by utilization of WPF, the volume or the amount of CMU is more appropriate. Crucially the prepared hollow CMU with 200 ×200 ×400 mm of dimensions (namely 8×8×16-inch blocks), meet the performance requirement of ASTM C140-14[87], especially with the similar strength. The mix proportion and physical properties for normal concrete and papercrete are listed in Table 33 and

Table 34, respectively. Physical properties were tested according to previous experimental results, and the mix proportion factors of papercrete where w/c, NHL, WPF-C and WPF-A is 0.48, 15%, 2% and 2%, respectively, complied the previous experimental design method to maintain a comparable 28-day compressive strength to the conventional concrete block.

Table 33 Materials and mix proportion for 1 m^3 normal concrete and papercrete.

CMU	Raw Materials (kg/m^3)						
	Cement	NHL	Sand	Gravel	WPF	Tap water	Superplasticizer
Conventional	354.17	/	626.77	1238.57	/	170	17.71
Papercrete	293.96	53.13	614.23	1213.8	15.2	199.37	17.71

Table 34 Major properties of normal concrete block and PB.

CMU	Density	Absorption	28-day Compressive Strength	Thermal Conductivity
	kg/m^3	%	MPa	W/m·K
Conventional	2385.21	3.47	8.87	1.82
Papercrete	2103.38	3.97	8.51	1.36

System boundary: To reach the target of investigation on the reasonability of using WPF as an alternative in concrete based on the LCA, not only the environmental impact caused by CMU production, also the potential benefits from avoided WPF disposal should be considered. Aiming to produce one functional unit defined previously, the production system started from all raw materials including upstream production to the finished product transported to the construction site. It is important that WPF is regarded as a raw material in a PB production system while WPF is discarded and treated in a conventional CMU production system.

Ideally, an integrated life cycle of a product, from cradle to grave. However, this research only considers the phases starting from raw materials to the use on-site as above described, the phases of installation, use, maintenance, demolishment and disposal were excluded. Several reasons were considered to limit this system boundary for evaluation: a) The raw materials production was reported to have the most environmental impact contribution for building blocks[139]. b) The configuration and properties of the blocks for PB and conventional CMU were identical. Meanwhile, there was no reliable and practicable data for PB installation, use and disposal. Therefore, it is assumed that the follow-up processes (after installation) will not differ significantly, the consumption and emissions were approximately equivalent.

Overall, the completed production system for manufacturing 1 m^3 CMU included two sections in this study, CMU production and WPF disposal, namely accounting for the cradle to construction site prepared for installation, as well as the expanded boundary caused by WPF disposal. Fig. 39 illustrated the profile of PB production combining WPF disposal, the avoided conventional disposal of WPF in the highlighted

after waste sorting processes. The raw materials production, transportation, WPF disposal and CMU production phases were marked. There were four scenarios established according to the different treatments for WPF. The differences of scenarios in Table 35 listed were described as following: scenario-1 to 3 contained the conventional CMU production, particularly, scenario-1 involved the incineration of WPF; scenario-2 involved landfill of WPF; scenario-3 involved the manufacture of recycled paper by using WPF; scenario-4 was a completed papercrete production procedure.

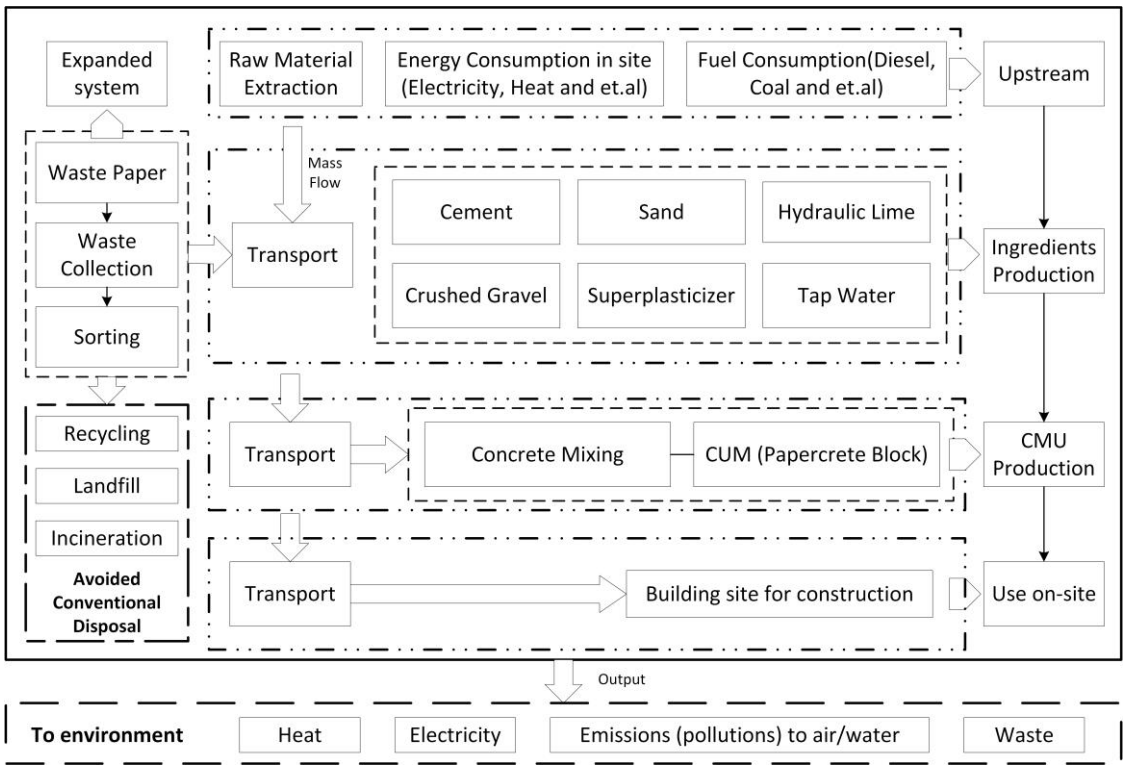

Fig. 39 System boundaries of PB production combining waste paper disposal (cradle to the site).

Table 35 The description of various scenarios for concrete block production coming with WPF disposal.

Scenario name	Description	Differences
Scenario-1	Conventional concrete block with the incineration of WPF.	WPF is treated by incineration to generate electricity or heating.
Scenario-2	Conventional concrete block with the landfill of WPF	WPF is treated with Municipal Waste for landfill.
Scenario-3	Conventional concrete block combing with the treatment of WPF for recycled paper	WPF is collected and processing for re-pulp, including all production processes.

Scenario-4	PB production processes	NHL and WPF are used to replace the 15% and 2% of cement by volume, totally 2% of aggregate in volume is replaced by WPF. Only involving WPF collection and sorting.

5.2.2 Life cycle inventory analysis

The LCI aims to It is required to clarify the allocation of the inputs and outputs, including mass flow in and out of the processes, specific substance of emissions and types of energy consumptions, during the LCI stage. Typically, a production system consisting of complex unit processes involved numerous input and output of mass and energy flow, thus some specialized software was used to allocate and establish the LCI and LCA model for auxiliary calculation, such as GaBi, SimaPro, TEAM and et. al[140]. In this study, openLCA 1.9, a user-friendly LCA software developed in Germany, was selected to calculate, evaluate, and interpret the established production system based on the LCI allocation.

The specific source and representative geographical code quoted of inventory data were listed in Table 36, which were reliable data sources. **Raw materials production**: the inventory data for all ingredients including Portland cement (CEM Ⅰ), NHL, sand, gravel, superplasticizer and tap water, along with other consumed materials such as fuel and energy, were obtained from Ecoinvent v3.6. **Manufacture of CMUs**: For conventional CMUs, the data of the concrete block production process from Ecoinvent database v3.6, involved the all processes of normal concrete block manufacture, including formation in a mould, air-dry and package. The transports and infrastructure during this process were included as well. However, the LCI of PB mixing and production, which is not available in existing literature or database, was established based on ingredients. As previously described and experimental results,

a comparable inventory of normal concrete mixing (25-30 MPa) and CUMs production was selected from the Ecoinvent database with relevance to the RoW geographical context, where entire manufacturing procedures (material treatment and mixing), energy, fuel and relevant infrastructure were involved. Meanwhile, papercrete production and PB production were under overall considered, which means the transportation between papercrete production and block manufacture was ignored. The activities of this production started from reception of raw ingredients at the concrete batching plant gate, the end of activities was ready-prepared products at the construction site before the delivery. **Disposal of WPF**: The different treatment of WPF was adopted in four scenarios, thus the inventory data of treatment was used from the database, only considering the newspaper. In scenario-1 and 2, WPF was treated as a part of municipal waste, where after sorted and transported for incineration or landfill. In scenario-3, after a set of pre-treatments WPF was used to produce the new newsprint. In scenario-4, WPF as a raw material of concrete was collected, sorted, and transported to the concrete mixing factory. **Transportation**: The internal transportation of each activity has been included in raw materials production phases. The defined transportation phases only involved the carriage between different stages, with various modes of transportation such as lorry, rail and et.al, as well as the default transport distance of regional statistical data. The calculation of the amount of transport in $ton \cdot km$ required for an average 1 kg of specific product by a given type of shipping is as following shown[141]:

$$T_{rp} = \frac{m_{stm} d_{stm} WWM}{m_{tot}} \quad (5\text{-}1)$$

where m_{stm} is the amount of the reference product transported by the specific mode of transportation in one year in the world; d_{stm} is the required transport

distance for total reference product; WWM is the wet mass of reference product; m_{tot} is the total yield of the reference product globally.

Table 36 Data source and region of LCI for major unit processes in the system.

Processes	Geographical code
Raw material production -Portland Cement[142–144]	
-Gravel and Sand[142,145]	RoW
-NHL[142,146] -Superplasticizer[147]	GLO and RoW
Concrete mixing plant[148,149] -Mixing -CMU production	RoW
-concrete mixing factory	GLO
Transportation[141] -transport model as the market -Transport by truck	GLO
Disposal -waste paper for incineration[150] -waste paper for landfill[151] -waste paper for recycling[152–154] -WPF production[155]	Row

RoW and GLO is the rest of the world and global data, where GLO is the average data for all countries globally, while RoW (Rest-of -the-World) is the GLO-based data and adjusted with considering the uncertainty.

5.2.3 Life Cycle Impact Assessment

To interpret the life cycle inventories based on these numerous impact data and types, LCIA was preformed to classify categories of environmental impact to specific indicators based on quantitative data of LCI, to explain the influence on the environment or human. The main steps of LCIA comprised characterization, normalization and weighting, specifically in the characterization stage the impact categories or indicators were calculated by multiplying the characterization factors relying on the contribution of each burden[156]. In the normalization and weighting stages, the midpoint indicators were further classified into the limited endpoint

according to the reference value (e.g. the average CO2 emissions globally in the year 2002), this processes aimed to evaluate the extent of contribution caused by the investigated system compared to the reference value within a specific time and area[157,158].

Accordingly, two types of indicators, midpoint, and endpoint method, were classified based on issue-orientation or damage-orientation. Midpoint indicators were more specific and directly related to LCI while endpoint indicators were more subjective with higher uncertainty, thus midpoint was appropriate to evaluate the specific contribution of burden and endpoint was applicable for production comparison[134,159]. As ISO 14040[127], ISO 14044[128] required, both two methods were recommended to use for enough interpretation and reasonable discussion.

Several assessment methods derived from these two approaches were available, such as CML 2001, Eco-indicator 99, ReCiPe, ILCD (Internal Reference Life Cycle Data System) and TRACI[129] as presented in Table 37, which is summarized according to the LCIA manual[129], especially the diagram of ReCiPe adopted by using openLCA and Ecoinvent 3.6[160] in this study was illustrated in Fig. 40, presenting the pathways of impact category calculation in midpoint and endpoint.

Table 37 Methodologies used for LCA[129].

Methodology	Inventor	Approach	
		Midpoint	Endpoint
CML	CML		√
Eco-indictor	PRé		√
EDIP97 –EDIP	DTU	√	
EPS	IVL		√
Impact	EPFL	√	√
LIME	AIST	√	√
LUCAS	CIRAIG	√	
ReCiPe	RUN + PRé + CML +RIVM	√	√
Swiss Ecoscarcity	E2+ ESU-services	√	

TRACI	US EPA	√
MEEuP	VhK	√

ReCiPe method integrated with the Ecoinvent v3.6 database contains the midpoint approach and the endpoint approach. There are three major perspectives for environmental assessment, H (Hierarchist), E (Egalitatain) and I (Individualist), resulting in a difference in the characterization, normalization and weighting factors[161]. Several representative indexes of LCA in the ReCiPe midpoint method are adopted to support the product decision by means of summarized assessment. Totally 18 different environmental impact categories are evaluated: agricultural land occupation ($ALOP, m^2a$), climate change ($GWP, kg, CO_2\ eq$), fossil depletion ($FDP, kg, oil\ eq$), freshwater ecotoxicity ($FETP, kg, 1{,}4\_\mathrm{DCB}\ eq$), freshwater eutrophication ($FEP, kg, P\ eq$), human toxicity ($HTP, kg, 1{,}4\_\mathrm{DCB}\ eq$), ionizing radiation ($RP\_HE, kg, U235\ eq$), marine ecotoxicity ($METP, kg, 1{,}4\_DCB\ eq$), marine eutrophication ($MEP, kg, N\ eq$), metal depletion ($MDP, kg, Fe\ eq$), natural land transformation ($NLTP, m^2$), ozone depletion ($ODP, kg, CFC\_11\ eq$), particulate matter formation ($PMFP, kg, PM_{10}\ eq$), photochemical oxidant formation ($POFP, kg, NMVOC\ eq$), terrestrial acidification ($TAP100, kg, SO_2\ eq$), terrestrial ecotoxicity ($TETP, kg, 1{,}4\_\mathrm{DCB}\ eq$), urban land occupation ($ULOP, m^2a$) and water depletion (WDP, m^3). Further, the after characterization, ReCiPe endpoint provides the normalization and weighting standards to convert the characterized impact indicators to be three specified categories for comparison. Table 38 show the different weighting method of ReCiPe, where in this study ReCiPe (H/A) method was adopted[162].

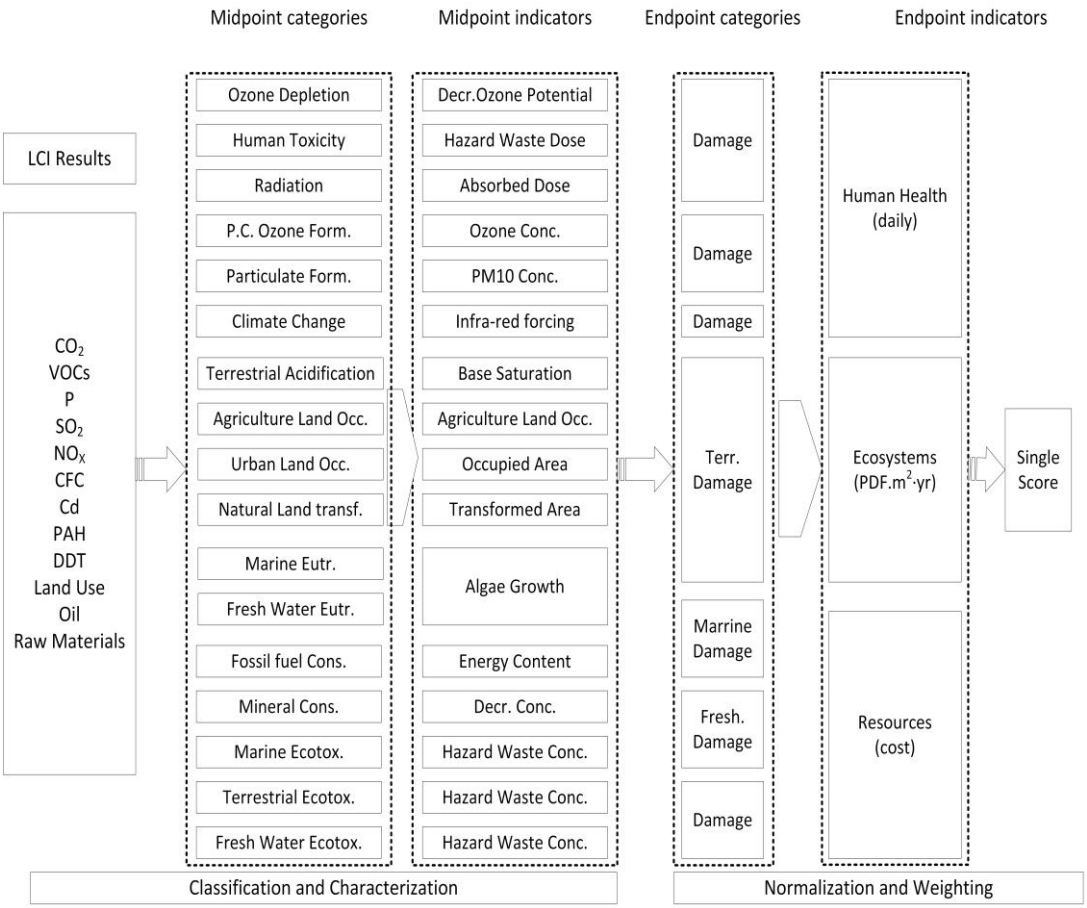

Fig. 40 The diagram of ReCiPe methodology involving midpoint and endpoint impact categories.

Table 38 Weighting factors of the ReCiPe method for normalization procedure.

ReCiPe method	Weighting value
ReCiPe (H/A)	Eco = 400; Hum = 400; Res = 200
ReCiPe (H/H)	Eco = 400; Hum = 300; Res = 300
ReCiPe (H/E)	Eco = 500; Hum = 300; Res = 200

5.3 Results and discussion

The major objectives of the LCIA are to expound the environmental impact of each technological process in the defined production system, by means of the comparisons between PB production and conventional concrete block production with system expansion of WPF disposal. The sensitivity analysis based on the mix proportion and transport distance was investigated to ascertain the changes caused by investigated factors.

5.5.1 Midpoint results analysis of different scenarios

Table 39 summarizes the characterized impact of four concrete block production scenarios by means of the Recipe Midpoint (H) method to investigate the environmental benefit of the given functional unit. Overall compared to the conventional concrete with the incineration of WPF, there is no remarkable improvement of PB production in terms of the life cycle perspective. Most impact indicators of scenario-3 achieve a favourable level, indicating paper recycling is still the most appropriate treatment, which is demonstrated by several studies[158,163]. GWP100, MDP, NLTP, ODP, POFP, TETP, and WDP of scenario-1 achieved a slight reduction compared to the other three scenarios. The main reasons causing the decrease of environmental indicators include: The consumption of natural aggregate is reduced slightly. Particularly, there is a significant increase of ALOP for scenario-4, compared to the minimum ALOP obtained in scenario-3 (expanded system of recycling paper production), increasing fourfold. The increase of land occupation is reasonable, considering the upstream of WPF production, a set of factories are required to be constructed, such as sorting and fibre production plant.

Although compared to scenario-3, there is no remarkable improvement on environmental impact for the utilization of WPF in CMUs, even increasing the part environmental impact, the midpoint indicators of scenario-4 presented comparable results to scenario-1 (incineration scheme), and better than scenario-2, where except for the increase of ALOP, GWP100, HTP, MEP, MDP, NLTP, ODP, POFP, TETP and WDP decreased by 4.8%, 7.3%, 6.3%, 7.8%, 9.2%, 11.1%, 24.2%, 7.4% and 1.6%, respectively.

The partly reduction of carbon dioxide emissions is due to the utilization of NHL replacing cement content, as discussed in the literature review section, compared with the production of cement, energy consumption and carbon dioxide emissions during the production of NHL is saved. Table 40 shows the comparison results of LCA between cement production and NHL production of 1 kg unit. The benefit of using NHL replacing Portland cement is demonstrated by this comparison.

Table 39 Recipe Midpoint (H) characterized impacts calculated for all scenarios, referred to as a functional unit of 1 m^3 of concrete block.

Impact Indicators	Unit	PB Production	Conventional Concrete Production		
		Scenario-4	Scenario-1	Scenario-2	Scenario-3
ALOP	m^2a	95.800	44.622	17.927	50.611
GWP100	kg CO_2-Eq	471.346	477.629	472.401	494.903
FDP	kg oil-Eq	98.089	95.153	95.063	96.802
FETP	kg 1,4-DCB-Eq	3.839	3.599	3.516	3.772
FEP	kg P-Eq	0.134	0.113	0.119	0.122
HTP	kg 1,4-DCB-Eq	157.458	140.607	141.021	148.593
IRP_HE	kg U235-Eq	12.749	13.911	12.155	13.753
METP	kg 1,4-DCB-Eq	3.654	3.442	3.356	3.609
MEP	kg N-Eq	0.413	0.413	0.405	0.440
MDP	kg Fe-Eq	50.000	54.194	53.900	54.227
NLTP	m^2	0.187	0.206	0.206	0.206
ODP	kg CFC-11-Eq	0.000	0.000	0.000	0.000
PMFP	kg PM10-Eq	0.817	0.773	0.764	0.784
POFP	kg NMVOC	0.990	1.283	1.270	1.310
TAP100	kg SO_2-Eq	1.181	1.098	1.101	1.134
TETP	kg 1,4-DCB-Eq	0.101	0.108	0.265	0.109
ULOP	m^2a	9.725	9.620	9.577	9.744
WDP	m^3	2.186	2.206	2.245	2.223

Table 40 Comparison of the impact of the production of cement per unit (1 kg) and NHL per unit (1 kg) by characterization ReCiPe Midpoint (H/A).

Impact indicators	Unit	Cement, Portland	NHL
ALOP	m^2a	0.058	0.043
GWP100	kg CO_2-Eq	0.922	0.895
FDP	kg oil-Eq	0.088	0.113
FETP	kg 1,4-DCB-Eq	0.003	0.003
FEP	kg P-Eq	0.000	0.000
HTP	kg 1,4-DCB-Eq	0.130	0.133
IRP_HE	kg U235-Eq	0.014	0.014
METP	kg 1,4-DCB-Eq	0.003	0.003
MEP	kg N-Eq	0.001	0.001
MDP	kg Fe-Eq	0.013	0.010

NLTP	m^2	0.000	0.000
ODP	kg CFC-11-Eq	0.000	0.000
PMFP	kg PM10-Eq	0.001	0.001
POFP	kg NMVOC	0.002	0.002
TAP100	kg SO_2-Eq	0.002	0.002
TETP	kg 1,4-DCB-Eq	0.000	0.000
ULOP	m^2a	0.003	0.003
WDP	m^3	0.001	0.001

Fig. 41 to Fig. 44 shows the contribution of each process to the environmental impact. Cement production makes a major contribution to most environmental impact except for MDP, ULOP and WDP. Compared to scenario-1-3, the contribution of cement production to each environmental impact decreases in scenario-4 due to the reduction of cement usage. Especially, IRE_He, ODP POFP of WPF production obtain the environmental credits, the reduction caused by waste paper sorting and transportation processes [142,164], the possible reasons is due to the utilization of methane and avoided incineration, however, these credits are inapparent in the whole system.

Additionally, due to reducing the weight of concrete, the contamination caused by transport has a reduction (however this aspect is not remarkable and affected by distance and carrying capacity). The energy consumption in scenario-4 is generated from the manufacture of WPF (WPF collection, sorting and fabrication, etc.). However, the recovery of paper is a credit of positive environmental influent.

5.5.2 Endpoint results analysis of different scenarios

The damage categories (endpoint) are weighted and normalized from the previous 18 different potential impacts. The production processes mentioned in the midpoint method are further classified into 4 sections including raw material production (cement, aggregate, superplasticizer, tap water, and NHL production), concrete block production (concrete mixing and block manufacture), transportation (transport of

raw materials to the concrete factory and transport of concrete block to the site of use) and WPF disposal (or WPF production).

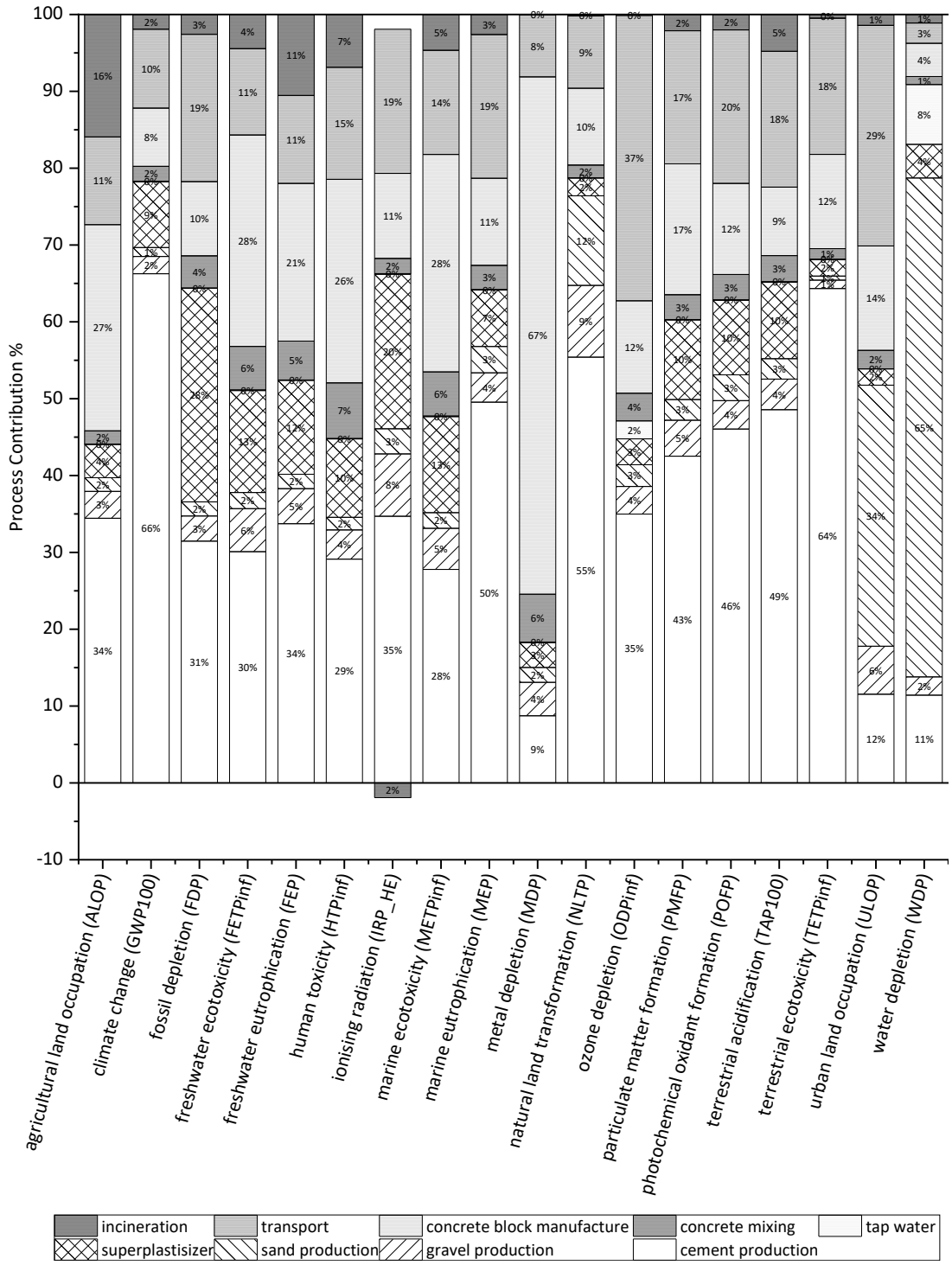

Fig. 41 Recipe Midpoint (H) characterized impacts for different steps of scenario-1, referred to a functional unit of 1 m^3 of PB.

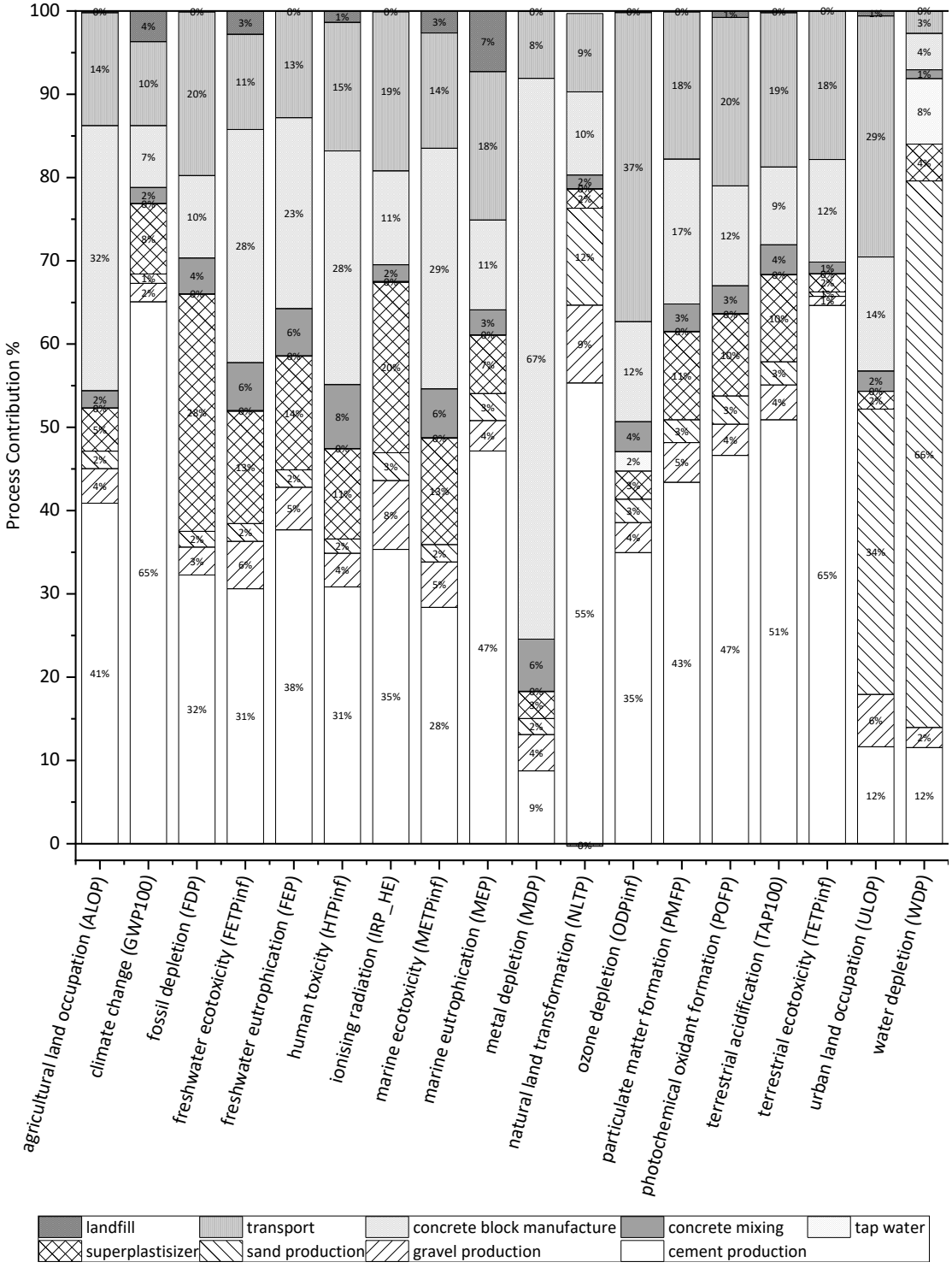

Fig. 42 Recipe Midpoint (H) characterized impacts for different steps of scenario-2, referred to a functional unit of 1 m^3 of PB.

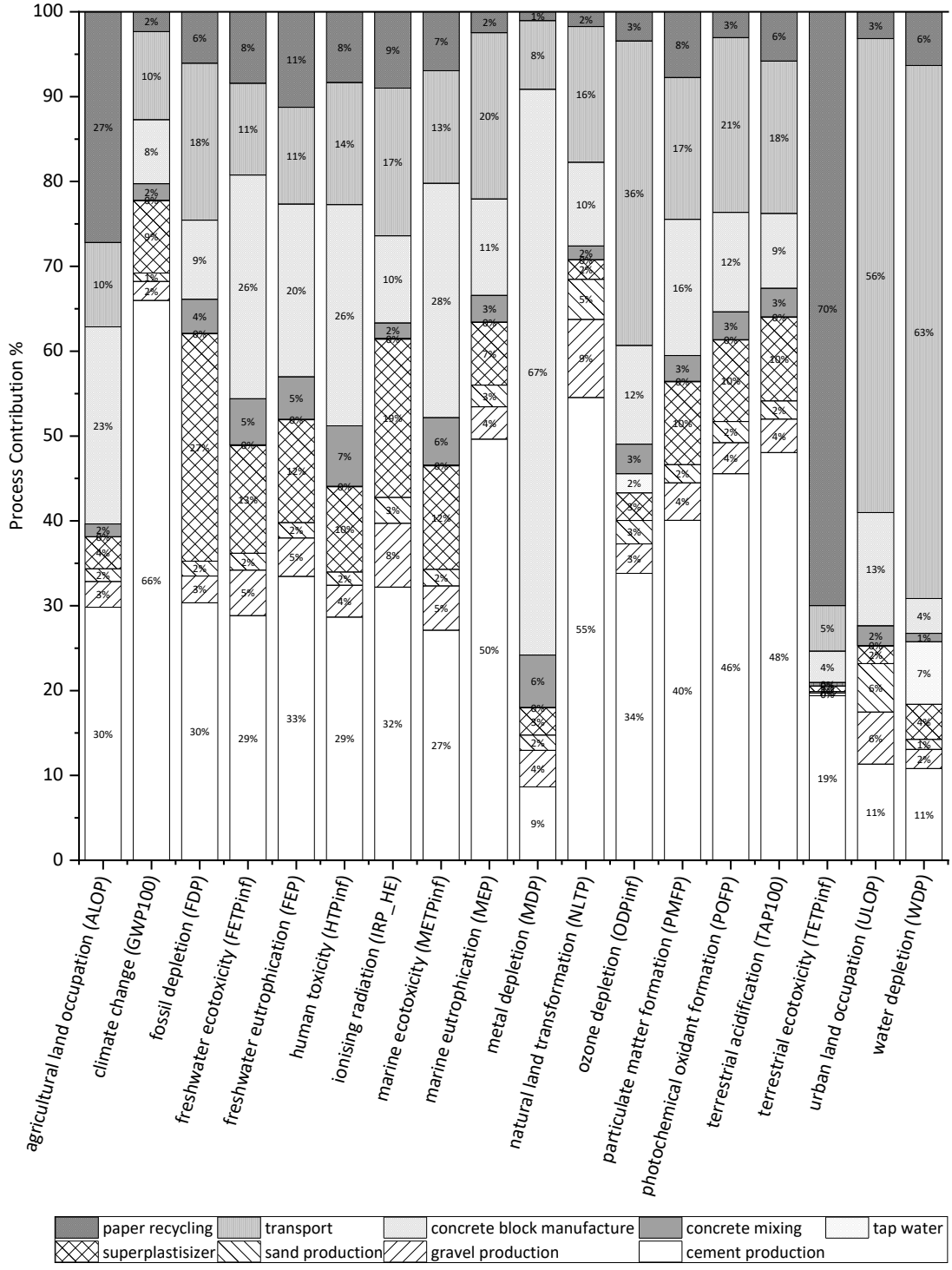

Fig. 43 Recipe Midpoint (H) characterized impacts for different steps of scenario-3, referred to a functional unit of 1 m^3 of PB.

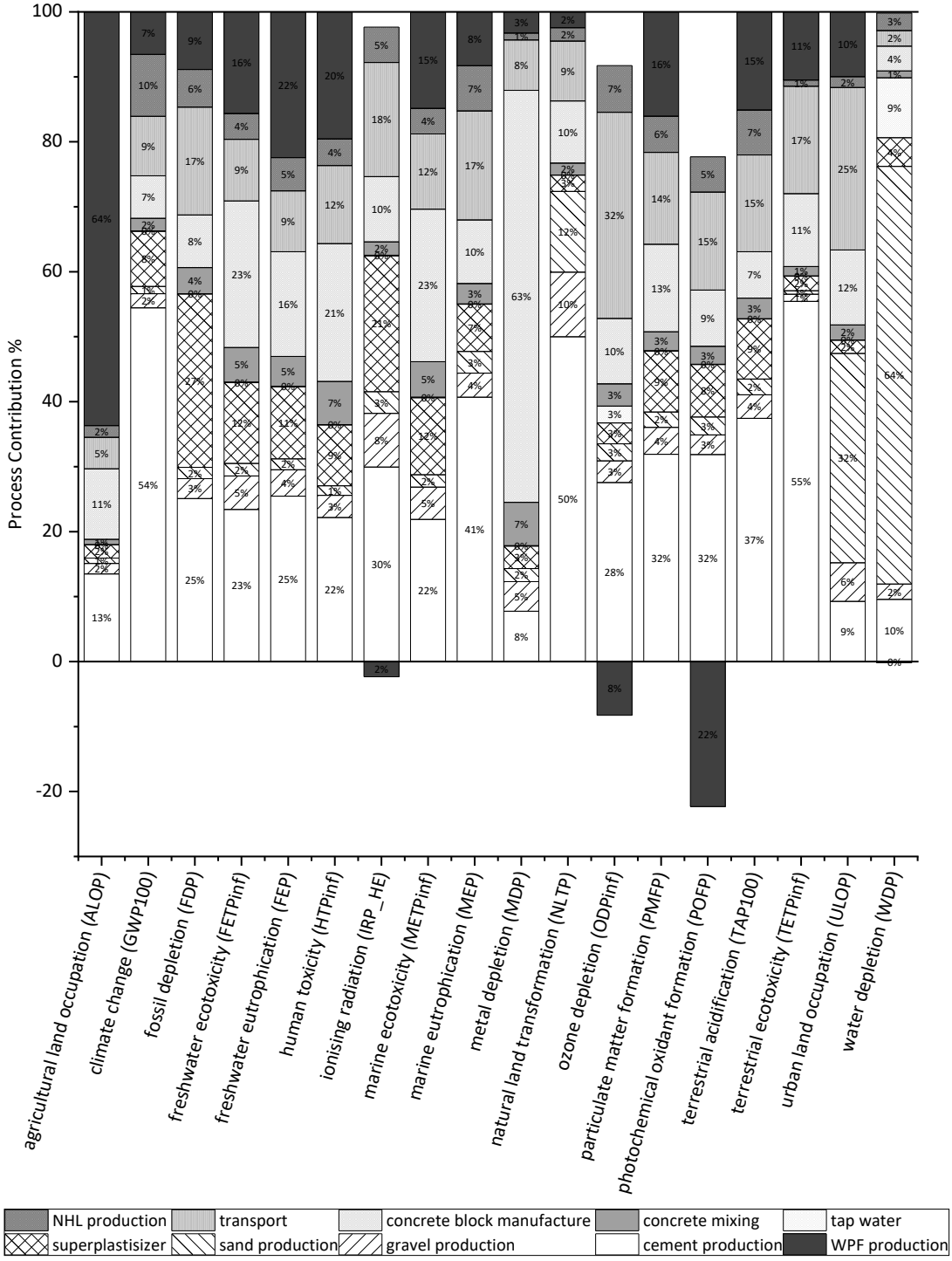

Fig. 44 Recipe Midpoint (H) characterized impacts for different steps of scenario-4, referred to a functional unit of 1 m^3 of PB.

In the case of ecosystem quality, the results of scenario-2, the incineration disposal of waste paper have a significant contribution to the increase of GWP, which is due to a large number of emissions to the air (such as CO_2, CO or VOCs), especially the contribution of GWP caused by incineration is more than 77%. There is a direct

relationship between various environmental indicator (energy consumption, GWP, EP, and HTP) and the incineration process, avoiding incineration of municipal waste can release the environmental impact efficiently. Nevertheless, the difference of GWP between scenario-1 and scenario-3 is not conspicuous. The results indicate the paper recycling process has little emissions to air. Major emissions during paper recycling procedures are derived from transport in the paper collection process. Furthermore, combing with the results of the previous comparison, the main environmental influence paper recycling make is due to energy consumption and organic pollution to water. The results of GWP100 demonstrate papercrete production by introducing a waste paper in mixes can reduce the greenhouse gas emissions efficiently even compared with conventional concrete, and major reduction processes are transportation and avoided appropriate incineration.

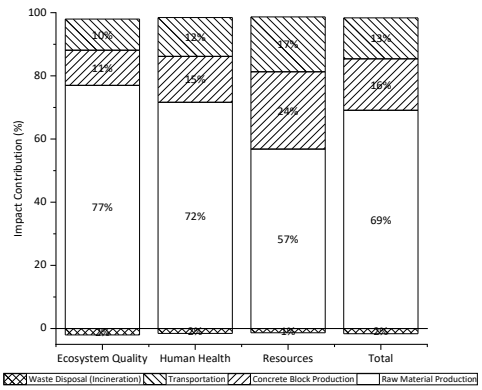

a) Scenario-1

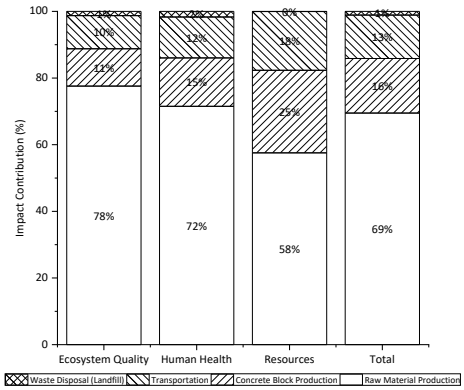

b) Scenario-2

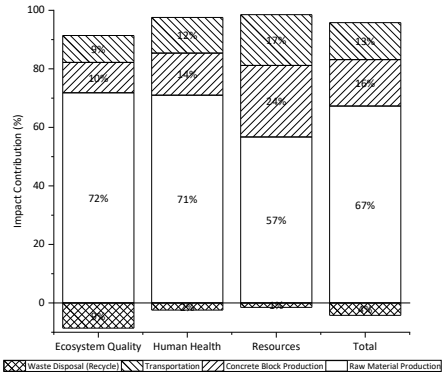

c) Scenario-3

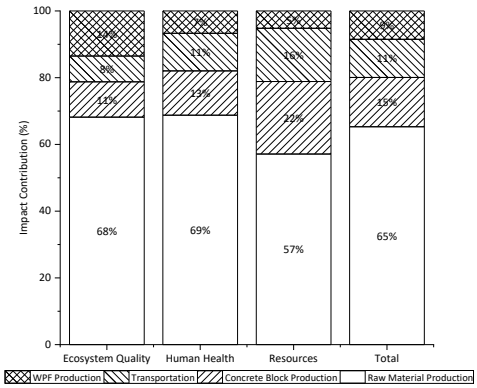

d) Scenario-4

Fig. 45 The impact contributions of papercrete production processes based on the endpoint method (scenario-4).

5.5.3 Sensitivity analysis of mix proportion

To access the effect of mixed proportion change on the environmental impact, since the environmental impact of NHL and cement is clarified previously, only WPF-C and WPF-A are modified. Table 41 shows the mix WPF replacement ratio in papercrete, the 28-day compressive strength with these mix proportion is comparable, around 8 MPa.

Table 41 Mix proportion for LCA comparison.

	w/c	NHL ratio	WPF-C	WPF-A
control	0.48	0	0	0
mix-1	0.48	15	2	2
mix-2	0.48	15	4	0
mix-3	0.48	15	0	4

Fig. 46 indicates the change of environmental indicators with mixing proportions varying. All indicators of scenario-4 with mix-2 achieve the lowest level compared to other scenarios. The increase in the replacement of cement make a positive effect on the environment. The total point of environmental damage for Scenario-4 with mix-1 is only comparable to scenario-2, namely the landfill disposal. However, the benefit of increasing WPF-C from 2% to 4% is remarkable, the energy consumption and emissions avoided from cement production, aggregate production and transport are more significant than that from the production of WPF. Additionally, the change of scenarios with mix-3 indicates the negative influence of WPF production is much larger than the benefit of avoided aggregates production.

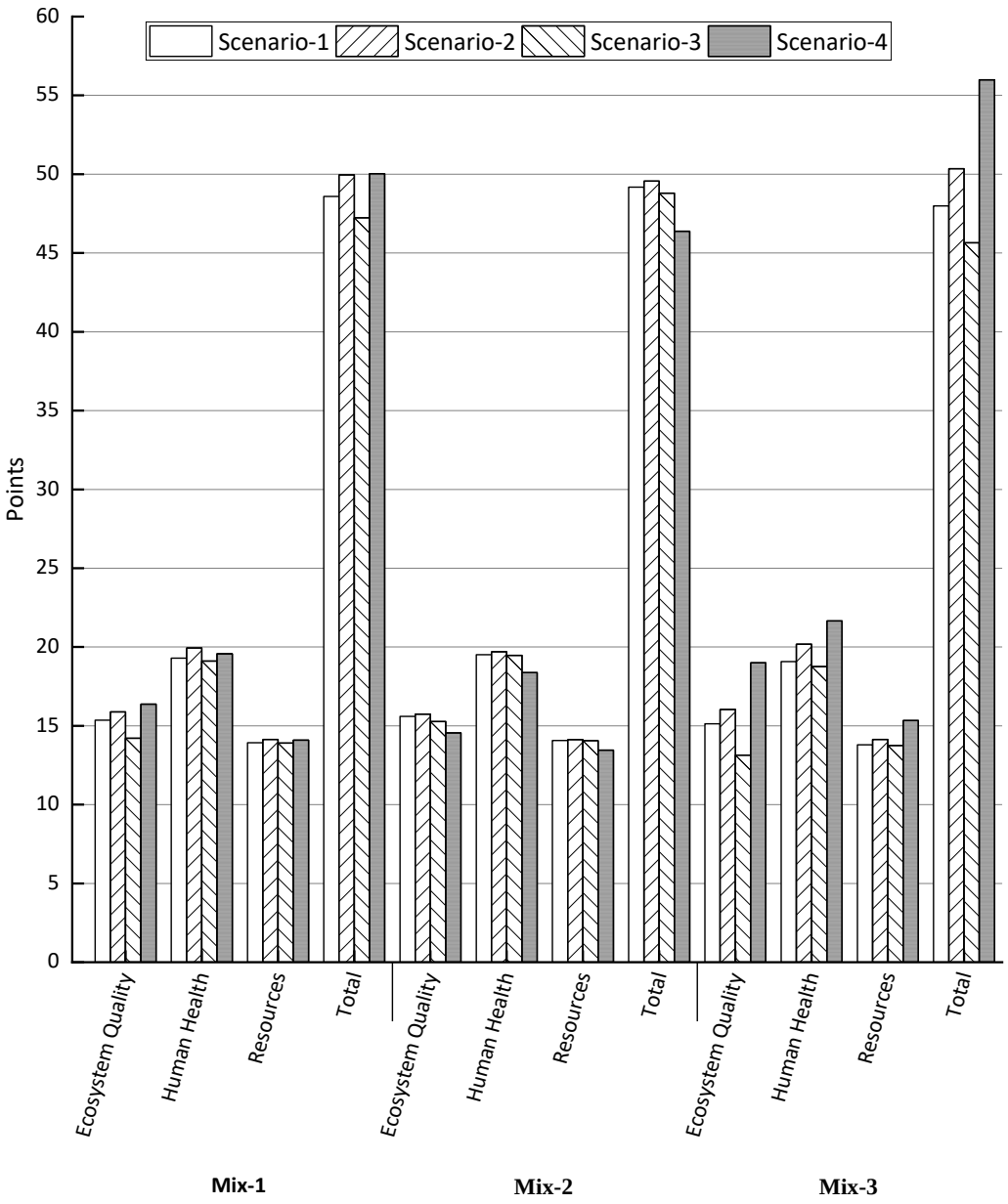

Fig. 46 The environmental indicators of each scenario with corresponding mix proportion based on endpoint method.

5.5.4 Sensitivity analysis of transport distance

It is predictable for the influence of transport distance on the environmental impact, thus, in this section, only scenario-3 and scenario-4 with mix-1 are selected for comparison. Fig. 47 shows that a simulation of transport distances for all transportation activities is conducted, by fixing the distance factor. For the total damage environment indicator, the limiting distance lower is 5 times. It is important

to mention that the analysis was performed for all impact categories, however, terrestrial ecotoxicity one stood out over the others.

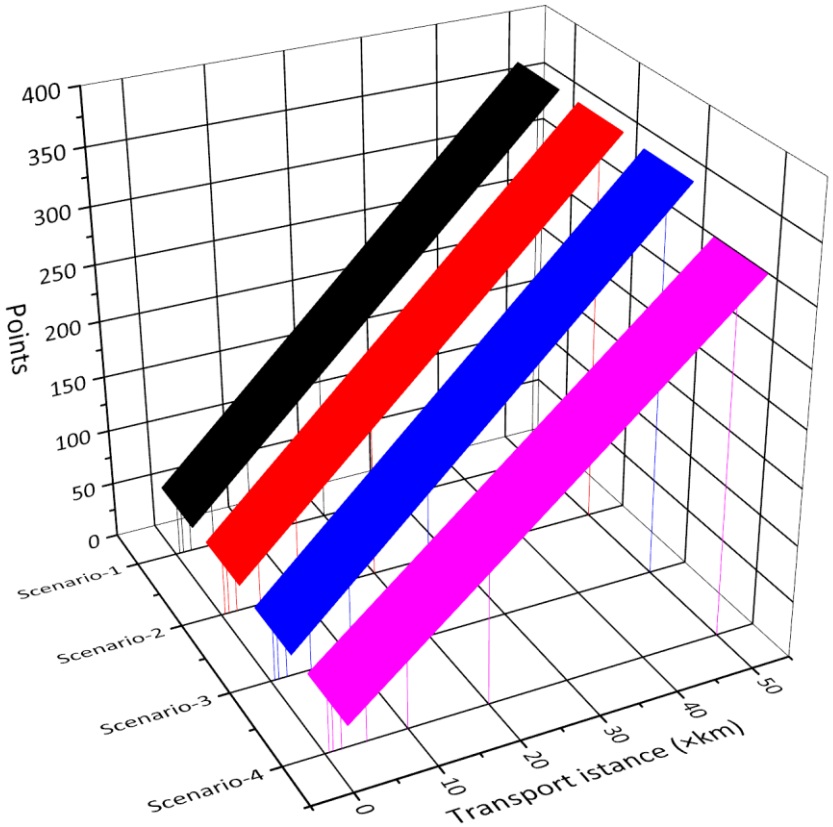

Fig. 47 Sensitivity analysis for all transportation distances, in terms of total damage point.

5.4 Summary

A cradle-to-gate LCA of papercrete combing with waste paper disposal procedures was conducted to evaluate if using waste paper as a replacement of concrete ingredients. LCA results for 1 m^3 of papercrete demonstrate using waste paper as a construction material is an environmentally friendly scheme. Compared with the waste paper incineration scheme, every environmental indicator improves, which has more than 70% reduction in greenhouse gas emissions. The most contribution is attributed to avoid incineration and reduction of cement use. However, in comparison with conventional concrete production, while waste paper recycled for

paper-making, the environmental indicator adopted in this study has a slight improvement; the difference of GWP is negligible.

Additionally, the use of hydraulic lime was demonstrated to achieve environmental credit due to the reduction of energy consumption and carbon dioxide emissions compared to cement production. The sensitivity analysis for transport distance and mix proportion was conducted for investigation. The weight reduction was also a vital advantage of papercrete, reducing transportation consumption and emission to achieve environmental benefits. Meanwhile, the environmental impact indicator presented the replacement of cement by WPF indeed benefit from reducing environmental impact, while the replacement of aggregate by WPF was not significant. The environmental impact of WPF production was considerable to cement production.

In summary, LCA results indicated the scheme of replacing cement was better than that of replacing aggregate with regard to environmental impact, and it was efficient to relieve the energy consumption and pollution to the environment for both concrete production and paper disposal. Papercrete production achieved environmental credit when the transportation distance increased.

Chapter 6 Conclusion and suggestion for future work

6.1 Introduction

This study was conducted to investigate the properties of the concrete block by introducing the waste paper fibre. To establish a systematic mix proportion method, w/c, dosage of NHL, and WPF are investigated based on RSM on the density, water absorption, 7-day compressive strength, 28-day compressive strength, softening coefficient and thermal properties to satisfy the requirement of concrete masonry unit in ASTM. The predictive model for all properties is established to guide the mixing design of the PB. ANOVA and the validation for the RSM model are carried out. Additionally, the SEM test and ultrasonic test are conducted to studies the mesoscopic structure and the compactness of the PB.

The environmental influence of PB production is investigated by means of LCA. An expanded system, including concrete production and waste disposal, is created to study the environmental contributions of a given functional unit of 1 m^3 PB.

6.2 Conclusion

In this study, according to the experimental results obtained, several conclusions were achieved as follow:

1) The significant variables and interactions were investigated on w/c, HL ratio, WPF-C and WPF-A in papercrete based on RSM, it is clear that the weight of PB decreases by 20% within an acceptable range. The reduction of compressive strength is significant by introducing WFP to replace the cement or aggregates. Slight increase of strength, water absorption, softening coefficient and SEM demonstrates that HL can improve the interface between cement and WPF when the relatively low ratio of

WPF, thus relieve the negative influence of WPF on the strength. In addition, due to the improvement in bonding, the density and thermal performance decrease slightly. Thermal conductivity decreases by 55.7% in the experimental range, which means thermal insulation is improved double by using WPF.

2) Based on the RSM results, the predictive functions for designed properties were validated, the developed models of density, water absorption, 7-day and 28-day compressive strength, softening coefficient and thermal conductivity for the PB was achieved by using the modified quadratic model with errors of less than 14%, and an optimized mix proportion was achieved by maximizing compressive strength and minimum density and absorption, which satisfied the requirement of building blocks in ASTM standard.

3) The LCA results demonstrate the feasibility of papercrete, compared to conventional concrete block production process with waste paper disposal. With the same substitution rate to cement and aggregates, the environmental influence is comparable to the convectional CMU production combining with a landfill of WPF. The utilization of HL reduces the consumption of cement so that the energy consumption and emissions are saved. Additionally, the increase of the substitution rate of cement by WPF or the decrease of the substitution rate of aggregate by WPF has a positive influence on the whole production system for achieving environmental credit, even comparable to the CMU production with WPF recycling scheme. It is vital that the manufacturing of WPF is not eco-friendly enough, which is just comparative to the landfilling. The increase of the transport distance makes the environmental benefit of PB production distinct due to the reduction of CMUs' weight.

6.3 Recommendations for future work

According to the studies and output previously, several suggestions for further research work can be conducted to improve the integrity of the papercrete study, which is summarized as follows:

The studies establish the predicate model by using RSM and investigate the effect of w/c, NHL and WPF

The present research focuses on the physical properties of papercrete, some physical or chemical properties can be conducted for the comparison of different test standards. For example, the resistance to carbonization or sorptivity involved in Chinese standards.

The studies focus on the softening coefficient expect for meeting the requirement of ASTM, thus some potentially improved properties can be tested and verified in future work, such as acoustics properties or free-thaw tests.

This study focuses on the LCA of papercrete involving in the “cradle to gate” of production. Further studies could be undertaken to investigate the integrated life span of PB, considering the improvement of the insulating properties.

Bibliography

[1] Sakai K, Noguchi T. The sustainable use of concrete. CRC press; 2012.

[2] Munasinghe M. Sustainable Development in Practice: Sustainomics Methodology and Applications. J Clean Prod 2009;15:253–8.

[3] Halliday S. Sustainable construction. Routledge; 2008.

[4] Harrison J. The role of materials in sustainable construction. Mater. Forum, vol. 30, Citeseer; 2006.

[5] Zabalza Bribián I, Valero Capilla A, Aranda Usón A. Life cycle assessment of building materials: Comparative analysis of energy and environmental impacts and evaluation of the eco-efficiency improvement potential. Build Environ 2011;46:1133–40. https://doi.org/http://dx.doi.org/10.1016/j.buildenv.2010.12.002.

[6] Nejat P, Jomehzadeh F, Taheri MM, Gohari M, Abd. Majid MZ. A global review of energy consumption, CO2 emissions and policy in the residential sector (with an overview of the top ten CO2 emitting countries). Renew Sustain Energy Rev 2015;43:843–62. https://doi.org/http://dx.doi.org/10.1016/j.rser.2014.11.066.

[7] Hong J, Shen GQ, Feng Y, Lau WS, Mao C. Greenhouse gas emissions during the construction phase of a building: a case study in China. J Clean Prod 2015;103:249–59. https://doi.org/http://dx.doi.org/10.1016/j.jclepro.2014.11.023.

[8] Robert A, Kummert M. Designing net-zero energy buildings for the future climate, not for the past. Build Environ 2012;55:150–8. https://doi.org/http://dx.doi.org/10.1016/j.buildenv.2011.12.014.

[9] Petek Gursel A, Masanet E, Horvath A, Stadel A. Life-cycle inventory analysis of concrete production: A critical review. Cem Concr Compos 2014;51:38–48. https://doi.org/http://dx.doi.org/10.1016/j.cemconcomp.2014.03.005.

[10] Valipour M, Yekkalar M, Shekarchi M, Panahi S. Environmental assessment of green concrete containing natural zeolite on the global warming index in marine environments. J Clean Prod 2014;65:418–23. https://doi.org/http://dx.doi.org/10.1016/j.jclepro.2013.07.055.

[11] Sjöström C. Approaches to sustainability in building construction. Struct Concr 2008.

[12] Van den Heede P, De Belie N. Environmental impact and life cycle assessment (LCA) of traditional and 'green' concretes: Literature review and theoretical calculations. Cem Concr Compos 2012;34:431–42. https://doi.org/http://dx.doi.org/10.1016/j.cemconcomp.2012.01.004.

[13] Vieira DR, Calmon JL, Coelho FZ. Life cycle assessment (LCA) applied to the manufacturing of common and ecological concrete: A review. Constr Build Mater 2016;124:656–66. https://doi.org/http://dx.doi.org/10.1016/j.conbuildmat.2016.07.125.

[14] Habert G, Bouzidi Y, Chen C, Jullien A. Development of a depletion indicator for natural resources used in concrete. Resour Conserv Recycl 2010;54:364–76. https://doi.org/http://dx.doi.org/10.1016/j.resconrec.2009.09.002.

[15] Oh BK, Choi SW, Park HS. Influence of variations in CO2 emission data upon environmental impact of building construction. J Clean Prod 2017;140, Part:1194–203. https://doi.org/http://dx.doi.org/10.1016/j.jclepro.2016.10.041.

[16] Akashi O, Hanaoka T, Matsuoka Y, Kainuma M. A projection for global CO2 emissions from the industrial sector through 2030 based on activity level and technology changes. Energy 2011;36:1855–67. https://doi.org/http://dx.doi.org/10.1016/j.energy.2010.08.016.

[17] Feiz R, Ammenberg J, Baas L, Eklund M, Helgstrand A, Marshall R. Improving the CO2 performance of cement, part I: utilizing life-cycle assessment and key performance indicators to assess development within the cement industry. J Clean Prod 2015;98:272–81. https://doi.org/http://dx.doi.org/10.1016/j.jclepro.2014.01.083.

[18] Metz B. IPCC Special Report on Carbon dioxide Capture and Storage. Econ Polit Clim Chang 2005.

[19] Worrell E, Price L, Martin N, Hendriks C, Meida LO. CARBON DIOXIDE EMISSIONS FROM THE GLOBAL CEMENT INDUSTRY. Environ Resour 2001;26:303–29.

[20] Meyer C. The greening of the concrete industry. Cem Concr Compos 2009;31:601–5. https://doi.org/http://dx.doi.org/10.1016/j.cemconcomp.2008.12.010.

[21] Habert G, Billard C, Rossi P, Chen C, Roussel N. Cement production technology improvement compared to factor 4 objectives. Cem Concr Res

2010;40:820–6.
https://doi.org/http://dx.doi.org/10.1016/j.cemconres.2009.09.031.

[22] Price L, Hasanbeigi A, Lu H, Wang L. Analysis of Energy-Efficiency Opportunities for the Cement Industry in Shandong Province, China. Lawrence Berkeley Natl Lab 2009.

[23] Randl N, Steiner T, Ofner S, Baumgartner E, Mészöly T. Development of UHPC mixtures from an ecological point of view. Constr Build Mater 2014;67, Part C:373–8.
https://doi.org/http://dx.doi.org/10.1016/j.conbuildmat.2013.12.102.

[24] Knoeri C, Binder CR, Althaus HJ. Decisions on recycling: Construction stakeholders' decisions regarding recycled mineral construction materials. Resour Conserv Recycl 2011;55:1039–50.
https://doi.org/10.1016/j.resconrec.2011.05.018.

[25] Van den Heede P, De Belie N. Environmental impact and life cycle assessment (LCA) of traditional and 'green' concretes: Literature review and theoretical calculations. Cem Concr Compos 2012;34:431–42.
https://doi.org/10.1016/j.cemconcomp.2012.01.004.

[26] Siddique R. Waste Materials and By-Products in Concrete. Springer Berlin 2008.

[27] Damtoft JS, Lukasik J, Herfort D, Sorrentino D, Gartner EM. Sustainable development and climate change initiatives. Cem Concr Res 2008;38:115–27.

[28] Flower DJM, Sanjayan JG. Green house gas emissions due to concrete manufacture. Int J Life Cycle Assess 2007;12:282–8.

[29] O'Brien KR, Ménaché J, O'Moore LM. Impact of fly ash content and fly ash transportation distance on embodied greenhouse gas emissions and water consumption in concrete. Int J Life Cycle Assess 2009;14:621–9.

[30] Turk J, Cotič Z, Mladenovič A, Šajna A. Environmental evaluation of green concretes versus conventional concrete by means of LCA. Waste Manag 2015;45:194–205. https://doi.org/http://dx.doi.org/10.1016/j.wasman.2015.06.035.

[31] Napolano L, Menna C, Graziano SF, Asprone D, D'Amore M, de Gennaro R, et al. Environmental life cycle assessment of lightweight concrete to support recycled materials selection for sustainable design. Constr Build Mater 2016;119:370–84. https://doi.org/http://dx.doi.org/10.1016/j.conbuildmat.2016.05.042.

[32] Anastasiou EK, Liapis A, Papayianni I. Comparative life cycle assessment of concrete road pavements using industrial by-products as alternative materials. Resour Conserv Recycl 2015;101:1–8. https://doi.org/http://dx.doi.org/10.1016/j.resconrec.2015.05.009.

[33] Zhang J, Liu G, Chen B, Song D, Qi J, Liu X. Analysis of CO 2 Emission for the Cement Manufacturing with Alternative Raw Materials: A LCA-based Framework ☆. Energy Procedia 2014;61:2541–5.

[34] Manuel JS. How do paper houses stack up? Environ Health Perspect 2002;110:A126. https://doi.org/10.1289/ehp.110-a126.

[35] Fuller BJ, Fafitis A, Santamaria JL. The paper alternative. Civ Eng YORK THEN RESTON- 2006;76:72.

[36] US-EPA. Wastes - Resource Conservation - Common Wastes & Materials – Paper Recycling, 2012. http://www.epa.gov/wastes/conserve/materials/paper/.

[37] 2015 Annual Report of China's Paper Industry. China Pap Newsletters n.d.:99–111.

[38] Lin B, Zheng Q. Energy efficiency evolution of China's paper industry. J Clean Prod 2017;140, Part:1105–17. https://doi.org/http://dx.doi.org/10.1016/j.jclepro.2016.10.059.

[39] CEPI. Preliminary Statistics 2015. Confed Eur Pap Ind 2015:1–3.

[40] Liang S, Zhang T, Xu Y. Comparisons of four categories of waste recycling in China's paper industry based on physical input–output life-cycle assessment model. Waste Manag 2012;32:603–12. https://doi.org/http://dx.doi.org/10.1016/j.wasman.2011.10.020.

[41] Modak N, Spence K, Sood S, Rosati JA. Building a Comprehensive Mill-Level Database for the Industrial Sectors Integrated Solutions (ISIS) Model of the U.S. Pulp and Paper Sector. PLoS One 2015;10.

[42] Acharya PK, Patro SK. Use of ferrochrome ash (FCA) and lime dust in concrete preparation. J Clean Prod 2016;131:237–46. https://doi.org/http://doi.org/10.1016/j.jclepro.2016.05.042.

[43] Detwiler R, Tennis PD. The Use of Limestone in Portland Cement : A State-of-the-Art Review. Eb227 Skokie Portl Cem Assoc 1996.

[44] Barbhuiya SA, Gbagbo JK, Russell MI, Basheer PAM. Properties of fly ash concrete modified with hydrated lime and silica fume. Constr Build Mater 2009;23:3233–9.

[45] Acharya PK, Patro SK. Effect of lime and ferrochrome ash (FA) as partial replacement of cement on strength, ultrasonic pulse velocity and permeability of concrete. Constr Build Mater 2015;94:448–57. https://doi.org/http://doi.org/10.1016/j.conbuildmat.2015.07.081.

[46] Kanellopoulos A, Nicolaides D, Petrou MF. Mechanical and durability properties of concretes containing recycled lime powder and recycled aggregates. Constr Build Mater 2014;53:253–9. https://doi.org/http://doi.org/10.1016/j.conbuildmat.2013.11.102.

[47] Walker R, Pavia S, Mitchell R. Mechanical properties and durability of hemp-lime concretes. Constr Build Mater 2014;61:340–8. https://doi.org/http://doi.org/10.1016/j.conbuildmat.2014.02.065.

[48] Elfordy S, Lucas F, Tancret F, Scudeller Y, Goudet L. Mechanical and thermal properties of lime and hemp concrete (“hempcrete”) manufactured by a projection process. Constr Build Mater 2008;22:2116–23.

[49] Wolfe R, Gjinolli AE. Assessment of cement-bonded wood composites as means of using low-valued wood for engineered applications. Int. wood Eng. Conf., 1996, p. 74–80.

[50] Pavasars I, Hagberg J, Borén H, Allard B. Alkaline Degradation of Cellulose: Mechanisms and Kinetics. J Polym Environ 2003;11:39–47.

[51] Mármol G, Santos SF, Savastano Jr. H, Borrachero M V, Monzó J, Payá J. Mechanical and physical performance of low alkalinity cementitious composites reinforced with recycled cellulosic fibres pulp from cement kraft bags. Ind Crops Prod 2013;49:422–7. https://doi.org/http://doi.org/10.1016/j.indcrop.2013.04.051.

[52] Yun H, Jung H, Choi C. Mechanical properties of papercrete containing waste paper. 18th Int. Conf. Compos. Mater., 2007.

[53] Sangrutsamee V, Srichandr P, Poolthong N. Re-Pulped Waste Paper-Based Composite Building Materials with Low Thermal Conductivity. J Asian Archit Build Eng 2012;11:147–51.

[54] Akinwumi II, Olatunbosun OM, Olofinnade OM, Awoyera PO. Structural evaluation of lightweight concrete produced using waste newspaper and office paper. Civ Environ Res 2014;6:160–7.

[55] Aigbomian EP, Fan M. Development of Wood-Crete building materials from sawdust and waste paper. Constr Build Mater 2013;40:361–6. https://doi.org/http://dx.doi.org/10.1016/j.conbuildmat.2012.11.018.

[56] Subramani T, Shanmugam G. Experimental Investigation Of Using Papercrete And Recycled Aggregate As A Coarse Aggregate. Int J Appl or Innov Eng Manag 2015;4:323–32.

[57] Pivnenko K, Eriksson E, Astrup TF. Waste paper for recycling: Overview and identification of potentially critical substances. Waste Manag 2014;45:134–42. https://doi.org/10.1016/j.wasman.2015.02.028.

[58] Selvaraj R, Priyanka R, Amirthavarshini M, Prabavathy S. EVALUATION OF PAPERCRETE: An Innovative Building Material. Int J Eng Adv Res Technol 2015;1.

[59] Kumar BH, Prakash N. Studies on strength and weight loss of paper concrete. Proc Inst Civ Eng - Eng Sustain 2016;169:39–44. https://doi.org/10.1680/ensu.14.00057.

[60] Booya E, Ghaednia H, Das S, Pande H. Durability of cementitious materials reinforced with various Kraft pulp fibers. Constr Build Mater 2018;191:1191–200. https://doi.org/10.1016/j.conbuildmat.2018.10.139.

[61] Rao A, Jha KN, Misra S. Use of aggregates from recycled construction and demolition waste in concrete. Resour Conserv Recycl 2007;50:71–81.

[62] Chung JH, Kim BH, Choi HK, Choi CS. Development of Papercrete due to Paper mixing ratio. Hanyang Univ Seoul, Korea 2015.

[63] Anandaraju K, Raj BJR, VijayaSarathy R. Experimental Investigation of Papercrete Brick. Int J Mach Constr Eng 2015;2:2394–3025.

[64] Arya RK, Kansal R. Utilization of Waste Papers to Produce Ecofriendly Bricks. Int J Sci Res 2016;5.

[65] Kawashima S, Shah SP. Early-age autogenous and drying shrinkage behavior of cellulose fiber-reinforced cementitious materials. Cem Concr Compos 2011;33:201–8. https://doi.org/10.1016/j.cemconcomp.2010.10.018.

[66] Jil Tushar Sheth SJ. Paper Crete: A Sustainable Building Material. Strateg. Technol. Complex Environ. Issues-A Sustain. Approach, 2014.

[67] Santamaria J, Fuller B, Fafitis A. Structural properties of a new material made of waste paper. Comput Methods Exp Meas XIII, WIT Trans Model Simul 2007;46:557–67.

[68] Seyyedalipour SF, Kebria DY. Study of Utilization of Pulp and Paper Industry Wastes in Production of Concrete. Int J Eng Res Appl 2014;4.

[69] Deng YH, Furuno T. Study on Gypsum-Bonded Particleboard Reinforced with Jute Fibres. Holzforschung 2002;56:440–5.

[70] Jegatheeswaran D. Studies on strength, durability and structural properties of flyash based papercrete building bricks. Chennai n.d.

[71] Paper Houses. Mother Earth News 2000:46.

[72] Decard JD, West RP, Prichard SJ. THE IMPACT RESPONSE OF RECYCLED PAPER WASTE CONCRETE. Thomas Telford 2001.

[73] Modry S. USE OF WASTE PAPER AS A CONSTITUENT OF CONCRETE. Thomas Telford 2001.

[74] ISO EN. 717-2 (1996): Acoustics–Rating of sound insulation in buildings and of building elements–Part 2: Impact sound insulation. Int Organ Stand ISO, Geneva, Switz n.d.

[75] Grist ER, Paine KA, Heath A, Norman J, Pinder H. Structural and durability properties of hydraulic lime-pozzolan concretes. Cem Concr Compos 2015;62:212–23. https://doi.org/10.1016/j.cemconcomp.2015.07.001.

[76] Pozo-Antonio JS. Evolution of mechanical properties and drying shrinkage in lime-based and lime cement-based mortars with pure limestone aggregate. Constr Build Mater 2015;77:472–8. https://doi.org/10.1016/j.conbuildmat.2014.12.115.

[77] EN BS. 459-1: 2015 Building lime. Defin Specif Conform Criteria (Vol BS EN 459-1 2015, Pp 56) BSI Stand Ltd 2015.

[78] Lawrence RM, Mays TJ, Rigby SP, Walker P, Ayala DD. Effects of carbonation on the pore structure of non-hydraulic lime mortars 2007;37:1059–69. https://doi.org/10.1016/j.cemconres.2007.04.011.

[79] Lanas J, Alvarez JI. Masonry repair lime-based mortars : Factors affecting the mechanical behavior 2003;33:1867–76. https://doi.org/10.1016/S0008-8846(03)00210-2.

[80] Velosa AL, Cachim PB. Hydraulic-lime based concrete : Strength development using a pozzolanic addition and different curing conditions. Constr Build Mater 2009;23:2107–11. https://doi.org/10.1016/j.conbuildmat.2008.08.013.

[81] Spycha E. The effect of lime and cellulose ether on selected properties of plastering mortar. Procedia Eng 2015;108:324–31. https://doi.org/10.1016/j.proeng.2015.06.154.

[82] Liu H, Zhao Y, Peng C, Song S, López A. Lime mortars – The role of carboxymethyl cellulose on the crystallization of calcium carbonate. Constr Build Mater 2018;168:169–77. https://doi.org/10.1016/j.conbuildmat.2018.02.119.

[83] Fuller B. Formal Tests. Living Pap 2011. http://www.livinginpaper.com/tests.htm.

[84] ASTM C55-17. Standard Specification for Concrete Building Brick 2017. https://doi.org/10.1520/C0055-17.

[85] Vinet L, Zhedanov A. A “missing” family of classical orthogonal polynomials. J Phys A Math Theor 2011;44:1–4. https://doi.org/10.1088/1751-8113/44/8/085201.

[86] ASTM C129-17. Standard Specification for Nonloadbearing Concrete Masonry Units 2017. https://doi.org/10.1520/C0129-17.

[87] ASTM C140/C140M-18a. Standard Test Methods for Sampling and Testing Concrete Masonry Units and Related Units 2018. https://doi.org/10.1520/C0140_C0140M-18A.

[88] Environments A. Standard Specification for Cellulose Fibers for Fiber-Reinforced Concrete 1 2012;07:5–7. https://doi.org/10.1520/D7357-07R12.2.

[89] GB/T 4111-2013. Test method for the concrete block and brick 2013.

[90] ASTM C1058 / C1058M-10. Standard Practice for Selecting Temperatures for Evaluating and Reporting Thermal Properties of Thermal Insulation 2015.

[91] ASTM C687-18. Standard Practice for Determination of Thermal Resistance of Loose-Fill Building Insulation 2018.

[92] C1363-19 A. Standard Test Method for Thermal Performance of Building Materials and Envelope Assemblies by Means of a Hot Box Apparatus 2019.

[93] ASTM C1045-19. Practice for Calculating Thermal Transmission Properties Under Steady-State Conditions 2019.

[94] 2008 GB 8076. Concrete Mixtures 2008.

[95] ASTM D1480-15. Standard Test Method for Density and Relative Density (Specific Gravity) of Viscous Materials by Bingham Pycnometer 2015. https://doi.org/10.1520/D1480-15.

[96] ASTM C136 / C136M-14. Standard Test Method for Sieve Analysis of Fine and Coarse Aggregates 2014. https://doi.org/10.1520/C0136_C0136M-14.

[97] ASTM. Astm C33-03 2010;i:1–11. https://doi.org/10.1520/C0033.

[98] ASTM C127−15. Standard Test Method for Relative Density (Specific Gravity) and Absorption of Coarse Aggregate 2015. https://doi.org/10.1520/C0127-15.

[99] ASTM C128-15. Standard Test Method for Relative Density (Specific Gravity) and Absorption of Fine Aggregate 2015. https://doi.org/10.1520/C0128-15.

[100] TAPPI T 232. FIBER LENGTH OF PULP BY PROJECTION 2013:7.

[101] TAPPI T 233. FIBER LENGTH OF PULP BY CLASSIFICATION 2006:7.

[102] TAPPI T 234. COARSENESS OF PULP FIBERS 2012:6.

[103] Okubayashi S, Griesser UJ, Bechtold T. A kinetic study of moisture sorption and desorption on lyocell fibers. Carbohydr Polym 2004;58:293–9. https://doi.org/10.1016/j.carbpol.2004.07.004.

[104] Mohr BJ, Biernacki JJ, Kurtis KE. Supplementary cementitious materials for mitigating degradation of kraft pulp fiber-cement composites. Cem Concr Res 2007;37:1531–43. https://doi.org/10.1016/j.cemconres.2007.08.001.

[105] Mohr BJ, Biernacki JJ, Kurtis KE. Microstructural and chemical effects of wet/dry cycling on pulp fiber-cement composites. Cem Concr Res 2006;36:1240–51. https://doi.org/10.1016/j.cemconres.2006.03.020.

[106] Grist ER, Paine KA, Heath A, Norman J, Pinder H. The environmental credentials of hydraulic lime-pozzolan concretes. J Clean Prod 2015;93:26–37. https://doi.org/10.1016/j.jclepro.2015.01.047.

[107] American Concrete Institute. ACI 211.3R-02: Guide for selecting proportions for no-slump concrete. . ACI Comm 211 2009:1–26.

[108] ACI211.3R. Guide for Selecting proportions for No-Slump Concrete 2002.

[109] Box GEP, Wilson KB. On the experimental attainment of optimum conditions. J R Stat Soc Ser B 1951;13:1–38.

[110] Chang K-H. e-Design: computer-aided engineering design. Academic Press; 2016.

[111] Arora JS. Introduction to optimum design. Elsevier; 2004.

[112] Ahuja SK, Ferreira GM, Moreira AR. Application of Plackett-Burman design and response surface methodology to achieve exponential growth for aggregated shipworm bacterium. Biotechnol Bioeng 2004;85:666–75.

[113] Mohammed BS, Fang OC, Anwar Hossain KM, Lachemi M. Mix proportioning of concrete containing paper mill residuals using response surface methodology. Constr Build Mater 2012;35:63–8. https://doi.org/http://dx.doi.org/10.1016/j.conbuildmat.2012.02.050.

[114] Li W, Cai L, Wu Y, Liu Q, Yu H, Zhang C. Assessing recycled pavement concrete mechanical properties under joint action of freezing and fatigue via RSM. Constr Build Mater 2018;164:1–11. https://doi.org/10.1016/j.conbuildmat.2017.12.219.

[115] Rezaifar O, Hasanzadeh M, Gholhaki M. Concrete made with hybrid blends of crumb rubber and metakaolin: Optimization using Response Surface Method. Constr Build Mater 2016;123:59–68. https://doi.org/http://dx.doi.org/10.1016/j.conbuildmat.2016.06.047.

[116] Jahan A, Edwards KL, Bahraminasab M. 6 - Multiple objective decision-making for material and geometry design. In: Jahan A, Edwards KL, Bahraminasab MBT-MDA for S the S of EM in PD (Second E, editors., Butterworth-Heinemann; 2016, p. 127–46. https://doi.org/https://doi.org/10.1016/B978-0-08-100536-1.00006-0.

[117] Montgomery DC. Design and analysis of experiments. John wiley & sons; 2017.

[118] ASTM C1552-16. Standard Practice for Capping Concrete Masonry Units, Related Units and Masonry Prisms for Compression Testing 2016. https://doi.org/www.astm.org.

[119] Bolton W. 8 - System models. In: Bolton WBT-I and CS, editor. Instrum. Control Syst., Oxford: Newnes; 2004, p. 179–99. https://doi.org/https://doi.org/10.1016/B978-075066432-5/50008-5.

[120] Khuri AI, Mukhopadhyay S. Response surface methodology. Wiley Interdiscip Rev Comput Stat 2010;2:128–49. https://doi.org/10.1002/wics.73.

[121] Mtarfi NH, Rais Z, Taleb M, Kada KM. Effect of fly ash and grading agent on the properties of mortar using response surface methodology. J Build Eng 2017;9:109–16. https://doi.org/10.1016/j.jobe.2016.12.004.

[122] Khedari J, Suttisonk B, Pratinthong N, Hirunlabh J. New lightweight composite construction materials with low thermal conductivity. Cem Concr Compos 2001;23:65–70.

[123] Kim KH, Jeon SE, Kim JK, Yang S. An experimental study on thermal conductivity of concrete. Cem Concr Res 2003;33:363–71. https://doi.org/10.1016/S0008-8846(02)00965-1.

[124] C597 A. Standard Test Method for Pulse Velocity Through Concrete, ASTM International 2016.

[125] Bentchikou M, Guidoum A, Scrivener K, Silhadi K, Hanini S. Effect of recycled cellulose fibres on the properties of lightweight cement composite matrix. Constr Build Mater 2012;34:451–6. https://doi.org/10.1016/j.conbuildmat.2012.02.097.

[126] Ardanuy M, Claramunt J, Toledo Filho RD. Cellulosic fiber reinforced cement-based composites: A review of recent research. Constr Build Mater 2015;79:115–28. https://doi.org/10.1016/j.conbuildmat.2015.01.035.

[127] Finkbeiner M, Inaba A, Tan RBH, Christiansen K, Klueppel H-J. The New International Standards for Life Cycle Assessment: ISO 14040 and ISO 14044. Int J Life Cycle Assess 2006;11:80–5.

[128] ISO-14044. Environmental management:life cycle assessment: requirements and guidelines 2006.

[129] European Commission - Joint Research Centre - Institute for Environment and Sustainability. International Reference Life Cycle Data System (ILCD) Handbook : Analysing of existing Environmental Impact Assessment methodologies for use in Life Cycle Assessment. Eur Comm 2010:115.

[130] Harrison GP, Maclean E (Ned) J, Karamanlis S, Ochoa LF. Life cycle assessment of the transmission network in Great Britain. Energy Policy 2010;38:3622–31. https://doi.org/10.1016/j.enpol.2010.02.039.

[131] Petek Gursel A, Masanet E, Horvath A, Stadel A. Life-cycle inventory analysis of concrete production: A critical review. Cem Concr Compos 2014;51:38–48. https://doi.org/10.1016/j.cemconcomp.2014.03.005.

[132] Hacker JN, De Saulles TP, Minson AJ, Holmes MJ. Embodied and operational carbon dioxide emissions from housing: A case study on the effects of thermal mass and climate change. Energy Build 2008;40:375–84. https://doi.org/10.1016/j.enbuild.2007.03.005.

[133] Damineli BL, Kemeid FM, Aguiar PS, John VM. Measuring the eco-efficiency of cement use. Cem Concr Compos 2010;32:555–62. https://doi.org/10.1016/j.cemconcomp.2010.07.009.

[134] Vieira DR, Calmon JL, Coelho FZ. Life cycle assessment (LCA) applied to the manufacturing of common and ecological concrete: A review. Constr Build Mater 2016;124:656–66. https://doi.org/10.1016/j.conbuildmat.2016.07.125.

[135] Kleijer AL, Lasvaux S, Citherlet S, Viviani M. Product-specific Life Cycle Assessment of ready mix concrete: Comparison between a recycled and an ordinary concrete. Resour Conserv Recycl 2017;122:210–8. https://doi.org/10.1016/j.resconrec.2017.02.004.

[136] Deschamps J, Simon B, Tagnit-Hamou A, Amor B. Is open-loop recycling the lowest preference in a circular economy? Answering through LCA of glass powder in concrete. J Clean Prod 2018;185:14–22. https://doi.org/10.1016/j.jclepro.2018.03.021.

[137] Evangelista BL, Rosado LP, Penteado CSG. Life cycle assessment of concrete paving blocks using electric arc furnace slag as natural coarse aggregate substitute. J Clean Prod 2018;178:176–85. https://doi.org/10.1016/j.jclepro.2018.01.007.

[138] Bakshi BR. Life Cycle Impact Assessment. Sustain Eng 2019:297–316. https://doi.org/10.1017/9781108333726.016.

[139] Galán-Marín C, Rivera-Gómez C, García-Martínez A. Embodied energy of conventional load-bearing walls versus natural stabilized earth blocks. Energy Build 2015;97:146–54. https://doi.org/10.1016/j.enbuild.2015.03.054.

[140] Ortiz O, Castells F, Sonnemann G. Sustainability in the construction industry: A review of recent developments based on LCA. Constr Build Mater 2009;23:28–39. https://doi.org/10.1016/j.conbuildmat.2007.11.012.

[141] Borken-Kleefeld J, Weidema BP. Global default data for freight transport per product group. Manuscr Spec Ecoinvent 2013;3.

[142] Kellenberger D, Althaus HJ, Jungbluth N, Künniger T, Lehmann M, Thalmann P. Life cycle inventories of building products. Final Rep Ecoinvent Data v2 0 No 2007;7.

[143] Hedrick JB, James B. Mineral commodity summaries 2010. US Geol Surv Reston, VA 2010:128–9.

[144] Boesch ME, Hellweg S. Identifying improvement potentials in cement production with life cycle assessment. Environ Sci Technol 2010;44:9143–9. https://doi.org/10.1021/es100771k.

[145] Künniger T, Werner F, Richter K. Ökologische Bewertung von Kies, Zement und Beton in der Schweiz. Schweizerische Mater Forschungsanstalt EMPA, Dübend 2001.

[146] Prusinski JR, Marceau ML, VanGeem MG. Life cycle inventory of slag cement concrete. Eighth CANMET/ACI Int. Conf. Fly Ash, Silica Fume, Slag Nat. Pozzolans Concr., American Concrete Institute Farmington Hills; 2004, p. 1–26.

[147] Althaus HJ, Chudacoff M, Hischier R, Jungbluth N, Osses M, Primas A. Life cycle inventories of chemicals. Ecoinvent Rep 2007;2.

[148] Marceau ML, Bushi L, Meil JK, Bowick M. Life cycle assessment for sustainable design of precast concrete commercial buildings in Canada. Green Build Libr 2012;1.

[149] Marceau M, Nisbet MA, Van Geem MG. Life cycle inventory of portland cement concrete. Portland Cement Association; 2007.

[150] Doka G. Updates to Life Cycle Inventories of Waste Treatment Services-part II: waste incineration. Doka Life Cycle Assessments, Zurich, 2013 2013.

[151] Doka G. Life cycle inventories of waste treatment services 2007.

[152] Association E-EA. Environmental profile report for the European Aluminium Industry, Life cycle inventory data for aluminium production and transformation processes in Europe. EAA, Brussels 2008:12–72.

[153] Hischier R. Life cycle inventories of packaging and graphical paper. Final Rep Ecoinvent Data v2 0 No 2007;11.

[154] Rentz O, Krippner M, Hähre S, Schultmann F. Report on best available techniques (BAT) in copper production. Deutsch-Französisches Inst Für Umweltforsch Univ Karlsruhe (TH), Karlsruhe, Ger 1999.

[155] Treichel A. BMW Baureihenarchiv· Der neue BMW 1er 3-Türer· 13. Mai 2012· bimmerarchiv. de 2012.

[156] Wang JJ, Tingley DD, Mayfield M, Wang YF. Life cycle impact comparison of different concrete floor slabs considering uncertainty and sensitivity analysis. J Clean Prod 2018;189:374–85. https://doi.org/10.1016/j.jclepro.2018.04.094.

[157] Monteiro H, Freire F. Life-cycle assessment of a house with alternative exterior walls: Comparison of three impact assessment methods. Energy Build 2012;47:572–83. https://doi.org/10.1016/j.enbuild.2011.12.032.

[158] Corcelli F, Fiorentino G, Vehmas J, Ulgiati S. Energy efficiency and environmental assessment of papermaking from chemical pulp - A Finland case study. J Clean Prod 2018;198:96–111. https://doi.org/10.1016/j.jclepro.2018.07.018.

[159] Bare JC, Hofstetter P, Pennington DW, Udo de Haes HA. Life cycle impact assessment workshop summary. Midpoints versus endpoints: The sacrifices and benefits. Int J Life Cycle Assess 2000;5:319–26. https://doi.org/10.1007/BF02978665.

[160] Wernet G, Bauer C, Steubing B, Reinhard J, Moreno-Ruiz E, Weidema B. The ecoinvent database version 3 (part I): overview and methodology. Int J Life Cycle Assess 2016;21:1218–30. https://doi.org/10.1007/s11367-016-1087-8.

[161] Goedkoop M. A damage oriented method for life cycle impact assessment. Eco-Indicator 99 1999.

[162] Hischier R, Weidema B, Althaus H-J, Bauer C, Doka G, Dones R, et al. Implementation of Life Cycle Impact Assessment Methods Data v2.2 (2010). Ecoinvent Rep No 3 2010:176.

[163] Schmidt JH, Holm P, Merrild A, Christensen P. Life cycle assessment of the waste hierarchy - A Danish case study on waste paper. Waste Manag 2007;27:1519–30. https://doi.org/10.1016/j.wasman.2006.09.004.

[164] Werner F, Althaus H-J, Künniger T, Richter K, Jungbluth N. Life cycle inventories of wood as fuel and construction material. Final Rep Ecoinvent Data v2 0 No 2007;9.

Appendix

According to the requirement of CMU, the data of configuration, density, compressive strength, thermal conductivity, and ultrasonic velocity test for samples of PB are listed from Table A.1-Table A.4.

Table A.1 Density and water absorption

		immersed weight (Wi)	saturated weight (Ws)	oven-dry weight (Wd)	Density (kg/m^3)	Absorption (%)
1	1	11.172	20.17	18.205	2023.23	10.79
	2	11.682	20.631	18.522	2069.73	11.39
	3	12.078	21.022	18.81	2103.09	11.76
2	1	10.902	19.776	17.54	1976.56	12.75
	2	11.027	20.002	18.1	2016.71	10.51
	3	10.644	19.844	17.605	1913.59	12.72
3	1	10.936	19.85	17.571	1971.17	12.97
	2	11.105	20.332	17.89	1938.88	13.65
	3	10.569	19.478	17.051	1913.91	14.23
4	1	10.846	20.127	18.478	2010.42	9.90
	2	10.96	19.76	17.881	2001.67	9.87
	3	11.061	19.943	18.338	2028.64	9.49
5	1	10.49	19.251	16.803	1922.46	14.24
	2	10.611	19.558	17.299	1956.02	15.10
	3	11.115	20.12	17.473	1943.11	14.48
6	1	9.876	18.71	16.027	2374.43	1.57
	2	10.306	19.214	16.368	2353.65	8.38
	3	9.73	18.153	15.602	1886.41	5.56
7	1	9.622	18.526	15.548	1700.50	19.53
	2	9.408	18.088	15.299	1787.85	21.09
	3	10.02	19.01	16.024	1787.35	19.88
8	1	11.627	20.541	19.325	2167.94	6.29
	2	11.751	20.242	19.104	2249.91	5.96
	3	10.932	19.57	18.411	2131.40	6.30
9	1	9.984	18.256	15.805	1690.67	14.29
	2	10.561	19.377	16.81	1686.21	13.97
	3	10.252	19.809	17.2	1753.25	13.53
10	1	12.387	21.757	20.388	1602.15	13.32
	2	11.49	19.813	18.735	1603.39	13.40
	3	11.612	20.51	19.064	1695.32	13.35
11	1	11.056	20.009	17.171	1845.03	16.48
	2	10.606	19.509	16.84	1803.02	18.50
	3	9.98	18.974	16.436	1868.16	16.23
12	1	9.231	19.133	16.741	1685.60	8.61
	2	9.306	19.402	17.024	1589.31	9.47
	3	9.208	18.505	16.3	1731.21	8.12

13	1	9.897	18.76	16.024	1814.24	16.74
	2	8.958	17.864	15.312	1837.45	17.39
	3	10.19	19.038	15.902	1852.31	16.35
14	1	10.628	19.62	17.406	2175.88	6.71
	2	11.007	20.022	17.672	2250.99	5.75
	3	10.924	20.002	17.488	2142.50	7.58
15	1	11.585	20.611	17.947	1935.72	12.72
	2	9.749	18.298	16.353	1960.29	13.30
	3	9.943	18.703	16.948	1926.42	14.38
16	1	9.869	18.458	15.847	2014.65	9.15
	2	9.849	18.515	15.625	2020.18	11.10
	3	9.418	17.458	15.02	1995.76	11.51
17	1	11.058	20.037	18.56	1988.37	14.84
	2	11.04	19.416	18.012	1912.86	11.89
	3	10.487	19.87	18.693	1934.70	10.36
18	1	9.007	19.85	18.277	1910.66	15.51
	2	8.624	20.28	18.525	1906.76	15.27
	3	9.049	19.429	17.97	1799.73	15.17
19	1	9.874	18.48	16.061	1866.26	15.06
	2	9.075	17.288	14.724	1792.77	17.41
	3	9.789	18.5	16.037	1841.01	15.36
20	1	8.698	17.122	14.325	1746.18	19.15
	2	8.857	16.46	13.593	1762.56	18.23
	3	8.345	15.648	13.053	1782.42	18.63
21	1	11.03	20.251	17.727	1917.93	14.57
	2	11.58	20.834	18.101	1933.50	13.06
	3	10.955	19.902	17.385	1940.37	15.15
22	1	10.343	19.04	16.182	1860.64	17.66
	2	10.031	19.314	16.849	1815.04	14.63
	3	10.482	19.211	16.535	1894.26	16.18
23	1	9.018	20.075	17.715	2067.05	7.96
	2	8.935	19.855	17.509	2150.43	7.79
	3	9.189	19.16	16.904	1992.22	6.30
24	1	10.801	19.81	18.15	1917.90	16.53
	2	11.1	20.02	18.02	1891.50	15.85
	3	10.986	19.951	17.892	1827.44	15.44
25	1	11.021	20.134	18.321	1990.95	8.92
	2	10.771	19.753	17.979	2031.93	10.51
	3	10.914	19.851	18.13	2064.63	8.75
26	1	10.59	19.729	17.013	1861.58	15.96
	2	10.691	19.319	16.549	1918.06	16.74
	3	10.805	20.16	17.881	1911.38	12.75
27	1	11.748	20.07	19.76	1807.97	17.07
	2	12.569	20.673	19.074	1719.29	16.67
	3	11.433	22.966	21.756	1797.24	19.72

Table A.2 7-day and 28-day compressive strength

	Gross Area (m^2)	7-days Max.force (N)	P_7(MPa)	SD (7-day)	28-days Max. force (N)	P_{28} (MPa)	SD (28-day)

	1	0.04023	206.03	5.12		252.7	6.28	
1	2	0.04055	193.82	4.78	0.18	250.3	6.17	0.06
	3	0.04220	204.85	4.85		261.1	6.19	
	1	0.04060	191.68	4.72		246.05	6.06	
2	2	0.03998	188.21	4.71	0.10	234.1	5.86	0.11
	3	0.04023	182.98	4.55		236.11	5.87	
	1	0.04096	160.39	3.92		226.56	5.53	
3	2	0.04034	151.69	3.76	0.08	228.9	5.67	0.17
	3	0.04023	156.73	3.90		214.4	5.33	
	1	0.04133	207.04	5.01		266.51	6.45	
4	2	0.04071	195.38	4.80	0.11	256.4	6.30	0.09
	3	0.04122	204.2	4.95		259.7	6.30	
	1	0.04147	173.54	4.18		229.72	5.54	
5	2	0.04122	169.51	4.11	0.07	227.3	5.51	0.07
	3	0.03998	161.81	4.05		215.91	5.40	
	1	0.04023	118.2	2.94		168.51	4.19	
6	2	0.04034	122.39	3.03	0.08	161.1	3.99	0.10
	3	0.03888	111.99	2.88		156.695	4.03	
	1	0.04206	93.89	2.23		130.04	3.09	
7	2	0.04060	82.72	2.04	0.10	128.71	3.17	0.14
	3	0.04158	86.12	2.07		120.45	2.90	
	1	0.04060	244.21	6.02		312.1	7.69	
8	2	0.04023	232.9	5.79	0.12	303.3	7.54	0.19
	3	0.04034	240.4	5.96		319.35	7.92	
	1	0.04023	137.73	3.42		201.1	5.00	
9	2	0.04085	139.12	3.41	0.16	198.34	4.86	0.18
	3	0.04133	129.78	3.14		191.61	4.64	
	1	0.04060	232.1	5.72		285.95	7.04	
10	2	0.04034	220.51	5.47	0.41	277.37	6.88	0.17
	3	0.04096	201.2	4.91		295.78	7.22	
	1	0.04060	120.93	2.98		180.51	4.45	
11	2	0.04023	135.88	3.38	0.21	189.8	4.72	0.19
	3	0.04071	125.69	3.09		177.51	4.36	
	1	0.04060	161.12	3.97		220.8	5.44	
12	2	0.04133	171.88	4.16	0.15	215.67	5.22	0.14
	3	0.04133	159.71	3.86		226.56	5.48	
	1	0.04071	96.51	2.37		129.6	3.18	
13	2	0.04038	85.41	2.12	0.19	131.53	3.26	0.17
	3	0.04012	99.3	2.47		140.51	3.50	
	1	0.04096	169.65	4.14		220.6	5.39	
14	2	0.04133	177.58	4.30	0.10	233.8	5.66	0.14
	3	0.03998	164.7	4.12		221.7	5.55	
	1	0.04060	168.25	4.14		230.1	5.67	
15	2	0.04147	169.44	4.09	0.06	243.6	5.87	0.12
	3	0.04096	164.8	4.02		240.7	5.88	
	1	0.04096	112.39	2.74		161.12	3.93	
16	2	0.04071	114.47	2.81	0.23	149.38	3.67	0.13
	3	0.04133	98.68	2.39		157.88	3.82	
1	1	0.03841	201.13	5.24	0.08	269.8	7.02	0.18

7	2	0.03939	200.42	5.09		262.33	6.66	
	3	0.04049	206.75	5.11		276.71	6.83	
18	1	0.03920	195.18	4.98		248.66	6.34	
	2	0.04019	205.5	5.11	0.10	279.92	6.97	0.31
	3	0.04071	200.08	4.92		272.83	6.70	
19	1	0.04060	125.71	3.10		164.77	4.06	
	2	0.04060	122.53	3.02	0.15	168.83	4.16	0.18
	3	0.04133	115.69	2.80		157.51	3.81	
20	1	0.04071	84.36	2.07		105.31	2.59	
	2	0.04060	76.82	1.89	0.10	128.22	3.16	0.31
	3	0.04060	83.72	2.06		125.91	3.10	
21	1	0.04133	154.36	3.74		234.91	5.68	
	2	0.04071	169.12	4.15	0.22	208.72	5.13	0.38
	3	0.04060	154.78	3.81		201.29	4.96	
22	1	0.04060	130.1	3.20		178.53	4.40	
	2	0.04133	125.42	3.03	0.11	164.3	3.98	0.22
	3	0.04071	122.23	3.00		175.1	4.30	
23	1	0.04060	159.7	3.93		219.66	5.41	
	2	0.04060	169.34	4.17	0.12	222.7	5.49	0.20
	3	0.04133	166.83	4.04		239.17	5.79	
24	1	0.04071	185.01	4.55		246.05	6.04	
	2	0.04060	180.14	4.44	0.06	249.43	6.14	0.28
	3	0.04060	184.2	4.54		266.9	6.57	
25	1	0.04133	180.06	4.36		248.71	6.02	
	2	0.04071	190.17	4.67	0.16	262.8	6.46	0.23
	3	0.04060	183.33	4.52		258.5	6.37	
26	1	0.04071	152.79	3.75		186.2	4.57	
	2	0.04060	135.34	3.33	0.21	219.11	5.40	0.41
	3	0.04060	146.11	3.60		205.4	5.06	
27	1	0.04133	277.43	6.71		329.7	7.98	
	2	0.04060	263.09	6.48	0.26	344.9	8.50	0.38
	3	0.04060	251.64	6.20		314.68	7.75	

Table A.3 28-day compressive strength of PB with water immersion.

		Gross Area (m2)	28-days Max. force (N)	P_{28} (MPa)	SD
1	1	0.03972	210.80	5.31	
	2	0.03982	200.91	5.04	0.15
	3	0.04257	214.70	5.04	
2	1	0.04060	199.30	4.91	
	2	0.03998	189.62	4.74	0.09
	3	0.03998	191.25	4.78	
3	1	0.04096	176.72	4.31	
	2	0.04034	178.54	4.43	0.14
	3	0.04023	167.23	4.16	
4	1	0.04133	231.33	5.60	
	2	0.04071	222.56	5.47	0.07
	3	0.04122	225.42	5.47	
5	1	0.04147	177.34	4.28	0.06
	2	0.04122	175.48	4.26	

	3	0.03998	166.68	4.17	
	1	0.04049	125.36	3.10	
6	2	0.04060	118.89	2.93	0.08
	3	0.03862	115.64	2.99	
	1	0.04206	91.29	2.17	
7	2	0.04060	90.35	2.23	0.10
	3	0.04158	84.56	2.03	
	1	0.04060	273.40	6.73	
8	2	0.04023	265.69	6.60	0.17
	3	0.04034	279.75	6.93	
	1	0.04023	149.02	3.70	
9	2	0.04085	146.97	3.60	0.14
	3	0.04133	141.98	3.44	
	1	0.04060	248.78	6.13	
10	2	0.04034	241.31	5.98	0.15
	3	0.04096	257.33	6.28	
	1	0.04060	132.86	3.27	
11	2	0.04023	139.69	3.47	0.14
	3	0.04071	130.65	3.21	
	1	0.04060	172.89	4.26	
12	2	0.04133	168.87	4.09	0.11
	3	0.04133	177.40	4.29	
	1	0.04071	92.92	2.28	
13	2	0.04038	94.31	2.34	0.12
	3	0.04012	100.75	2.51	
	1	0.04096	176.04	4.30	
14	2	0.04133	186.57	4.51	0.11
	3	0.03998	176.92	4.43	
	1	0.04060	179.71	4.43	
15	2	0.04147	190.25	4.59	0.09
	3	0.04096	187.99	4.59	
	1	0.04096	119.55	2.92	
16	2	0.04071	110.84	2.72	0.10
	3	0.04133	117.15	2.83	
	1	0.03841	228.52	5.95	
17	2	0.03939	222.19	5.64	0.15
	3	0.04049	234.37	5.79	
	1	0.03920	214.84	5.48	
18	2	0.04019	241.85	6.02	0.27
	3	0.04071	235.73	5.79	
	1	0.04060	124.73	3.07	
19	2	0.04060	127.80	3.15	0.14
	3	0.04133	119.24	2.89	
	1	0.04071	72.35	1.78	
20	2	0.04060	88.09	2.17	0.22
	3	0.04060	86.50	2.13	
	1	0.04133	182.06	4.41	
21	2	0.04071	161.76	3.97	0.29
	3	0.04060	156.00	3.84	

	1	0.04060	133.36	3.29	
22	2	0.04133	122.73	2.97	0.165241
	3	0.04071	130.80	3.21	
	1	0.04060	172.43	4.25	
23	2	0.04060	174.82	4.31	0.15646
	3	0.04133	187.75	4.54	
	1	0.04071	203.19	4.99	
24	2	0.03950	209.02	5.29	0.226372
	3	0.04060	220.66	5.44	
	1	0.04133	207.18	5.01	
25	2	0.04071	218.91	5.38	0.19291
	3	0.04060	215.33	5.30	
	1	0.03998	140.08	3.50	
26	2	0.04060	165.16	4.07	0.287217
	3	0.04023	156.11	3.88	
	1	0.04085	295.39	7.23	
27	2	0.04096	310.10	7.57	0.266936
	3	0.04001	281.84	7.04	

Table A.4 Thermal conductivity of PB at 28 days.

		T1	T2	L	λ_T	Average λ_T
1	1	20	37.10	200	1.15	1.09
	2	21.2	36.80	203	1.03	
2	1	18.3	34.10	204	1.00	1.01
	2	18.5	34.10	201	1.02	
3	1	19.6	30.05	200	0.84	0.89
	2	20	30.05	200	0.94	
4	1	19.5	39.16	202	1.18	1.16
	2	20.1	39.16	201	1.14	
5	1	21.1	28.70	200	0.85	0.85
	2	21.2	28.70	203	0.85	
6	1	19.8	25.32	202	0.73	0.745
	2	19.8	25.32	202	0.76	
7	1	20	20.93	202	0.60	0.62
	2	20.2	20.93	202	0.64	
8	1	18.4	43.89	200	1.33	1.315
	2	18.7	43.89	200	1.30	
9	1	20.3	26.00	201	0.75	0.765
	2	20.2	26.00	197	0.78	
10	1	21.3	43.21	205	1.25	1.275
	2	21	43.21	201	1.30	
11	1	19.6	26.67	203	0.80	0.795
	2	19.6	26.67	201	0.79	
12	1	20.3	29.37	200	0.89	0.87
	2	20.3	29.37	201	0.85	
13	1	20.5	22.96	200	0.68	0.68
	2	20.9	22.96	201	0.68	
14	1	18.7	30.05	203	0.88	0.89
	2	18.5	30.05	201	0.90	

15	1	20.9	30.38	201	0.94	0.895
	2	20.4	30.38	202	0.85	
16	1	18.8	25.32	201	0.75	0.745
	2	19	25.32	200	0.74	
17	1	21.4	41.19	202	1.23	1.215
	2	21.3	41.19	201	1.20	
18	1	19.6	39.84	203	1.17	1.175
	2	19.6	39.84	203	1.18	
19	1	20.5	25.66	202	0.78	0.755
	2	20.7	25.66	199	0.73	
20	1	18.4	19.92	199	0.60	0.585
	2	18.9	19.92	202	0.57	
21	1	20.8	29.71	203	0.88	0.875
	2	20.8	29.71	200	0.87	
22	1	21	26.33	201	0.77	0.78
	2	21.3	26.33	202	0.79	
23	1	19.9	31.73	202	0.98	0.94
	2	19.3	31.73	202	0.90	
24	1	22.5	37.47	202	1.18	1.11
	2	22.3	37.47	203	1.04	
25	1	21.9	38.15	195	1.14	1.13
	2	21.8	38.15	197	1.12	
26	1	20.7	27.01	200	0.80	0.75
	2	20.7	27.01	200	0.70	
27	1	17.8	44.90	202	1.30	1.325
	2	18	44.90	202	1.35	